

# **Wings over Wairio:**

Using UAV imagery to perform fine-scale mapping of wetland vegetation

---

A Thesis

submitted to the Victoria University of Wellington  
in fulfilment of the requirements for the Degree of  
Master of Science (GIS)

by

Patrick Hipgrave

---

Victoria University of Wellington

2020

Abstract of a Thesis submitted in partial fulfilment of the requirements for the Degree of Master of Geographic Information Science.

## **Wings over Wairio:**

Using UAV imagery to perform fine-scale mapping of wetland vegetation

by

Patrick Hipgrave

Differentiating between species of plants in aerial imagery is often challenging and, in some cases, can be impossible without significant field data collection. However, remote sensing technology is developing to the point where it is increasingly possible to eliminate the need for extensive fieldwork entirely and conduct non-disruptive monitoring of fragile environments. The increasing availability of UAV platforms with integrated high-resolution cameras and low-cost image processing software is also making remote sensing operations accessible to those outside the scientific community with an interest in environmental monitoring. This project trialled an emerging set of image analysis techniques called 'object-based image analysis' to create fine scale maps of a recovering wetland area, based on aerial photographs collected using a consumer-grade UAV (unmanned aerial vehicle). The effects of including additional ancillary data (such as digital surface models (DSMs) and multispectral imagery) in the classification process were also assessed to compare the ability of a standard digital camera to produce high-accuracy classifications to that of a more specialised multispectral sensor. The inclusion of this extra information was found to significantly improve classification accuracy in almost all cases, making a strong argument for the inclusion of ancillary data whenever possible, especially when considering the ease with which ancillary datasets can be produced. The high-resolution (between 2 and 4cm/pixel) imagery provided sufficient detail to observe 28 distinct land cover classes in total, with around 20 classes per image. While the number of classes in the classification scheme may have imposed limits on the overall accuracy of the classified maps, several classes were classified with a high (70% or greater) level of accuracy, including two invasive species, showing that the object-based school of image classification has potential to be a powerful tool for detecting and tracking individual vegetation types.

# Acknowledgements

Acknowledgement and thanks are due to...

My supervisors, Dr Mairead de Roiste, and Dr Stephen Hartley for their support and advice. Extra thanks are owed to Stephen, who generously loaned me his UAV, without which this project could never have got off the ground.

Further thanks are owed to Dez Tessler, for his assistance and willingness to let me loose with the School's Matrice. And also for his patience in putting up with perhaps the least co-operative sales department in the Southern Hemisphere. In the same vein, Dr James Quilty of the School of Engineering must be thanked for his trust and loan of his RedEdge Camera, which proved so essential in pursuit of this project's goals. Oliver Wigmore of the Antarctic Research Centre has my gratitude for helping me with last-minute clarifications and guidance. Likewise, thanks to Andrew Rae for getting the necessary software up and running. And to the ITS team at VUW who stepped in when the computers stopped co-operating.

To Ducks Unlimited and the Department of Conservation, for their permission to use the Wairio wetland as my study site and for providing clearance to fly there.

To Mum and Dad, for the constant supply of encouragement, tea and biscuits, and without whose incessant pestering to sign up for the MGIS programme in the first place, I wouldn't be writing this.

To the team at No. 2 (Hutt City) Squadron, Air Training Corps, who were always able to provide me with distractions when I needed a break and for putting up with me going on about how brilliant drones are.

# Table of Contents

<b>Abstract</b> .....	<b>ii</b>
<b>Acknowledgements</b> .....	<b>iii</b>
<b>Table of Contents</b> .....	<b>iv</b>
<b>List of Tables</b> .....	<b>vi</b>
<b>List of Figures</b> .....	<b>vii</b>
<b>Terms &amp; Abbreviations</b> .....	<b>viii</b>
<b>Chapter 1 Introduction</b> .....	<b>1</b>
1.1 Introduction .....	1
1.2 Research Questions & Objectives .....	2
1.3 The Wairio Wetland Block.....	3
1.4 Thesis Structure .....	4
<b>Chapter 2 Literature</b> .....	<b>6</b>
2.1 Aerial Remote Sensing .....	6
2.1.1 The Use of UAVs for Remote Sensing .....	6
2.2 New Zealand’s Wetlands.....	8
2.3 Wetland Vegetation Mapping .....	9
2.3.1 Ancillary Data Sources – Digital Surface Models .....	9
2.3.2 Ancillary Data Sources – Multispectral Imagery.....	10
2.4 Image Classification Techniques .....	11
2.4.1 Manual Interpretation & Digitisation .....	11
2.4.2 Pixel-Based Classification .....	11
2.4.3 Object-Based Classification .....	12
2.5 Change Detection.....	13
<b>Chapter 3 Methodology</b> .....	<b>14</b>
3.1 Study Area .....	14
3.2 Survey Flights.....	19
3.2.1 Multispectral Imagery Collection .....	23
3.3 Image Processing – Mosaic & Surface Model Generation .....	24
3.4 Image Classification.....	24
3.4.1 Input.....	25
3.4.2 Segmentation .....	25
3.4.3 Creating Training Data .....	29
3.4.4 Object-Based Classification .....	31
3.5 Accuracy Assessment .....	32
3.5.1 Image Preparation .....	33
3.5.2 Creating Reference Data for Ground-Truthing.....	33
3.5.3 Confusion Matrices.....	36
3.5.4 Analysis of Accuracy Results.....	36
3.6 Change Detection.....	38
3.6.1 Flood Patterns .....	39

<b>Chapter 4 Classification &amp; Change Detection Results .....</b>	<b>41</b>
4.1 Classification Results .....	41
4.1.1 Seasonal Flights .....	41
4.1.2 Class-Specific Results .....	43
4.1.3 Multispectral Imagery Tests .....	46
4.1.4 Class-Specific Results .....	47
4.2 Change Detection.....	49
4.2.1 Land / Water Change by Surface Area .....	49
4.2.2 Change Visualisation.....	50
4.2.3 Descriptive.....	52
4.2.4 Comparative Maps.....	54
<b>Chapter 5 Discussion &amp; Evaluation .....</b>	<b>58</b>
5.1 Classification Accuracy .....	58
5.1.1 Higher-Accuracy Classifications (OA: >70%).....	60
5.1.2 Moderate Accuracy (OA: 60%-69%) .....	60
5.1.3 Poor Accuracy (OA: <60%) .....	61
5.1.4 Confusions.....	61
5.1.5 Implications of Accuracy .....	63
5.1.6 Accuracy vs. Usability.....	63
5.2 Potential Causes of Error.....	65
5.3 Convenience of UAV Mapping.....	69
5.3.1 UAV Logistics & Ease of Use .....	69
5.3.2 Operational Capability .....	71
5.3.3 Non-Disruptive Operation.....	72
5.3.4 Post-Flight Processes .....	73
5.4 Improving Effects of the DSM.....	74
5.5 Multispectral Camera Imagery Tests .....	76
5.5.1 Data Quality Issues .....	77
5.5.2 Benefits of additional ancillary data .....	80
5.6 Evaluation.....	82
5.6.1 Survey Flights .....	82
5.6.2 Image Processing.....	83
<b>Chapter 6 Conclusions .....</b>	<b>84</b>
6.1 Research Question One.....	84
6.2 Research Question Two.....	85
6.3 Future Research Opportunities .....	86
<b>Bibliography .....</b>	<b>87</b>
<b>Appendix A: Class Example Images .....</b>	<b>92</b>
<b>Appendix B: Confusion Matrices .....</b>	<b>97</b>
<b>Appendix C: Full-Page Maps .....</b>	<b>115</b>
C.1 True-Colour Camera Orthomaps .....	115
C.2 Multispectral Camera Imagery .....	127

## List of Tables

Table 3.1: Band Combinations for Segmentation and Classification .....	26
Table 3.2: List of Classes.....	29
Table 3.3: Spectral Properties used for Classification.....	32
Table 3.4: Textural Properties used for Classification.....	32
Table 3.5: Defining Characteristics of Classes .....	34
Table 3.6: List of change detection 'generic' classes .....	39
Table 4.1: Overall Classification Accuracy & Kappa Scores .....	41
Table 4.2: Analysis of deviance of LME for the effect of ancillary DSM data and Season on Overall Accuracy (n = 24 values from Table 4.1).....	42
Table 4.3: Analysis of deviance of LME for the effect of ancillary DSM data and Season on Overall Kappa (n = 24 values from Table 4.1) .....	43
Table 4.4: Per Class Accuracy .....	44
Table 4.5: Overall Accuracy and Kappa with different combinations of ancillary data .....	46
Table 4.6: Analysis of deviance of LME for the effect of ancillary data in the form of a DSM and/or multispectral infrared on Overall Accuracy assessed in late Summer (n = 12 values from Table 4.5).....	47
Table 4.7: Analysis of deviance of LME for the effect of ancillary data in the form of a DSM and/or multispectral infrared on Overall Kappa assessed in late Summer .....	47
Table 4.8: Class-Specific Accuracy (Multispectral Camera).....	48
Table 5.1: Classes Ranked by Overall Accuracy (OA) .....	59
Table 5.2: Classes and their Common Conclusions.....	62
Table 5.3: Contrasting Classification Accuracy between schemes with many and few classes based on March 2019 imagery .....	83

## List of Figures

Figure 1: Boundary of the Wairio Wetland (approximate) Imagery dates from 2018 .....	4
Figure 2: Image Capture, Processing and Classification Process Diagram .....	14
Figure 3: Outline of the four stages of the Wairio Wetland (Imagery from 2018) .....	15
Figure 4: Stage One of the Wairio Wetland Block, imagery Captured by Patrick Hipgrave (June 2018) .....	16
Figure 5: Stage Two of the Wairio Wetland Block, imagery Captured by Patrick Hipgrave (June 2018) .....	17
Figure 6: Stage Three of the Wairio Wetland Block, imagery Captured by Patrick Hipgrave (June 2018) .....	18
Figure 7: Comparison of water colouration within a stage .....	31
Figure 8: Accuracy Assessment Process Diagram .....	33
Figure 9: Land/Water Change in Stage One .....	50
Figure 10: Land/Water Change in Stage Two .....	51
Figure 11: Land/Water Change in Stage Three .....	52
Figure 12: Stage One - changes over time .....	55
Figure 13: Stage Two - changes over time .....	56
Figure 14: Stage Three - changes over time .....	57
Figure 15 : Example of the Blackberry Patch maps given to the contractor. Extracted from a Map created by Stephen Hartley (2019). .....	64
Figure 16: Demonstration of edge effects in the classified imagery (Stage two, October 2018) .....	66
Figure 17: Two Kahikatea trees in stage one blend into the background in the leftmost image (Winter, 2018), but are clearly visible in the image to the right (Spring, 2018). .....	75
Figure 18a & 18b: Comparing RGB-Only (above) and DSM-Inclusive Classifications (below) of stage two (June 6 <sup>th</sup> , 2018) .....	76
Figure 19: Extract from Stage One Orthomosaic (April 2019) showing the blurred areas. ....	77
Figure 20: The mounting arrangement for the RedEdge Camera .....	78
Figure 21a & 21b: Comparison of base orthomosaics (above) and DSM resolution (below) between the two cameras. ....	81

## Terms & Abbreviations

**CAA** - Civil Aviation Authority

**DOC** – Department of Conservation

**DU** – Ducks Unlimited

**DEM** – Digital Elevation Model

**DSM** – Digital Surface Model

**FWHM** – Full Width at Half Maximum

**GIS** – Geographic Information Systems / Science

**GPS** – Global Positioning System

**LiDAR** – Light Detection and Ranging

**MS** – Multispectral

**OA** – Overall Accuracy

**OBIA** – Object Based Image Analysis

**PA** – Producer’s Accuracy

**NIR** – Near Infrared

**RE** – Red Edge

**RGB** – Red, Green, Blue

**SVM** – Support Vector Machine

**UA** – User’s Accuracy

**UAV** – Unmanned Aerial Vehicle

# Chapter 1

## Introduction

### 1.1 Introduction

Wetland environments may change rapidly over time, therefore precise tracking of temporal changes in wetland surface cover requires more frequent monitoring. While the use of Unmanned Aerial Vehicles (UAVs) as aerial remote sensing platforms is not a novel concept and neither is object-based image classification of vegetation, there is currently a dearth of studies that deal with the subject in relation to the environment of New Zealand. Additionally, none of the studies that deal specifically with wetlands e.g. (Cordeiro & Rossetti, 2015; Lechner, Fletcher, Johansen, & Erskine, 2012) focused on a wetland that was undergoing restoration at the time.

There is also a disagreement within the literature regarding the effect that the additional of ancillary data might have on the results of their image classification. Some, for instance Kim, Madden, & Xu, (2010) and Waser *et al* (2008) argue in favour of the inclusion of topographic or multispectral variables alongside visible-spectrum imagery, some (Campbell & Whyne, 2011) suggest improvements are not guaranteed, and others (Pande-Chhetri, Abd-Elrahman, Liu, Morton, & Wilhelm, 2017; Dronova, et al., 2012) make no reference to the matter at all. It is possible that this phenomenon that has occurred due the development and adoption of UAV technology for various applications outpacing the understanding of the relationship between method and data quality (Dandois, Olano, & Ellis, 2015).

Many users of UAVs are comparative novices, particularly in New Zealand wetlands, where many wetland restoration projects are undertaken by volunteers with no particular training in ecological science or remote sensing. Such projects are often conducted without access to the scientific expertise, equipment, and sources of funding of career scientists. However, the widespread adoption of UAVs and availability of low-cost image processing software is likely to increase their use by amateur wetland restoration teams. Given that the 'gold standard' of remote sensing typically involves the use of expensive multispectral sensor suites, the quality of studies conducted by those without access to these high-quality sensors is an unknown quantity. It may be that adding multispectral ancillary data does not improve the accuracy of classification to a degree that would justify the associated additional expense. A reliable classification scheme may simply require data that can easily be produced from 'off-the-shelf' sensors and aerial platforms that are easily accessed and operated by the general public.

## 1.2 Research Questions & Objectives

The use of UAVs as remote sensing platforms is expanding at an increasingly rapid pace. Despite this, there have been no wetland monitoring projects conducted via UAV whose duration extended beyond a single survey covering one instance in time, either in New Zealand or elsewhere.

Additionally, there appears not to be a consistent view on the merits of the inclusion of ancillary data sources. Therefore, this project will conduct a year-long monitoring programme of a recovering wetland area whilst simultaneously examining how the accuracy of object-based image analyses may be improved with the addition of a range of ancillary data types.

This project will answer two primary research questions:

1. Test the proposition that UAVs can provide accurate and convenient assessment of changes in vegetation and water coverage over time, using a recovering wetland area as a case study.
2. To what extent is the accuracy of the image classification process improved with the addition of ancillary data, such as digital surface models or near infrared imagery?

To answer these questions, the project will use object-based image analysis of orthomosaics captured with a UAV to pursue several objectives, namely:

- Create a series of classified raster images to represent vegetation and surface cover at seasonal intervals.
- Compare the results of the image classification process when ancillary (surface model or near-infrared) data is included in concert with the true-colour imagery.
- Compare the extent of the target classes in the captured images with that evident in previously gathered data to look for changes over time.
- Assess the feasibility of using a UAV for gathering ground-truthing data for post-classification verification of results and remote identification of plants.

On completion, this project will have provided several important contributions to the literature surrounding aerial remote sensing of vulnerable environments. First and foremost, it will provide evidence in support of the inclusion of ancillary data in the classification of aerial imagery by documenting the effect that different varieties of ancillary data have on the results of the image classification. At the same time, it will test and report the ability of an object-based approach to provide species-specific classifications in an environment with a high degree of heterogeneity both within and between a large number of land cover classes. Additionally, it will provide evidence of the ability of a research team with limited experience, personnel, budget and time to gather imagery and

process it into maps with much greater levels of detail than might otherwise be available without recourse to contracting professional UAV operators or GIS technicians. It will also support the assertion that UAVs are well-suited to surveying fragile environments as put forward by Anderson & Gaston, (2013) among others. This will be done by demonstrating the ability of UAVs to operate within such an environment without causing harm or disruption to the local flora or fauna. Protecting the latter from UAV-induced distress is both an ethical and legal concern constraining the wider use of UAVs in both New Zealand and elsewhere (Gonzalez & Johnson, 2017; Department of Conservation, 2019). Finally, the project will produce a valuable inventory of land cover and seasonal change within a recovering wetland area.

### **1.3 The Wairio Wetland Block**

This thesis uses the Wairio wetland as a case study to investigate the research questions posed above. The wetland at Wairio, in the Lower North Island of New Zealand has only recently begun to be restored to a state approaching its natural condition, having been drained and converted into farmland during the 1960s and 70s. As part of the clearance programme, most of the native forest and sedge was removed, and exotic grasses suitable for cattle grazing were planted in their place. The land passed into the ownership of the Department of Conservation (DOC) in 1987 but no serious efforts were made to reverse the ecological changes caused by two decades of agricultural development and the land remained open for occasional grazing for a number of years. In 2005, Ducks Unlimited New Zealand (DU) and DOC entered into a partnership to undertake restoration of the area (Ducks Unlimited, 2016).

Since then, several measures have been taken to restore the area into wetlands. A number of earth dams have been created to retain surface water in the site, resulting in large areas of former grassland now being permanently or semi-permanently flooded. A significant programme of re-planting is ongoing to restore native vegetation to the area. As a result, most of the vegetation is comprised of isolated, compact stands of native trees, including manuka and cabbage trees, with smaller plantations of toetoe and flax being scattered throughout the site. A few large kahikatea (*Dacrycarpus dacrydioides*) and totara (*Podocarpus totara*) trees are also present and are the only remnant of the original forest. Several species of exotic grasses, including tall fescue (*Lolium arundinaceum*) and Yorkshire fog (*Holcus lanatus*) are widespread and make up most of the ground cover in open areas, giving way to grasses, sedges and rushes that are more tolerant of aqueous conditions in proximity to bodies of water. Meanwhile an eradication programme is underway to control weeds which are still well-established in the area including blackberry and gorse bushes,

supplemented by recent incursions of *Bidens frondosa*.

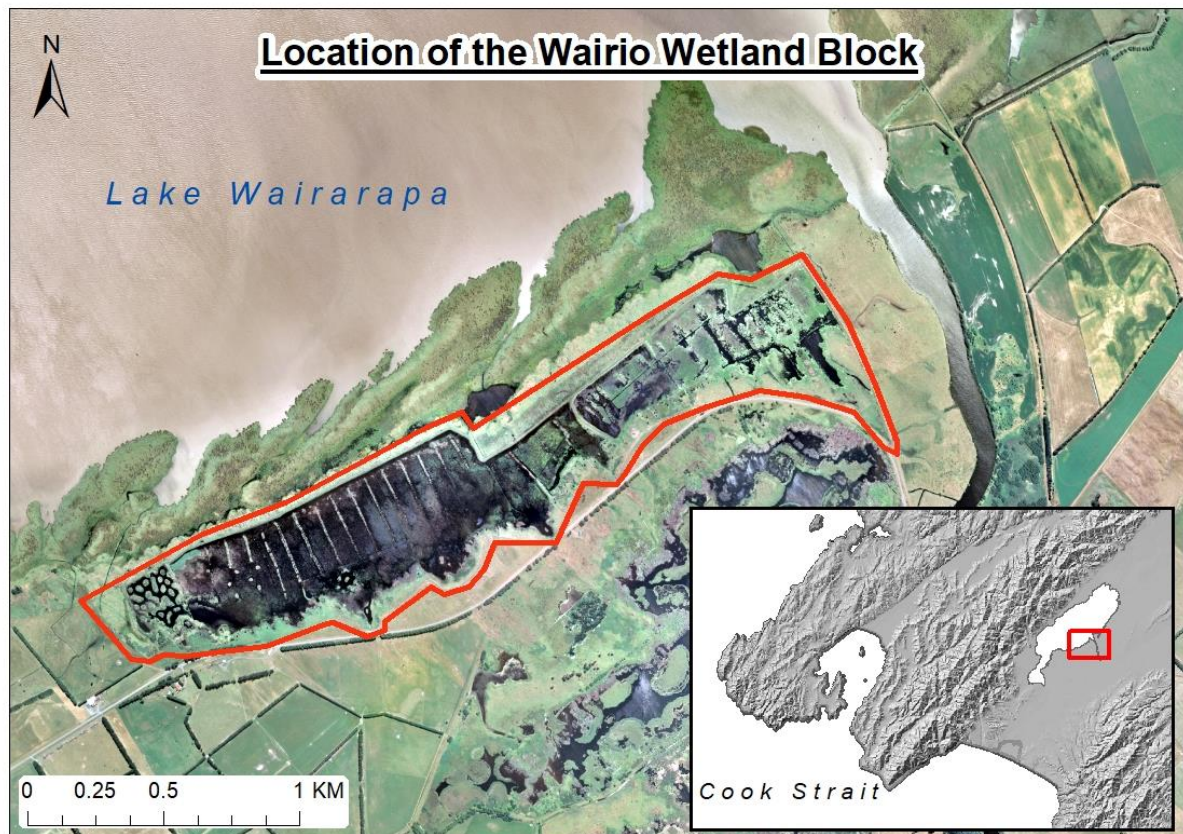


**Figure 1: Boundary of the Wairio Wetland (approximate) Imagery dates from 2018**

The restoration programme means that the vegetation present in the site should be changing at a faster rate and should exhibit a greater deal of variation over time than would be present in a natural wetland. Therefore, a monitoring programme that can document the seasonal and successional changes that occur within the wetland would be a boon to restoration efforts as it would allow for better measurements of the rate at which vegetation is recovering and spreading. This would serve to illustrate the degree to which the goals of the project are being met or whether a specific area requires more remedial work. Understanding seasonal fluctuations in water cover can also be useful for managing or predicting habitat and nesting sites for waterfowl, threatened species like the Australasian Bittern in particular. A programme that leveraged remote sensing techniques would also allow for better targeting of weed species that would be difficult to find on foot, owing to the difficulty in accessing parts of the wetland now that many areas of dry land are cut off by water.

## 1.4 Thesis Structure

Chapter 2 presents a review of the literature which has contributed to the development of this project, with a particular focus of the recent applications of UAVs for remote sensing and aerial photography, the wetlands of New Zealand and the field of image classification for mapping and change detection.

Chapter 3 provides the methodology of the project, beginning by covering the methodology used to plan and conduct the survey flights. Following this, the processes used to classify the imagery datasets into land cover classes will be detailed and finally the means by which the accuracy of the image classifications were assessed will be described.

Chapter 4 presents the results of the image classification process, including a description of the effects of the inclusion of ancillary data on the process as well as the surface cover maps of each site. The results of the accuracy assessments will also be discussed at this point. Chapter 4 also outlines the results of the change detection, describing the observed pattern of changes in the study areas over the course of the project.

Chapter 5 presents an evaluation of the projects methods and results, followed by the conclusions drawn from the project.

## Chapter 2

### Literature

#### 2.1 Aerial Remote Sensing

Photogrammetry is one of the oldest scientific uses of aerial images. Though satellite imagery has replaced aerial imaging as the go-to option for imaging very large expanses at once, the relatively low altitude of aerial shots allows for greater levels of detail in the photograph, with the advent of low-flying UAVs (Unmanned Aerial Vehicles) allowing for extremely detailed maps of topography and land cover to be produced over relatively small areas.

Aerial remote sensing is a comparatively cost-efficient method of gathering data over large expanses, whilst field surveys require significant logistical planning, can be time consuming and even be disruptive or damaging to the environment being surveyed (Bollard-Breen, Brooks, & Jones, 2015). Recent developments in remote sensing technologies have led to the development of new, low-impact methods of monitoring the environment from a distance and the use of conventional piloted aircraft or UAVs as airborne platforms for a wide array of scientific equipment allows for survey missions to be conducted without researchers needing to be physically present in the area. While satellite-based systems are theoretically capable of producing high-resolution<sup>1</sup> maps of wetland areas, the levels of heterogeneity present in wetland vegetation are such that precise classification of satellite imagery would be challenging without collecting spectral measurements in the field with which to 'train' the image classification process.

##### 2.1.1 The Use of UAVs for Remote Sensing

When monitoring wetland areas, capturing remotely-sensed data from an aerial platform has many advantages over on-site surveys. Though their use for environmental monitoring is still an emergent field, there has been an increase in their use over the last decade as small UAVs have become increasingly capable and affordable (Anderson & Gaston, 2013). Using UAVs to capture imagery allows for improved temporal and spatial resolutions in comparison to manned aircraft. The former advantage derives from the UAV's ability to be readied for flight and deployed more rapidly while the latter stems from the UAV's small size allowing it to be safely operated at very low altitudes (Giles & Billing, 2014), allowing for high spatial resolution image capture even with smaller or less advanced sensors than those that might be fitted to a full-size aircraft. Use of a self-piloted or autonomously operated UAV allows greater levels of user control over the final product as the surveyor is in full

---

<sup>1</sup> 30cm/pixel resolution from the Worldview-4 satellite is currently among the best commercially available offerings. For contrast, the resolution of the mages gathered by the UAV in this project is 2cm/pixel.

control over the parameters of the flight. By comparison, conventional aircraft are expensive to hire, operate and maintain (Kumar, 1997); while pilots require special training and qualifications to conduct survey flights, which are normally restricted by local aviation regulations to a greater degree than UAV flights are. Additionally, it is occasionally illegal or unsafe to operate a full-size aircraft in certain areas or below certain altitudes where UAVs may operate with impunity, although the reverse is also true and there are increasing calls for tighter regulation of UAV use (Shelley, 2018). All these factors combine to render conventional aircraft impractical to use for small scale surveys or for projects with limited budgets. UAVs are far more cost-effective than manned aircraft as after an initial purchase the UAV is reusable *ad infinitum* at no extra cost to the user beyond occasional maintenance and requires no fuel (at least in the case of smaller, battery-powered models) or specialist training to operate.

The use of UAVs as rapid, low-impact alternatives to ground surveys is a theme echoed in a number of papers, including Bollard-Breen, Brooks & Jones (2015), Chabot & Bird (2011), Johnson-Roberson, Murphy & Bongiorno (2013) and Anderson & Gaston (2013). All these studies cite advantages: such as the ability to easily access regions that are difficult for researchers to access on foot; providing very-high resolution images at low altitude, thus improving the researcher's ability to detect objects on the ground and the increasing affordability of UAV systems making aerial surveys more accessible to the scientific community. Commonly noted disadvantages include limited flight time and payload, vulnerability to inclement weather conditions, and poor image resolution at higher altitudes.

A further limitation of UAVs is related to the range of available sensors that may be employed. Whilst multi- and hyper-spectral sensors, as well as LiDAR sensors, are increasingly available and affordable, they remain considerably more expensive and offer poorer spatial resolution in comparison to RGB-only cameras that often come pre-equipped on most off-the-shelf UAVs. As well as this, many off-the-shelf UAVs are not capable of being fitted with additional sensors without undergoing significant modification. Consequently, research projects with a limited budget must be designed to make the most of high-resolution true-colour imagery. In order to do this, it is necessary to employ image analysis algorithms that can account for the textural and spatial characteristics of objects present in the images, as well as their spectral properties. The umbrella term for this category of image analysis methods is 'Object-Based Image Analysis' (OBIA), which will be discussed in detail in section 2.4.3.

Some comparable studies to this project include Pande-Chhetri, Abd-Elrahman, Liu, Morton, & Wilhelm (2017) who used RGB aerial imagery captured via UAV in combination with OBIA techniques to detect invasive weeds in a wetland area in southern Florida and compared the accuracy of object- and pixel-based methods for the same purpose. They found that OBIA consistently outperformed pixel-based approaches, with a peak classification accuracy of 70%, but required considerably more

work on the part of the user to adjust the parameters of the classification and refining the classified image to achieve the best possible results, a process which required specialist knowledge of the vegetation present – a quality which may not always be possessed by the surveyor. In 2015, Peña *et al.* evaluated a range of visible-light and multispectral cameras fitted to a UAV to detect weed seedlings based on the unique physical and spectral properties of the weed plants in contrast to their surrounds. They found that up to ~91% of the weed population in their study area could be detected through this method, which allowed for better targeting of weed eradication programs, thus removing the need to spray wide swathes of area with herbicide. Lechner, Fletcher, Johansen, & Erskine, (2012) also used a UAV to gather both visible-light and multispectral imagery with which to perform surface cover classification of swampland areas in the Blue Mountains of Australia. They noted that one of the primary difficulties was distinguishing between vegetation types where there was a lack of spectral contrast between classes.

## **2.2 New Zealand's Wetlands**

Wetland ecosystems occur on the borders of terrestrial and aquatic ecosystems, at the point where land and water overlap. As a result, wetlands are characterised by areas of permanent water, as well as areas that are frequently inundated. The variable water levels require that any plants that become established within the wetland must have a high tolerance for waterlogged soil, or be able to quickly re-colonise areas of dry land exposed as water withdraws.

Wetlands provide a number of important ecosystem services, including water purification, floodwater management and habitat provision. Despite this, it is estimated that less than 10% of New Zealand's wetlands remain (Ausseil, et al., 2008). Of that 10%, much of what remains exists in a highly altered state owing to clearance by fire following Māori settlement, and later by logging, further land clearances and the introduction of various weeds following the arrival of European settlers (Ausseil, et al., 2008). Many wetlands were drained and cleared following European settlement in order to use the land for agriculture or urban development and they remain highly susceptible to harm caused by human activity (Hansford, 2010). The ecological importance of wetland areas is reflected in the Resource Management Act (1991) in which wetlands are identified as high priority for protection and preservation. Consequently, maintaining accurate inventories of existing wetlands is critical to preventing further loss and conserving the remaining wetlands for the ecosystem services they provide.

As well as biological services, wetlands also represent areas of special social and cultural value to different groups. For Māori, wetlands have historically been vital sources of traditional foods and plant materials for use in construction and weaving. Tourists, nature-lovers and hunters are drawn to wetlands by the diversity of birdlife, the environment's natural aesthetic and the recreational

opportunities found within, which can also provide secondary economic benefits at a local scale via these persons patronising local businesses, paying for hunting licences, and so on.

## **2.3 Wetland Vegetation Mapping**

Combinations of aerial and satellite imagery are commonplace tools for wetland mapping at varying scales. Satellite mapping is usually used for mapping larger areas, and a single image can be used to classify an entire wetland system. This, combined with the frequency with which satellites can repeatedly cover a study area and the quantity of archival data available have played to the advantage of a number of mapping projects (Ozesmi & Bauer, 2002).

However, owing to the comparatively poor spatial resolution offered by satellite images most studies are often limited to rough classifications using generic surface types (Ruwaimana, et al., 2018). Species-specific classification of vegetation may become prohibitively difficult in such cases as the available spectral information is too limited to differentiate between species that occur in close proximity to one another, or that have too small a spatial footprint to be easily detected in imagery with a lower spatial resolution. Imagery gathered by aircraft allows for more detailed mapping and classification, but at the cost of reduced coverage area. Imagery gathered by UAV is often used when the highest possible level of precision is desired or in cases where smaller study areas are involved, as the limited flight endurance of most commercially-available models of UAV limits their range to strictly small-scale surveys of areas of a few dozen hectares (Anderson & Gaston, 2013).

### **2.3.1 Ancillary Data Sources – Digital Surface Models**

Wetland mapping projects often employ a range of remote sensing products in addition to true-colour imagery. Topographic data can be derived from several sources, including LiDAR, radar topographic mapping or stereo-photogrammetry and is commonly employed in conjunction with aerial photography (Li & Chen, 2005; Waser, et al., 2008; Kim, Madden, & Xu, 2010). Topographic data is usually represented in the form of Digital Elevation or Surface Models (DEM/DSM). These should not be confused for one another as they are used to represent elevation in different ways. DEMs represent a 'bare earth' raster grid, showing only the elevation of the ground, with features such as trees and building filtered out. A DSM does not filter out such features, so can represent both the height of an object above ground level and the elevation of ground level itself.

The use of digital surface models allows objects in an otherwise two-dimensional image to be given additional contextual characteristics that can distinguish them from their surroundings, which can be particularly useful where such objects might be otherwise indistinguishable from terrain when only considering spectral information. Typical applications include detecting tree stumps (Goldbergs, Maier, Levick, & Edwards, 2018), estimating forest structure (Mahlangu, et al., 2018), measuring

above-ground biomass (Lin, Wang, Ma, & Lin, 2018) and differentiating between mangrove species based on their comparative size (Cao, et al., 2018).

Approaches that include digital surface models for similar applications to those described here tend to have much higher levels of classification accuracy than those drawing solely on spectral information. For instance, Li & Chen (2005) tested a method of mapping wetlands that incorporated optical imagery from Landsat 7, SAR imagery and DEMs and found that their method correctly identified their target classes at a rate that varied between 71% and 92% depending on the class. This rate dropped to between 24% and 89% when employing only true-colour imagery. However, Campbell and Whyne (2011) noted in a review of image classification methods that the inclusion of a DSM does not always result in an improvement in classification accuracy. Puzinas (2017) found that including a DSM to aid land cover classifications actually decreased accuracy by around 2%, but their approach to selecting training data may have been the source of this reduction, rather than the DSM itself.

### **2.3.2 Ancillary Data Sources – Multispectral Imagery**

Multi- and hyperspectral data is increasingly available from earth observation satellites and from miniaturised sensors that may be fitted to aircraft or UAVs. The distinction between the two types lies in the number and width of discrete wavelength bands in the electromagnetic spectrum that a sensor may detect – the ‘spectral resolution’. Multispectral sensors can generally detect three to ten bands, which may include both visible and non-visible wavelengths. Common multispectral products include a range of infrared imagery, including Near Infrared (NIR) and Red Edge (RE), Thermal Infrared (TIRS). By contrast, hyperspectral sensors, such as NASA’s Airborne Visible / Infrared Imaging Spectrometer (AVIRIS) may detect in the region of two hundred discrete bands - AVIRIS detects 224.

The use of multi- and hyperspectral sensor allows for the spectral reflectance in the non-visible range to be leveraged to improve the accuracy of image classifications (Berhane, et al., 2018). The higher spectral resolution of these sensors allows them to distinguish between different surface types that appear alike to the eye, but feature different levels of reflectance in a non-visible wavelength. This is advantageous when mapping land cover types with high levels of heterogeneity in terms of the number of types present, but low levels of separation between types in the visible spectrum. This additional discriminatory power has resulted in the increasingly widespread adoption of beyond-visible spectrum imagery for wetland mapping. (Hirano, Madden, & Welch, 2003; Berhane, et al., 2018; Ramsey & Laine, 1997).

While this class of sensors are far more versatile than optical sensors, they are often limited by poor spatial resolution and increase the complexity of the procedures required for image processing

(Hirano, Madden, & Welch, 2003). However, the loss of spatial resolution in aerial multispectral imagery can be made up for by reducing the altitude of capture, so a multispectral sensor fitted to a low-flying UAV can acquire much more nuanced imagery than a space-based sensor or one mounted to a full-size aircraft (Ruwaimana, et al., 2018).

## **2.4 Image Classification Techniques**

Image classification refers to the practice of grouping collections of pixels in a reference image into several 'classes', based on the application of statistical or logical decision rules (Kavzoglu, 2017). In the context of remote sensing, this is done in order to convert the reference image into a thematic raster map of different types of land use or cover which may be drawn on for quantitative measurements of the spatial coverage of a given class, or changes in land cover over time. Image classification comes in a number of forms, from manual interpretation and digitisation of features to automatic 'unsupervised' classifications.

### **2.4.1 Manual Interpretation & Digitisation**

Visual interpretation of remotely sensed imagery is still a viable technique and remains in common use within aerial mapping projects. The practice is highly reliant on the interpreter being familiar enough with the types of vegetation present to reliably identify them in the photograph and also requires them to make consistent decisions based on their interpretation of the characteristics of objects visible in the image. To improve the consistency of their decisions, researchers may create a decision tree to inform their choice of classification. Characteristics that typically inform classification include shade (colour), texture, size, shape and position relative to other objects (Avery & Berlin, 1992). Though manual interpretation has been found to be more accurate than automated classification processes (Morgan, Gergel, & Coops, 2010), it also requires a greater investment of time and a greater level of skill on the part of the researcher to accurately trace the borders of features representing a given class (Wulder, 1998). As a result, the trend within the remote sensing community has been to increase the use of fully or partially automated pixel and object-based image classification techniques.

### **2.4.2 Pixel-Based Classification**

Prior to the advent of object-based classification methods, remote sensing was primarily conducted using either supervised or un-supervised forms of pixel-based classification. In both forms, the classification algorithm considers the spectral properties of each pixel in the image and assigns the pixel to a class based on these.

Unsupervised classifications will group pixels by dividing the range of spectral values present in the entire image into a defined number of classes and then assigning every pixel to the class it most closely matches. This method is a 'quick and dirty' form of classification that typically produces results that lack the level of detail present in supervised classifications but is much faster to process as it eliminates the need to devote time to creating training datasets for the classification algorithm. As such, it is most commonly used for initial exploratory analyses (Blaschke, 2010).

Supervised classifications differ as they sort pixels into classes which are based on the properties of groups of pixels identified by the user as being typical examples of the type of surface they represent, known as 'training data'. This allows the classifier to be tailored to identify certain types of surface while ignoring others. Supervised methods are generally preferred in situations where a greater degree of accuracy is desired, and the extra time taken to create the training data is not a limitation.

### **2.4.3 Object-Based Classification**

Object-based image analysis (OBIA) differs from other methods of classification as rather than classifying each individual pixel in the image based on the pixel's spectral properties, the process looks for contiguous clusters of pixels with similar spectral, spatial and geometric characteristics according to user-defined rules (Dronova, Gong, & Wang, 2011). These clusters are then presented as individual 'objects', segmenting the raster image into a collection of vector polygons. Following this, the user identifies polygons which serve as examples of the target object in a similar manner to supervised pixel-based classifications.

OBIA has been found to delineate objects more accurately in images with higher spatial resolutions and is consequently well-suited to analysing high-resolution images captured with a low-flying UAV but produces less precise results than from images taken from an aircraft or satellite (Pande-Chhetri, Abd-Elrahman, Liu, Morton, & Wilhelm, 2017). Object-based classification has been successfully used for vegetation mapping in a number of studies that sought to distinguish plant communities. As an example, Lopez-Granados, *et al.* (2016) classified imagery gathered via UAV to distinguish weeds growing in maize fields, allowing for more precise targeted herbicide spraying. The technique has also been proven to be effective in wetland areas with more dynamic relationships between water and plant coverage (Dronova, Gong, & Wang, 2011; Cordeiro & Rossetti, 2015). OBIA avoids the 'salt and pepper' effect that characterises errors in pixel-based methods, in which mis-classified pixels occur within clusters of pixels of a single other class, producing a speckled appearance. Object-based classifications also allows for additional spatial information from other sources to be included as ancillary data. For instance, a digital surface model can be included to help distinguish between trees and ground cover or small bushes of similar colour or texture.

## 2.5 Change Detection

A common method for providing a quantitative measurement of change in land cover over time is to conduct pixel-by-pixel comparisons of classified imagery, with one classified image correlating to one time period (Lu, Mausel, Brondizio, & Moran, 2005). Post-Classification comparisons allow the researcher to observe changes from one class into another, which means it is well suited to tracking change in variables that are not well represented by numerical values, such as changes in NDVI score (Inzamul & Basak, 2017). This method of change detection has been used in numerous studies to detect change over a range of periods, with some relevant examples being Munyati (2000) who used this to monitor the change in a Zambian floodplain over a 10-year period with a view to relating the observed changes to a period of reduced rainfall and increasing water abstraction and Laine & Ramsey (1997), who compared the condition of a coastal wetland following a hurricane to its condition prior to the weather event.

It is also possible to conduct change detection by manually interpreting the pre- or post-classification image for changes. While this method is less able to produce quantified results and is more dependant on the skills and knowledge of the user, visual interpretation has its own advantages such as being being able to compare multiple images at once, or leveraging those skills and knowledge to interpret textural or spatial differences that a machine-driven interpretation might miss (Bhatt, 2019).

Consequently, the manual method of change detection is still considered a valid method in spite of the array of digital means in common use. Mas and González (2015) applied manual interpretation techniques to improve the accuracy of land cover change detection in the state of Michoacán, Mexico. In this instance, manual interpretation was used as the arbiter in cases where their machine-driven methods for change detection produced uncertain results and to perform accuracy assessment of the final maps. Panigrahy *et al* (2010) also used visual interpretation in the absence of any machine-driven methods to monitor deforestation in western India. Manual methods are also useful in situations when the desired change variable is not well represented by spectral variables or changes in land cover, as demonstrated by Yamazaki, Yano and Matsuoka (2005), who compared satellite imagery to assess damage to buildings following the 2003 earthquake in Bam, Iran.

# Chapter 3

## Methodology

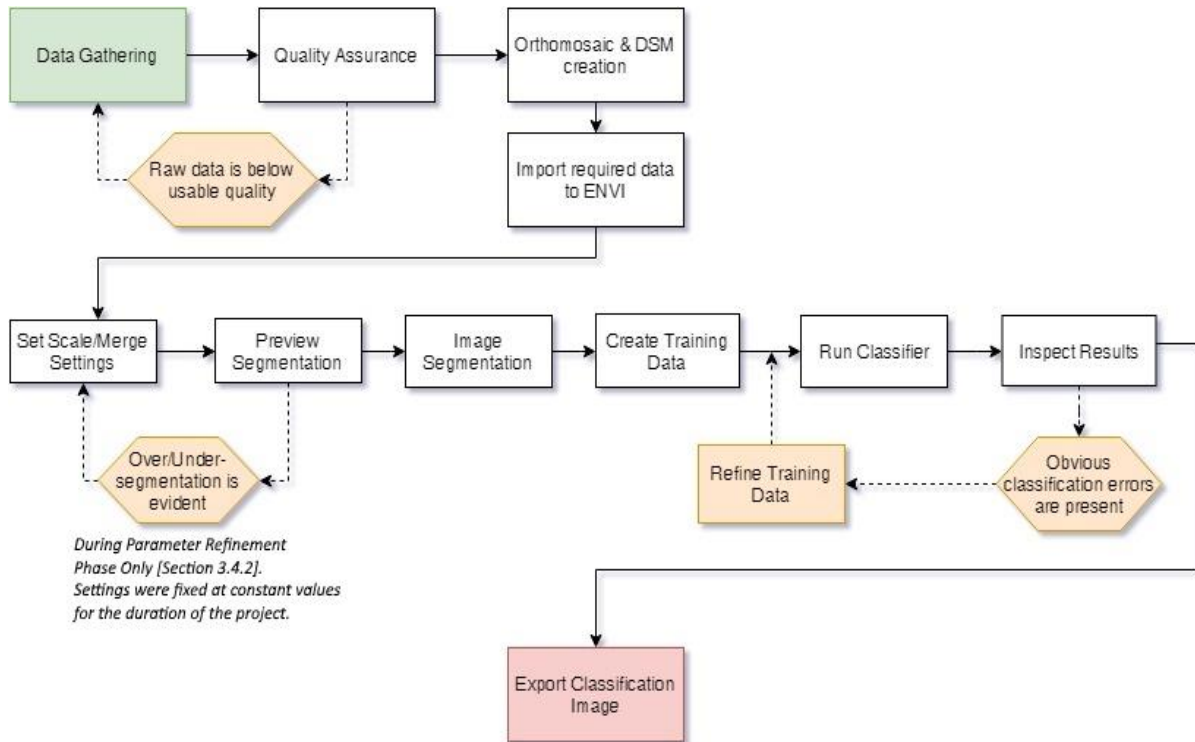


**Figure 2: Image Capture, Processing and Classification Process Diagram**

### 3.1 Study Area

This project focused on three out of four monitored subsections in the Wairio wetland, which are referred by those involved with the restoration process as ‘stages’, the borders of which are indicated in figure 3 below. Restoration efforts have been concentrated in these areas; thus, they were thought to be of more scientific interest and would be easier to use to validate the process used to capture and classify imagery. Each stage presents a unique combination of open water and land as well as distinct patterns of vegetation, therefore, consistent results across each stage will suggest the process employed in this project will be valid not just at Wairio, but also at similar wetlands nationwide.



**Figure 3: Outline of the four stages of the Wairio Wetland (Imagery from 2018)**

Stage one (see *fig. 4* below) at the western edge of the wetland has recently been flooded and depending on the current level between 30-50% of the 7.87ha site is now submerged. A number of small islands are scattered around the flooded section, which have been thickly planted with Flax and Toetoe as part of the re-vegetation programme. Raupō is prominent around the water's edge. The western edge of the stage is entirely covered in exotic grasses leftover from the period in which the land was in use as farmland, for instance Tall Fescue (*Lolium (previously Festuca) arundinacea*) and Yorkshire Fog (*Holcus lanatus*) which are also found in abundance in stage three.



**Figure 4: Stage One of the Wairio Wetland Block, imagery Captured by Patrick Hipgrave (June 2018)**

Stage two (*fig. 5*) is the largest of the three surveyed stages, with a total area of 8.25ha. It is approximately 50% aquatic by surface area, with most dry land concentrated in the southern and eastern sections of the site. Most vegetation is limited to ground cover and low shrubs around the stage borders, with occasional clusters of cabbage trees and flax bushes scattered throughout. As of June 2018, a large population of *Bidens frondosa* had become established in the southern part of the stage.



**Figure 5: Stage Two of the Wairio Wetland Block, imagery Captured by Patrick Hipgrave (June 2018)**

Stage three (fig. 6) is mostly terrestrial and covers 5.2ha with a small area of open water. However, much of the northern section of the stage is low-lying and often floods following prolonged periods of rain or in wetter seasons. The re-planting operations have produced several very tight clusters of Manuka (*Leptospermum scoparium*), Konunu (*Pittosporum tenuifolium*), Cabbage trees, Flax and Toetoe. Sedges (*Carex geminata* being the most common) are also present in moderate quantities and several patches of *Bidens frondosa* and Blackberry bushes are distributed around the stage. A few Kahikatea and Totara trees dating to the pre-settlement forest can be found here. Other rarer plants include *Coprosma robusta*, and *C. propinqua* and *Olearia virgata* which were planted as a part of the restoration programme.

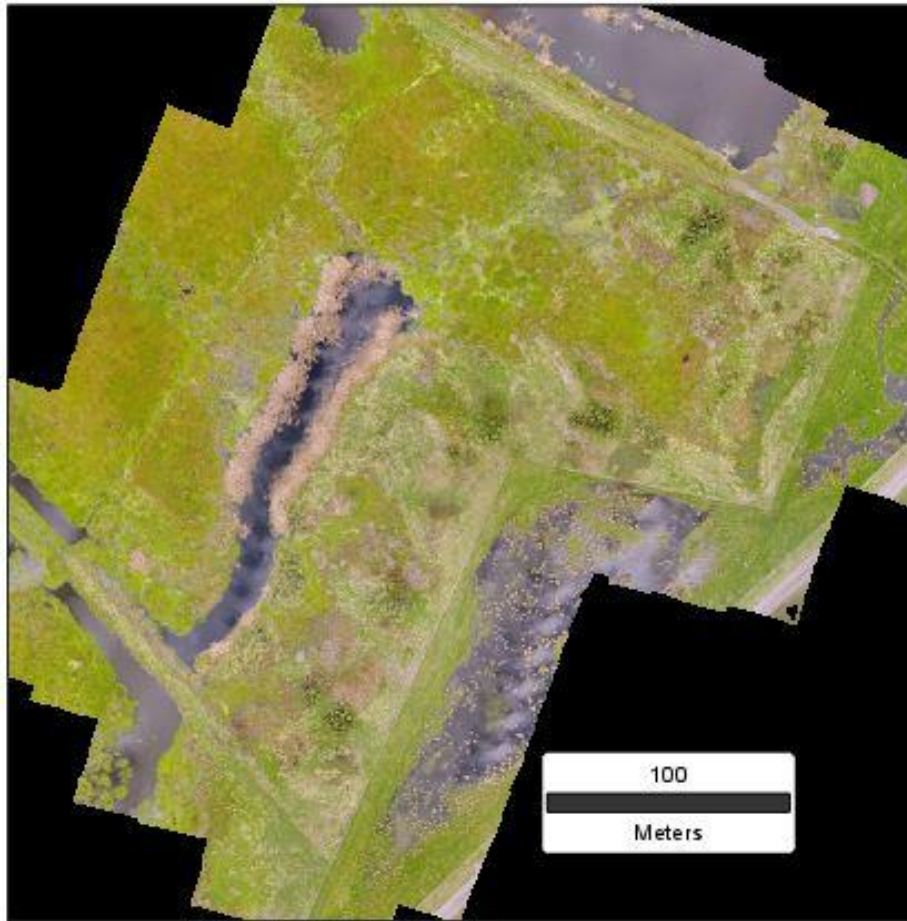


**Figure 6: Stage Three of the Wairio Wetland Block, imagery Captured by Patrick Hipgrave (June 2018)**

Stage four was not studied, as with an area of approximately 30 hectares it was too large to conduct UAV operations over without having several observers present to monitor the craft, as is mandated by Civil Aviation regulations (Civil Aviation Authority of New Zealand, 2018). To assess the feasibility of mapping a comparatively large area compared to the other stages, a trial flight over this stage was completed in June 2018. For this flight, an additional observer in radio contact with the UAV operator was present in order to fulfil the CAA requirement for constant line-of-sight contact with the UAV.

During this flight, it was proved that a single observer could not maintain visual contact with the drone as due to the layout of the stage, the UAV would occasionally be obscured by trees or up to a kilometre away from the operator – well out of visual range. While the UAV could complete the flight with the available number of batteries<sup>2</sup>, several safety issues were noted regarding operating a UAV beyond line-of-sight. The common factor in these issues was the method of communication between observer and pilot. With the UAV out of sight, the pilot is reliant on the observer for notification of

---

<sup>2</sup> Approximately 2 and a half batteries were requiring to complete the flight, which lasted approximately 50 minutes, including the time needed to land the UAV and swap used batteries for fresh ones.

hazards posed to the UAV, or problems with the UAV itself<sup>3</sup>. This means there is an additional delay in the pilot's ability to react in emergency situations posed by the need to wait for the observer to become aware of the hazard and contact the pilot. Given that a delay of only a second could make the difference between a crash and a successful evasion, this communication lag is undesirable. Moreover, there must be a clear method of communicating instructions to the pilot when they are flying blind. For instance, the command 'fly left' could be interpreted in at least three ways: left relative to the observer, relative to the UAV's current heading, or relative to the pilot. With two out of three interpretations being potentially dangerous, it is clear that beyond line-of-sight operations are not advisable for teams of operators and observers with little previous experience.

Given this safety issue, and conscious of the fact that the UAV was not my property to risk, I opted to eliminate the potential for accidents by not pursuing further flights over stage four. This decision did not hinder the project's aims, as the three remaining stages would still provide me with sufficient data to achieve my research aims.

### **3.2 Survey Flights**

Survey flights were conducted between June 2018 and March 2019. To facilitate gathering imagery to represent seasonal change, flights were conducted in June, September, January, and March.

True-Colour Imagery was captured using a DJI Phantom 4, a small quadrotor-type UAV. The Phantom 4 has an integrated 20-megapixel camera mounted on a ventral gimbal for stability and which, when flown at a height of 50 metres above ground level produces imagery with an average ground sampling distance of 1.96 centimetres per pixel. Using a quadrotor UAV is advantageous in a wetland environment as the UAV's ability to take off and land vertically<sup>4</sup> allows it to be operated safely even when open, flat terrain suitable for use as a landing site is scarce. A further advantage afforded by the UAV's small frame and VTOL capability is that it may be carried directly to the area to be flown over and launched onsite, thus conserving battery power, and reducing time in the air. However, quadrotor UAVs have a lower endurance range than fixed-wing types owing to their lower flight speed and inability to glide, thus the Phantom's endurance of 20-25 minutes per battery meant it was only possible to survey one of the wetland stages per flight and a limited number of batteries permitted no more than one hour of flight time per day – in effect, three survey flights over any of stages one, two and three.

---

<sup>3</sup> For instance, changes in pitch of the rotor noise implying an issue with the UAV's motor and/or rotors, or the UAV clearly struggling to fly against the wind.

<sup>4</sup> Commonly referred to as 'VTOL Capability' in aviation parlance.

To capture the imagery, the UAV was flown in a 'lawnmower' pattern at a constant height of 50 metres above ground level, this height was chosen in order to achieve a target resolution of 2 centimetres per pixel or better. Increasing the resolution beyond this point would have been prohibitive as it would have exponentially increased flight time, file size and processing time required in exchange for no significant improvement in the final product. Imagery was captured at intervals to achieve 80% forward and lateral overlap between images. This level of overlap exceeds the minimum necessary amounts to produce an orthomosaic<sup>5</sup> by a considerable degree, but was deemed desirable to facilitate more accurate mosaicking of the captured images into a single orthomosaic by increasing the number of tie points between adjacent images, which in turn improves the resolution of the mosaic and the accuracy of the digital surface model produced from the images.

Rather than manually flying the UAV, the aircraft's flight path was plotted using DroneDeploy - an autopilot application which autonomously controls the UAV's course and operates the camera independently of the UAV operator. This method keeps the flight altitude and the overlap between images constant as well as to optimise the aircraft's flight path to make the most of the limited battery capacity. Manual operation would have resulted in a greater risk of inconsistent overlap between images, making stitching the images harder, possibly causing distortion or reduced resolution in areas of the orthomosaic, or even gaps where no imagery was captured. One flight plan was created for each of the three stages and each plan was designed to capture not only the target stage but enough area outside the stage boundaries to act as a buffer against edge distortion in the resulting mosaic.

For the purposes of maintaining consistency between image datasets, all flights were conducted in an identical fashion, using the same flight plan and camera overlap settings. All flights were captured as close to solar noon – the time at which the sun is highest in the sky - as was practical, in order to increase the level of illumination of the terrain and reduce the appearance of shadows in the image as much as possible. An acceptable bracket of time for image capture was deemed to be within one hour before or after solar noon, except on overcast days where the appearance of shadows was much reduced.

The weather played a significant role in constraining the UAV's deployment. Because the UAV must fly in precise lines and at a low speed (10-15m/s), wind speeds equal to or greater than this could have the potential to blow the UAV off course. While the UAV can automatically adjust for occasional gusts, or constant wind speeds slower than its own velocity, it cannot compensate for constant winds above about 20 m/s and according to the manufacturer's guidelines, should not be flown under those conditions. Additionally, the UAV cannot operate in the rain, though very light drizzle -

---

<sup>5</sup> PrecisionMapper recommends at least 70% overlap (PrecisionMapper Support, 2018)

'spitting' to use a colloquial descriptor - is safe. Therefore, wind and rain forced the postponement of a few flights in spring and autumn. The optimal conditions for flight are therefore a partly cloudy or overcast day, with no precipitation and calm winds, ideally less than 5 m/s.

Every time a flight over a given area was conducted, the flight path used was identical to that used on the initial flight over the area being photographed, covering the same track in the same direction each time, thus ensuring that all objects in the survey area were photographed from the same perspective each time. While it is possible that small amounts of variation in flight path and altitude between flights may have been introduced by imprecision in the UAV's onboard GPS receiver<sup>6</sup>, this level of variance is low enough that it is unlikely that this would have any noticeable effect on the images.

The procedure for a typical survey flight is described below:

#### ***Pre-Flight Checks***

- Once on location, position UAV on flat ground that is suitable for use as a take-off/landing point.
- Insert battery and check charge level is sufficient for the planned flight.
- Check propellers are securely attached, the gimbal clamp is removed, and the memory card is inserted correctly. Finally, check the lens of the camera is free of any dirt and is undamaged.

#### ***Start Up***

- Power up the UAV and remote controller. Ensure the remote is set to 'P' (positioning) mode. Connect the mobile device to the controller via USB cable.
- Using the UAV's default interface app, check the internal compasses and gyroscopes are calibrated correctly and do not show any errors. If necessary, carry out a re-calibration. It is inadvisable to fly if the onboard sensors are displaying errors as this will reduce the accuracy of the aircraft's flight path, or at worst lead to a 'fly-away' error in which the aircraft ceases to respond to control inputs correctly.
- Confirm that 'obstacle avoidance' settings are switched on.
- Close DJI Go to prevent conflicts with DroneDeploy, then open DroneDeploy app. Select the appropriate flight plan and confirm the flight path has loaded correctly.
- Wait for the UAV to warm up and acquire a strong GPS positioning fix.
- Select the mission start option on the mobile app. The UAV will automatically start up, launch, and proceed to the initial point in the flight plan and will then complete the flight autonomously.

---

<sup>6</sup> DJI rates the Phantom 4 Pro's GPS unit's accuracy to within +/- 0.5m vertically, and +/- 1.5m horizontally.

### ***In Flight***

- If the UAV's battery requires changing, the app will detect this and return the UAV to its launch point and land. After changing the battery, relaunch the UAV using the app. The UAV will proceed to the point at which it aborted the survey flight and continue the mission.
- In the event of an emergency, the operator can assume manual control by switching the UAV into 'S' (sport) mode using the remote controller. This overrides the app, which otherwise blocks manual input on the controls.

### ***Landing & Post-Flight***

- The UAV will land automatically on or near the location it was launched from. The precision of the landing is affected by the quality of the UAV's GPS fix. Take manual control if the UAV appears to be descending into a hazardous area.
- On landing, DroneDeploy will shut down the UAV's motors and produce a preview image taken from the survey flight. Check the preview image for distortion or unusual colouring, which would indicate a fault with the camera settings.
- If the flight has completed to the user's satisfaction, shut down the UAV. Remove the rotors and battery and re-attach the gimbal clamp for transport.
- Copy imagery from the memory card to a computer for processing. File storage should be set up to ensure that imagery set from different sites and flights are kept separate and well labelled.

### ***Notes on safety & legal aspects***

New Zealand Civil Aviation legislation, specifically General Operating Rule Part 101 (Civil Aviation Authority of New Zealand, 2018) mandates that all remotely operated aircraft regardless of size are subject to the rules of the air, thus it is not always possible to operate a UAV in the manner or location desired without seeking authorisation from one or more external parties. Depending on the category of the airspace the flight takes place in, operators may be required to seek permission from local air traffic controllers. Additionally, landowners and local authorities have a right to dictate additional terms and conditions which UAV operators must adhere to in order to fly over their land.

The flights conducted as part of this project were covered under subsection 'E' of Civil Aviation Authority Rule Part 101 which covers lower-risk non-commercial flights. To ensure that the requirements for constant visual contact with the UAV were met, additional observers were brought in to assist in maintaining visual contact with the UAV. Since Lake Wairarapa is outside controlled airspace it was not necessary to notify aviation authorities about the flights, but for safety's sake a

notification was posted on Airshare<sup>7</sup> to warn any other aircraft that might happen to be operating in the same area. DOC requires that anyone wishing to operate a UAV over any area of conservation land apply for a permit and submit a risk assessment for their proposed flight. In this case my project was able to be conducted in accordance with a standing permit held by Victoria University of Wellington and so required no additional permission other than notifying the local DOC office of my intent to fly.

### 3.2.1 Multispectral Imagery Collection

In April 2019, a multispectral camera was made available to me and it became possible to pursue the use of multispectral data – specifically Near Infrared and Red Edge imagery. Whilst time constraints meant that only a single round of flights could be conducted, it was still desirable to pursue investigation into how classification accuracy might improve with the application of different combinations of ancillary data other than a DSM. Of particular interest was whether accuracy could be improved to greater levels than those achieved with data extracted from an ‘off-the-shelf’ camera, or whether the additional spectral resolution of the multispectral camera could compensate for the camera’s lower spatial resolution.

In general terms, the methodology for these flights remained the same as before, with a few minor differences to account for the different equipment used. These flights were conducted with a DJI Matrice 200 quadcopter, as the Phantom is not able to carry third-party cameras. The camera used was a Micasense RedEdge-M, which features a set of five imagers to gather red, green, blue, NIR and RE wavelengths independently.

<b>Band Number:</b>	<b>Band Name:</b>	<b>Centre Wavelength (nm)</b>	<b>Bandwidth FWHM (nm)</b>
<b>1</b>	Blue	475	20
<b>2</b>	Green	560	20
<b>3</b>	Red	668	10
<b>4</b>	Near IR	840	40
<b>5</b>	Red Edge	717	10

*RedEdge-M Image Bands (MicaSense Inc, 2017)*

These flights required the additional purchase and installation of a custom-designed mounting kit to fit the camera to the UAV as the RedEdge cannot be fitted directly to the Matrice’s gimbal mount. Part of the modifications required additional internal electrics to the UAV to power the camera from the UAV’s battery, which appeared to have the side-effect of reducing the flight endurance of the Matrice from around 30 minutes to 20 or less. Since the RedEdge camera has a narrower field of view

---

<sup>7</sup> A website operated by Airways NZ which allows UAV operators to register flights with the national air traffic control agency.

and cannot capture photos as quickly as the Phantom's camera the altitude of the flights was increased to 60 meters in order to maintain the 80% forward and side overlap used in the regular flights. This produced a spatial resolution of approximately 4cm/pixel. Processing the images followed the same methods outlined below.

### **3.3 Image Processing – Mosaic & Surface Model Generation**

The collected images from each flight over each stage were stitched into a single large image using PrecisionMapper, a cloud-based mapping and analytic service<sup>8</sup>. There were no processing options or parameters to specify, which has the advantage of limiting the potential for unintentional inconsistencies in the way the images are stitched. Each image has associated metadata detailing the UAV's height, spatial coordinates and camera angle added to its metadata automatically upon capture which PrecisionMapper extracts and uses to overlay each image correctly. The process then blends the images together along the overlapping areas, creating a single colour-corrected image.

PrecisionMapper also uses the raw images to create a digital surface model from the image. This is done by comparing the perspective difference between two overlapping images to establish the height of the object, a process known as stereophotogrammetry. This process creates a three-dimensional point cloud which in turn is used to generate a digital surface model (DSM). The accuracy of this process is significantly improved by having high levels of overlap between images as this increases the number of reference points the program can detect and compare between images, which in turn allows for a larger point cloud and a more nuanced representation of elevation in the DSM. PrecisionMapper allows for the DSM to be downloaded as an independent dataset from the orthomosaic, which is not a common feature of free online orthomosaic processing tools. The DSM created from each set of imagery was downloaded alongside the orthomosaic.

Creation of the DSM is a necessary step in proper orthomosaic creation and is not a peculiarity of PrecisionMapper. The DSM is used to 'orthorectify' the image, removing perspective distortion and so making sure that objects in the image retain their correct proportions and position. While the need to create a DSM can be avoided if the target area is entirely flat, such a situation is surely rare, and certainly not the case in any of the three stages at Wairio.

### **3.4 Image Classification**

All image classification was conducted using Harris Geospatial's ENVI 5.4, which includes an object-based image classification tool as part of the software's 'Feature Extraction' add-on. The object-based classification process is a multi-stage workflow.

---

<sup>8</sup> [www.precisionmapper.com](http://www.precisionmapper.com)

### **3.4.1 Input**

The first stage of the classification workflow was to load all the required data into the program. Specifically, the mosaicked image to be classified and any additional data used to support the segmentation and classification, known as ‘ancillary data’, which is used to give the image segmentation and classification algorithm additional information to work with. For instance, adding the DSM should improve the classifier’s ability to distinguish between low-lying ground cover and larger objects such as bushes or trees which might otherwise be hard to tell apart if they have a similar colouration and texture. Near Infrared imagery is also commonly used for this purpose, as two species that appear similar to the human eye may have very different degrees of spectral reflectance in non-visible element of the electromagnetic spectrum.

The imagery for each stage and season was classified individually and the DSM that was generated in tandem with a particular image and the NIR data (where applicable) were added as ancillary data, except when testing for the difference in classification accuracy caused by the lack of ancillary information. At this point, a processing mask was applied to confine the segmentation and classification algorithms and their outputs to within the border of the stage, as marked by the fence line around the border of each stage.

### **3.4.2 Segmentation**

The second stage of the classification workflow was to segment the image. Segmentation divides the image to be classified into groups of neighbouring pixels that have similar properties, which are known as ‘segments’.

#### *Segmentation Bands*

The segmentation algorithm evaluates only the original image’s spectral bands by default, but can be customised to consider one or more ancillary datasets. For this project, the segmentation band settings were set up so that segmentation would be based on all the bands of every raster dataset included, as shown in table 3.1 below.

**Table 3.1: Band Combinations for Segmentation and Classification**

<b>RGB Only</b>	<b>DSM</b>	<b>Multispectral</b>	<b>All Ancillaries</b>
Red, Green & Blue Bands			
	<b>DSM</b>	<b>Near Infrared</b>	<b>Near Infrared</b>
		<b>Red Edge</b>	<b>Red Edge</b>
			<b>DSM</b>

### *Choice of Algorithm*

ENVI features a choice of only two segmentation algorithms. The first, known as ‘Edge’ is optimised for detecting the edges of features, but relies on these being sufficiently well-defined in whatever imagery the algorithm is applied to. The second algorithm, called ‘Intensity’ is typically used to detect small differences in values such as those that might occur in a single-band image, whether these changes reflect different objects or not. This can lead to situations where multiple different objects in the real world are represented as a single object after segmentation, so the ‘Intensity’ algorithm was deemed unsuitable given the need for precise definition of objects in the image and was not used in accordance with the developer’s recommendations (ITT Visual Information Solutions, 2008).

### *Scale and Merge Settings*

The ‘edge’ algorithm is controlled by two parameters. The ‘scale level’ controls the maximum size of segmented areas of the image, and by extension the number of objects present after the segmentation process. Scale may have a value between 0 and 100, with larger values resulting in fewer objects. Scale should be given a value that prevents both ‘over-segmentation’, which results in a single object being represented by multiple segments and ‘under-segmentation’ where multiple objects are represented by a single segment. In contextual terms, scale must be adjusted so that each segment produced by the algorithm represents only one type of surface cover. After some experimentation, scale was fixed at a constant value of 20 for all iterations of the image classification process. For detail of how this figure was arrived at, see section 3.4.5.

The ‘merge level’ controls the algorithm’s ability to combine neighbouring segments with similar properties into a single segment. Like the scale setting, higher merge levels will reduce the number of individual segments produced, but increases the risk of under-segmentation. Following

experimentation, the merge level was fixed at 50. The scale and merge levels were kept constant so that this project could focus on the consequences of including (or not including) ancillary data during the classification process.

### *Parameter Refinements*

I opted not to investigate the effects that scale, merge, and algorithm settings would have on classification accuracy. Instead, I kept these parameters constant for all iterations of the classification process. To achieve this, it was necessary to determine what combination of parameters would be best suited for the range of situations and classification schema encountered in this project. This was done through a process of assessing previews of the segmentation image which adjusted in real time based on changes made to the segmentation settings. While this is a more subjective method of assessing the best combination of scale and merge factors in contrast to observing the effect of different settings on the final classification accuracy, visual assessment is a widely used method of testing the effects of segmentation settings (Zhang, Fritts, & Goldman, 2008). Moreover, the inherent subjectivity of this method can be overcome when a well-defined set of assessment criteria are in place (Gelasca, Ebrahimi, Farias, Carli, & Mitra, 2004).

I based my assessment of the quality of segmentation on the principles proposed by Haralick and Shapiro (1985), which in their original or adapted forms have become a *de facto* standard (Zhang, Fritts, & Goldman, 2008) specifically:

1. Regions should be uniform and homogeneous with respect to some characteristic(s).
2. Adjacent regions should have significant differences with respect to the characteristic on which they are uniform.
3. Region interiors should be simple and without holes.
4. Boundaries should be simple, not ragged, and be spatially accurate.

To test the settings to find the combination that best fit these criteria, I made use of ENVI's capability to offer the user a preview of the segmentation image as the scale and merge settings are being set. By visually examining the preview images with scale settings of 5, 10, 20, 40 and 60 I was able to gain an impression of what settings would offer the best results for my purposes. I tested the settings on the June imagery for each of the three stages simultaneously, in order to make sure that settings were transferrable between sites, rather than picking a setting that worked well in one location and relying on it being suited to the others.

The coarser scale setting of 60 tended toward under-segmentation with very obvious segments which contained multiple classes, meanwhile the fine scale settings of 5 and 10 typically resulted in

over-segmentation within objects with variable texture or colouration. The intermediate settings of 20 and 40 produced segments that appeared to be the best fit for the detectable objects in each image, with the former occasionally over-segmenting and the latter occasionally under-segmenting.

I opted to proceed with a scale level of 20, reasoning that for the purposes of the study it was better to have the borders between classes correctly delineated at the cost of increased processing time owing to the larger number of segments – offset somewhat by the merge setting - than to risk the chance of two separate surface types being conflated. A larger scale setting would have been viable if it were not for the fact that I needed a high degree of precision from the classification in order to be able to classify vegetation at species level. Coarser scales would have been better suited if more a more generic classification were desired. Once I had fixed on a scale setting, I introduced merge settings to the test. Merge levels were initially set at either 0, 25, 50, 75 and 90. A merge level of 50 proved to offer the best balance between reducing the total number of segments as much as possible whilst not merging segments that represented different classes.

A potential alternative to either manual assessment or assessment based on classification accuracy would have been to create a reference image by manually digitising the visible objects in the aerial photograph and comparing this to the automated segmentation. A manually digitised image would be much more precise than a computer-generated one (Graaf, Koster, Vincken, & Viergever, 1994), but to create such an image would have been enormously time-consuming given the desired level of precision required delineation of individual objects. A typical image classification workflow for this project would take in the region of 3-5 hours, including processing time. By contrast, manually digitising the reference image alone would be the work of several days, even though the survey areas are not large.

Since most of the literature on these subject deals with a range of different software suites, it was not possible to adopt the recommended settings used in other studies. As an example (Pande-Chhetri, Abd-Elrahman, Liu, Morton, & Wilhelm, 2017) describe the effect of scale settings for the segmentation process in some detail, to the point of identifying optimal settings for segmenting objects of different sizes, but the software they used (Trimble eCognition) measures 'scale' differently to ENVI as the parameter in their program may be set between 5 and 300 or more, while ENVI only permits a range of 1-100. This difference in the way software suites treat parameters with identical names and functions - but different programming of the underlying algorithm renders it unlikely that Pande-Chhetri *et al's* observation that a scale level of 40 was best for segmenting mixed communities of vegetation not dissimilar to those present in the Wairio study site would be directly applicable to ENVI's scale setting. It was therefore necessary to 'test and adjust' the classification workflow to establish a consistent set of parameters for future use.

### 3.4.3 Creating Training Data

Once the segmentation process was completed, a set of segments were manually classified in order to create a set of training data. Training sites were selected according to the following criteria:

1. Sites should be evenly distributed around the image, where the distribution of the relevant class allows this.
2. A minimum of five, but usually around 10 or more distinct sites was used for all classes. The number of segments this would represent would vary depending on the class<sup>9</sup>.
3. Training sites were at a minimum the size of the object they were intended to represent, for instance the whole head of a Cabbage Tree and all the segments it contained.
4. Where a distinct object was not visible (e.g. grasses), training sites included all segments within a minimum area of approximately 5m<sup>2</sup>.
5. The training sites should be representative of the majority of examples of that class.
6. If intra-class variability is high enough (see the example below) create subclasses to represent the different expressions of each class.

Training datasets needed to be redefined with each change in season as land cover changes in the wetland meant that data from a previous season might not be applicable to the current time. For instance, certain vegetation types would have gone dormant (as was the case for *bidens*) or been replaced by (or would have replaced) water as water levels rose and fell.

Table 3.2 below sets out each class, with a brief description of what it represents, along with when and where it was observed.

**Table 3.2: List of Classes**

<b>Class Name</b>	<b>Represents:</b>	<b>Observed:</b>	<b>When Evident:</b>
<b>Water</b>	All open water.	All stages	Constant
<b>Mixed Grasses</b>	Various exotic grass species that are too similar to distinguish.	All stages	Constant
<b>Brown Grass</b>	Exotic grasses, possibly in poor health that are distinctively brown in colouration	All stages	Winter & Spring

---

<sup>9</sup> Very homogenous classes like 'Water' and 'Azolla' tended towards fewer, larger segments, and around 20 segments in total would be used as training sites. Classes broken into smaller segments were represented by several hundred segments, but the training sites for these classes would cover roughly equivalent areas to the sites with larger segments

<b>Isolepis</b>	<i>Isolepis sp.</i>	All stages	Constant
<b>Yellow Isolepis</b>	<i>Isolepis sp.</i> that exhibits a distinctive yellow coloration.	Stage 1	Spring
<b>Reeds</b>	Raupō ( <i>Typha orientalis</i> )	All stages	Constant
<b>Rush</b>	Assorted <i>Juncus</i> species	All stages	Constant
<b>Sedge</b>	Various <i>Carex</i> species, primarily <i>C. geminata</i>	All stages	Constant
<b>Flax</b>	Flax/Harakeke ( <i>Phormium tenax</i> )	All stages	Constant
<b>Toetoe</b>	Toetoe ( <i>Austroderia toetoe</i> )	Stages 1 & 3	Constant
<b>Cabbage Tree</b>	Cabbage Tree/Ti kouka ( <i>Cordyline australis</i> )	All stages	Constant
<b>Manuka</b>	Manuka ( <i>Leptospermum scoparium</i> )	All stages	Constant
<b>Kahikatea</b>	Kahikatea or other tree significantly larger than the average in each stage.	All stages	Constant
<b>Other Tree 1</b>	Generic class - tree species with dark green colouration ( <i>Coprosma spp. etc</i> )	All stages	Constant
<b>Other Tree 2</b>	Generic class - tree species with brown colouration	All stages	Constant
<b>Other Tree 3</b>	Generic class - tree species with light green colouration. ( <i>Kowhai, Pittosporum etc</i> )	Stages 1,3	Constant
<b>Azolla</b>	Red Azolla ( <i>Azolla rubra</i> )	All stages	Spring – Summer
<b>Green Algae</b>	Unidentified water plant characterised by very light green colour, usually found on the water's surface at the edge of flooded areas	All stages	Winter-Autumn
<b>Mixed Algae</b>	Vegetation covering the surface of an area of water that appears to be a mix of Red Azolla and 'green algae'	Stages 2 & 3	Summer
<b>Yellow Algae</b>	Unidentified yellow water plant	Stage 2	Summer
<b>Blackberry</b>	Blackberry bush ( <i>Rubus sp.</i> )	Stage 1, 3	Constant
<b>Bidens</b>	<i>Bidens frondosa</i>	All stages	Winter & Spring
<b>Dry Bidens</b>	<i>Bidens frondosa</i> – while dormant, has a very distinct white/grey colouration	Stage 2	Spring
<b>Dry Vegetation</b>	Ground cover vegetation that is dead, dry, or dormant, characterised by light yellow to grey/white colouration	All stages	Constant
<b>Dormant Tree</b>	Tree that is either dead or dormant, characterised by grey colouration	All stages	Constant
<b>Waterlogged Grass</b>	Class representing grass or other ground cover that is submerged in, floating on, or emergent through standing water, but still visible above the surface	All stages	Most evident in Spring & Summer
<b>Mud</b>	Sediment exposed by retreating water	All stages	Autumn
<b>Shadow</b>	Area in shadow that is too dark to identify	All stages	Constant

It was found that it was sometimes necessary to have multiple sub-classes representing a single surface type, for instance the appearance of water could vary greatly depending on the water's

depth, turbidity or whether the surface was calm or not. In practice, this meant that several water subclasses would need to be defined as required: common examples included 'brown', 'blue' and 'rippled'.

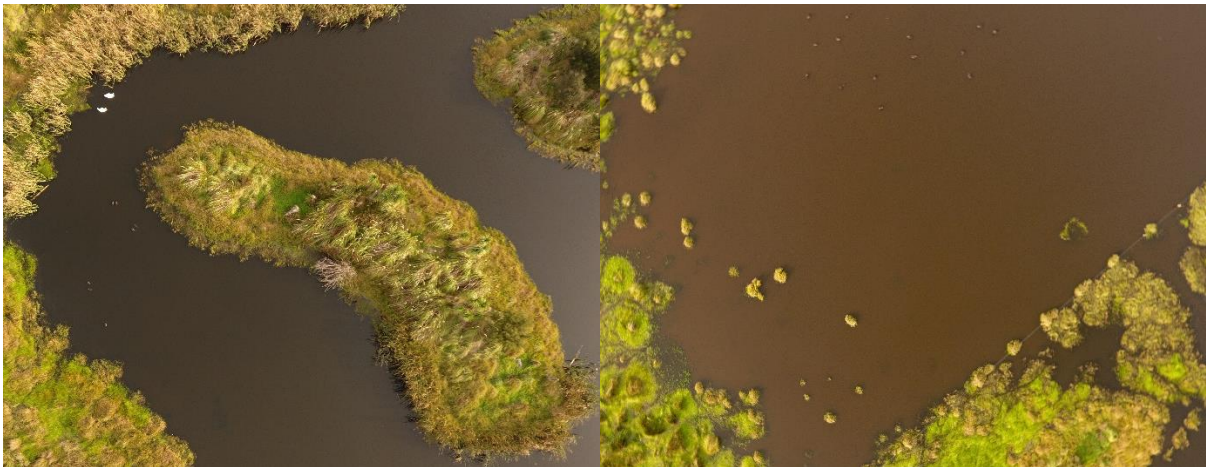


**Figure 7: Comparison of water colouration within a stage**

However, small levels of variation in colour and texture within the examples for a class are acceptable and even desirable as the classification algorithm has a threshold for determining whether a segment belongs to a given class. If the range of possible values that represent a class is narrow, there will be an increased chance that a segment that should be assigned to the target class but has slightly different values than those that fall within the acceptable range will be mis-classified.

### **3.4.4 Object-Based Classification**

#### *Choice of Algorithm & Algorithm Settings*

ENVI offers three choices of classification algorithm, but as the Support Vector Machine (SVM) algorithm has been found in other studies<sup>10</sup> to be a reliably accurate classifier, I opted to proceed using the SVM algorithm for consistency.

#### *Classification Bands*

Similar to the segmentation algorithm, the classification algorithm was set up so as to consider the values of all the available variables, including any ancillary data included in the workflow, as per table 3.1 above.

#### *Attributes*

---

<sup>10</sup> For instance, in Pande-Chhetri *et al* (2017), or Pal & Mather (2005) who found that the SVM algorithm consistently outperformed other algorithms when applied to surface cover classifications of UAV or satellite imagery respectively.

The classification algorithm was set to consider all spectral and textural properties of the segments, as follows:

**Table 3.3: Spectral Properties used for Classification**

<b>Spectral Attribute:</b>	<b>Description:</b>
<b>Spectral Maximum</b>	Maximum value of the pixels comprising the region in each band.
<b>Spectral Minimum</b>	Minimum value of the pixels comprising the region in each band.
<b>Spectral Mean</b>	Average value of the pixels comprising the region in each band.
<b>Spectral Deviation</b>	Standard deviation value of the pixels comprising the region in each band.

**Table 3.4: Textural Properties used for Classification**

<b>Textural Attribute:</b>	<b>Description:</b>
<b>Texture Range</b>	Average data range of the pixels comprising the region inside a kernel of a defined size.
<b>Texture Mean</b>	Average value of the pixels comprising the region inside the kernel.
<b>Texture Variance</b>	Average variance of the pixels comprising the region inside the kernel.
<b>Texture Entropy</b>	Average entropy value of the pixels comprising the region inside the kernel.

### 3.5 Accuracy Assessment

To quantify the effects that ancillary data had on improving classification accuracy, it was necessary to test both the overall and class-specific accuracy of the classifier, with and without ancillary data.

To assess accuracy, I first created my own set of ‘ground-truth’ data with which to judge the classifier’s accuracy. The creation of the reference datasets (described in section 3.5.2) and the accuracy assessment was conducted using ArcGIS Pro 2.1 and is illustrated in figure 8.

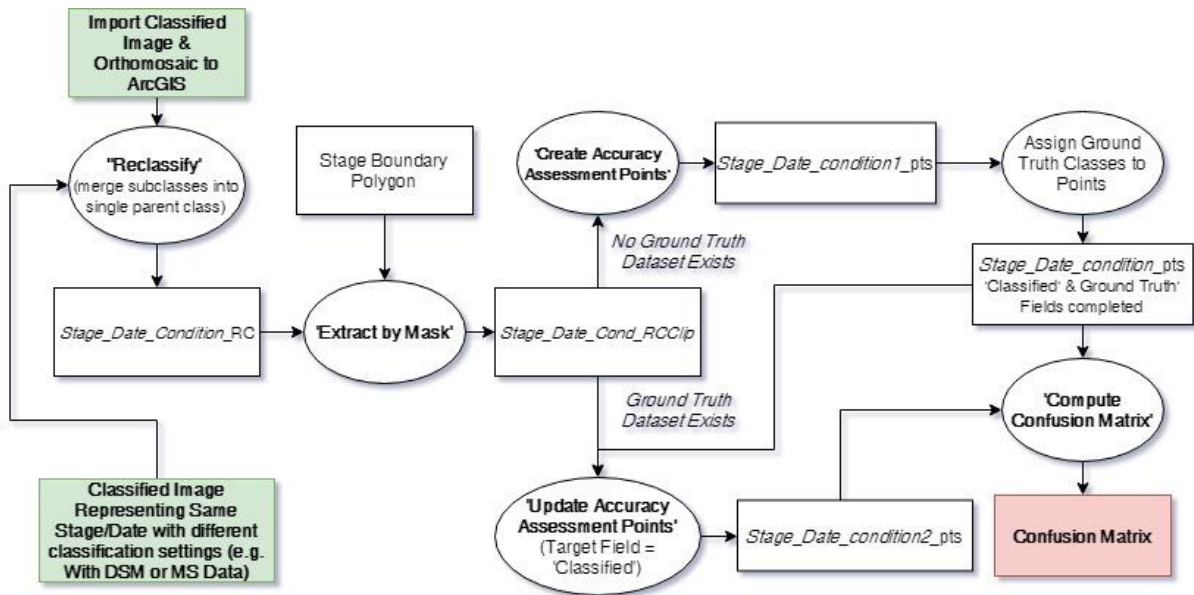


Figure 8: Accuracy Assessment Process Diagram

### 3.5.1 Image Preparation

The classified images produced in ENVI were reclassified in ArcGIS Pro to combine some of the subclasses created in the training stage into a single class. For instance, the Spring classification for stage two included three separate 'Water' classes to account for differences in colour caused by depth or surface reflection, which were combined into a single class for the purposes of assessing accuracy. Reducing the number of classes where possible is desirable as this helps offset the reduction in accuracy inherent in classification schemes with larger numbers of classes. However, subclasses representing the same species that were significantly distinct from one another were left as individual classes. An example of this include the 'Isolepis' & 'Yellow Isolepis' classes, the latter of which is believed to represent Isolepis in either poor health or at a different stage in its growth pattern. A further example is the 'Mixed Grass' & 'Dry Vegetation' classes. While much of the 'Dry Vegetation' class represents dry grass stalks and so could arguably be counted among the mixed grass species, there was enough potential for overlap with other non-grass species to keep them apart.

### 3.5.2 Creating Reference Data for Ground-Truthing

Several methods of creating a reference image were considered. The most precise method would have been to manually digitise the class boundaries from the aerial photographs but this would have been time-consuming and potentially prone to error if the boundaries between classes were insufficiently distinct (Green & Hartley, 2000). Therefore, I opted to use a series of reference points distributed so as to create a stratified random sample of the actual surface cover in each site. Reference data was created for each site individually and was updated with each set of seasonal

imagery to account for changes in surface cover or water levels. The boundaries for the reference data were determined by a shapefile marking the fence boundary of each stage. Keeping all the reference points inside the stage ensured that all the reference points could be assigned a value from the classified images and that their ground truth value would not be that of a type of surface that was not included in the classification process – for instance the gravel paths bordering some of the stages.

To ensure that the reference dataset was suitably comprehensive, each dataset contained at least 1000 points, a figure determined from the general rule of thumb that for each class in the dataset there should be at least 50 points (Lillesand, Kiefer, & Chipman, 2004). Although some classifications included fewer than 20 classes, the minimum was kept at 1000 for consistency.

To keep the allocation of ground truth data consistent in the event that the surface cover was not readily identifiable, I noted the identifying characteristics of each class to use these as a reference. The final decision of which class to apply would be based on which set of traits best matched what was evident in the image. Table 3.5 below lists these in full. However, the 2 cm/pixel resolution of the aerial photographs meant it was possible to determine what type of surface cover to assign to each point quite easily, as even classes with similar characteristics listed below could be easily differentiated. Photos of each class can be found in appendix A.

**Table 3.5: Defining Characteristics of Classes**

<b>Class Name:</b>	<b>Colour</b>	<b>Texture &amp; Appearance</b>	<b>Shape</b>	<b>Size</b>	<b>Position</b>
<b>Mixed Grass</b>	Light to Dark Green	Rough. May grow in obvious tufts	N/A	Low ground cover	Widespread
<b>Brown Grass</b>	Brown	Rough texture, low-lying vegetation in grassed areas	N/A	Small patches	Mixed in with other grasses
<b>Isolepis</b>	Bright Green	Smooth	N/A	Low ground cover	Usually near water or lower-lying areas
<b>Waterlogged Grass</b>	Green or Brown	Rough	N/A	Small	Always in/bordering water
<b>Bidens</b>	Dark brown or grey (when dormant)	Rough. Often forms a clear linear pattern.	N/A	Small	Variable
<b>Dry Bidens</b>	Grey/White	Rough. Often forms a clear linear pattern.	N/A	Small	Variable
<b>Dry Vegetation</b>	Pale yellow to off-white/grey	May be smooth or rough	N/A	Low ground cover	N/A
<b>Reeds</b>	Yellow (Winter/Autumn) or Green (new shoots)	Rough	Long, thin leaves	Small-Medium (~1m high)	Always in/bordering water
<b>Rush</b>	Dark Green	Smooth, grows in small clusters	Round cluster with pointed leaves	Small (<1m high)	Usually near water
<b>Water</b>	Blue (various shades), Black, Brown	Smooth. Ripples may give a rougher appearance. Reflected light/cloud may be visible.	N/A	N/A	N/A

<b>Manuka</b>	Dark, Brown-tinged green	Rough	Roughly circular	Small Tree	Usually in clusters of other trees
<b>Flax</b>	Mid to Dark Green	Rough	Circular plant. Thick, long leaves	Medium sized	Usually grows in clusters
<b>Toetoe</b>	Light Green, appearing grey/white at edges	Rough	Circular plant. Long, thin leaves	Medium Size	In clusters, often near water.
<b>Cabbage Tree</b>	Light Green, occasionally with yellowish accents	Rough	Compact circular heads, (<1m diameter)	Medium-sized tree but typically only the head is visible	No pattern, may be either individual plants or groups in close proximity
<b>Sedge</b>	Dark Green or Brown	Rough	Thin leaves often grow in a regular linear pattern	Small	Grows in patches several meters in diameter. Found on open ground
<b>Kahikatea</b>	Mid- to Dark-green	Rough. Often distinguishable by a large shadow or patches of bare branch	Round	Large. Usually large enough to cast a shadow under certain lighting conditions	Isolated individual plants
<b>Yellow Isolepis</b>	Yellow. Occasional green tint	Smooth	N/A	Low ground cover.	Within or bordering green Isolepis patches
<b>Azolla</b>	Pink or Red	Smooth	N/A	Always on the surface of a body of water.	Always on the surface of a body of water.
<b>Green Algae</b>	Light 'lime' green	Smooth	N/A	Surface cover	Always on the surface of a body of water.
<b>Mixed Algae</b>	Mix of green and red within the same segment	Smooth	N/A	Surface cover	Always on the surface of a body of water.
<b>Yellow Algae</b>	Yellow	Smooth	N/A	Surface cover	Always on the surface of a body of water.
<b>Other Tree 1</b>	Dark Green, variable patterns caused by leaves	Rough, with dark patches representing gaps in leaves	Roughly circular or oval shape	Variable from ~1m high or more. May cast shadow	No pattern, may be individual plants or cluster of several

<b>Other Tree 2</b>	Brown	Rough, with dark patches representing gaps in leaves	Roughly circular or oval shape	Variable from ~1m high or more. May cast shadow	No pattern, may be individual plants or cluster of several
<b>Other Tree 3</b>	Light green	Rough, with darker patches representing gaps in leaves	Roughly circular or oval shape	Variable from ~1m high or more. May cast shadow	No pattern, may be individual plants or cluster of several
<b>Blackberry</b>	Dark Green, may have patches of yellow brown during autumn/winter	Rough, often has a speckled appearance	Variable	Ground cover. Grows in patches of >1m diameter.	N/A
<b>Mud</b>	Grey or light brown. Grey mud occasionally has a blue tinge	Typically smooth. May show rivulet patterns formed by flowing water	N/A	N/A	In locations previously covered by or now bordering water
<b>Shadow</b>	Grey to black. May be tinted the colour of whatever surface type it obscures.	Depending on strength of the shading may be either smooth (completely black) or rough (underlying surface shows through)	Variable	N/A	N/A
<b>Dormant Tree</b>	Grey	Rough. Depending on species, multiple boughs may be visible	Round or elongated oval, depending on perspective	Medium. May cast shadow	Isolated individuals

### 3.5.3 Confusion Matrices

Once each set of reference points was complete, ArcGIS Pro’s image analysis tools were used to add a value representing the surface type as determined by the image classifier at the same point. I then created a confusion matrix to compare my ‘ground truth’ values to the ‘classified’ value, allowing me to determine how often each class was correctly identified and which classes the classification algorithm struggled to distinguish between. The matrix presents class-specific accuracy measurements representing the rate at which each class was correctly assigned in the form of ‘user’s accuracy’ and ‘producer’s accuracy’ (UA and PA), and two measure of the classifications’ total accuracy, ‘overall accuracy’ and ‘Kappa’ (Campbell & Whyhne, 2011).

### 3.5.4 Analysis of Accuracy Results

A linear mixed effects (LME) model was used to test the effect of season and ancillary DSM data on overall accuracy and kappa, using “stage” as a random factor representing spatial replication (equation 1). Analysis of deviance was performed on the fitted model using the “Anova” function of the car package, and type two sum of squares.

$$lme(Accuracy \sim DSM + Season, random = \sim 1 | Stage)$$

(Equation One)

A separate LME model was used to test the main and interactive effects of DSM and infra-red ancillary data in one season, replicated across the three stages. Analysis of deviance was performed on the fitted model with type three sum of squares due to the interaction term in the model (eqn 2)

$$\text{lme}(\text{Accuracy} \sim \text{DSM} * \text{Infrared}, \text{random} = \sim 1 | \text{Stage})$$

(Equation Two)

Models were fitted in the programming language R. The results of the Autumn surveys were treated as a reference point for the effect of season on classification accuracy, therefore they do not appear in the tables of results in chapter four.

To confirm whether the inclusion of the DSM in the classification process had a measurable and statistically significant effect, I extracted the UA and PA values for each class from the confusion matrices. This allowed me to amass up to 24 data points<sup>11</sup> for each class under both sets of conditions (with and without ancillary DSM data). To provide a measure of the accuracy for a given class across the course of the project, I recorded the mean of both sets of measurements and used the difference between each set of means to provide the average improvement when the DSM was applied.

To determine whether this difference was statistically significant, I performed a paired t-test on the individual data points for both UA and PA to compare the DSM-inclusive and DSM-excluded results.

The analysis of the classification accuracy using data acquired from the multispectral sensor followed an identical method. The changes in overall accuracy and kappa under four conditions were subjected to the LME model described above and the difference in class specific accuracies between conditions 1 and 4 (as below) was determined and tested for significance.

*Conditions for Multispectral Sensor Imagery Tests:*

1. The visible (red, green, and blue bands) only
2. The visible bands and a DSM
3. The visible bands, NIR and RE
4. The visible bands, a DSM and both multispectral bands.

---

<sup>11</sup> One point for each accuracy measurement from each time the class was observed in one of the survey flights. Four flights over three stages allow for a maximum of 24 points.

### 3.6 Change Detection

To conduct change detection (quantified in terms of net change in surface area), it was necessary to simplify the classified images. The primary motivation for this was to make up for the low accuracy with which some classes were classified (this is detailed in chapter four), minimising the loss of reliability in the results by reducing the number of areas where change might be shown because of incorrect classification, rather than actual change (Green & Hartley, 2000). Additionally, the low accuracy rate of certain classes would make it difficult to determine what quantitative measurements of change were valid, and which were influenced to any degree by incorrect classification.

To provide example of why this was necessary: the classes representing different types of tree were often mistaken for one another by the classifier. Leaving these as separate classes during change detection would result in an apparent change from one class to another where in fact, none occurred. Given the short interval between images, it was unlikely that a Cabbage Tree would have supplanted a *Pittosporum* in the space of three months. Consequently, an indication that this *had* occurred would in all probability be incorrect and unhelpful for any scientific application. Combining these classes into one would avoid this issue.

The second motivation was so that the results would be easier to interpret and display, as with 20 classes per image the number of possible combinations of changing classes would have been too great to convert into meaningful results with ease. In a classification involving 20 classes, up to 20 possible change states exist for each class: 'no change' and one for change from the first class to another. This has the potential to produce up to 400 different indications of change between seasons for a single stage, each of which would be treated as a unique value in the resulting raster. So many values would have been impossible to accurately display on a map. Additionally, this meant that in the region of 3600<sup>12</sup> quantified measures of change could be expected, all of which would need to be suspect owing to the levels of accuracy obtained.

Therefore, the classified images were reclassified into five classes (see table 3.6) according to their size and typical growth zone.

---

<sup>12</sup> Assuming each classification has 20 classes - 400 between each season: (Winter-Spring, Spring-Summer and Summer-Autumn) = 1200. 1200 x three stages = 3600.

**Table 3.6: List of change detection 'generic' classes**

<b>Change Detection Class</b>	<b>Contains:</b>
Water	Water
Aquatic and semi-aquatic emergent vegetation	Isolepis, Yellow Isolepis, Waterlogged Grass, Raupō, Rushes, Red Azolla
Terrestrial Ground Cover	Mixed Grasses, dry vegetation, <i>bidens</i> , dry <i>bidens</i> , blackberry, sedge
Terrestrial Substantial Vegetation	Flax, Toetoe, All six tree classes: Manuka, Kahikatea, Cabbage Tree, Other Trees 1-3
Shadow	Shadow

Change detection efforts were focused on documenting the changing balance of water and land in the study areas, as it was not clear that the image classifications were precise enough to give a reliable idea of the expansion or retreat of any individual species.

Since several classes representing land cover were classified with an average accuracy of 50% or less – effectively worse than random odds, it would not be justifiable to use these results to carry out change detection to quantify seasonal or successional changes in land cover as the potential for error is too great. However, water was consistently classified with a very high level of accuracy (90% or greater in most cases), thus measurements of change in water levels would be far more reliable than change in other classes and still of scientific value in the context of a wetland considering the implications of water levels for the prediction of habitat distribution for local bird species, or planning the re-planting of native plants – planting types that are not flood-resistant in flood-prone areas would not be advisable. Using generic classes as above would be quite capable of providing a reliable representation of the changing patterns of water and solid ground.

### **3.6.1 Flood Patterns**

To map changes in flood extent, I identified areas of permanent water and land and the distribution of aquatic vegetation and water in each set of seasonal imagery to determine areas that occasionally flood. Combining these allowed me to map the change in water coverage in each of the three stages.

Terrestrial Ground Cover, Substantial Vegetation and Shadow were treated as 'permanent land' for the purposes of this test, on the assumption that the species contained in these classes are not especially flood resistant and would have been supplanted by flood-tolerant species of aquatic vegetation if their position was waterlogged.

Aquatic vegetation is a reliable indicator of the presence of water, as the species present cannot exist if water is not present at their base, or has not recently covered the site. For instance, *isolepis* is known to prefer poorly drained, permanently damp soil (New Zealand Plant Conservation Network, 2019). Therefore, if *isolepis* is present in a location, it is reasonable to infer that the location is at least retaining more water from rain or occasional flooding. Likewise, Raupō can only grow at the water's edge as the roots must be either submerged or in waterlogged soil. Therefore, if Raupō flourishes in an area, that area must be at least occasionally underwater, if not permanently so.

## Chapter 4

### Classification & Change Detection Results

#### 4.1 Classification Results

##### 4.1.1 Seasonal Flights

Flights were conducted at seasonal intervals of approximately 3-4 months. As multispectral imagery was not available until the Summer of 2019, it was only possible to measure the effects of introducing a DSM to the classifier for the seasonal imagery, the effects of including multispectral imagery has been dealt with as a special case study and are presented in 4.1.3.

Table 4.1 presents two measurements of the accuracy of each classification, Overall Accuracy and Cohen's Kappa coefficient (Kappa for short). 'Overall Accuracy' represents the proportion of the ground-truthing reference points that were correctly classified. 'Kappa' reflects the difference between the actual level of agreement between the reference data and the classified image and the level of agreement that would be expected in a purely random classification (Congalton & Green, 2008). Therefore, a Kappa of 0.5 would indicate that the classified map was 50% more accurate than would be the case if the assignment of classes were entirely random. Each set of results in the table below represents the results of an independent classification process with unique training data, however the methodology used to obtain them was identical in each case.

**Table 4.1: Overall Classification Accuracy & Kappa Scores**

Stage	Season	No DSM		DSM Included		Difference	
		Overall Accuracy	Kappa	Overall Accuracy	Kappa	Overall Accuracy	Kappa
One	Winter	41%	0.35	69%	0.65	+28%	+0.30
	Spring	60%	0.54	72%	0.68	+12%	+0.14
	Summer	45%	0.40	54%	0.49	+9%	+0.09
	Autumn	53%	0.48	55%	0.51	+2%	+0.03
Two	Winter	53%	0.59	67%	0.65	+14%	+0.06
	Spring	62%	0.57	66%	0.60	+4%	+0.03

	<i>Summer</i>	69%	0.60	74%	0.66	+5%	+0.06
	<i>Autumn</i>	68%	0.62	71%	0.66	+3%	+0.04
<b>Three</b>	<i>Winter</i>	52%	0.46	73%	0.70	+21%	+0.24
	<i>Spring</i>	57%	0.52	71%	0.67	+14%	+0.15
	<i>Summer</i>	57%	0.53	63%	0.60	+5%	+0.07
	<i>Autumn</i>	57%	0.50	63%	0.57	+6%	+0.07
<b>Average over all Stages &amp; Seasons:</b>		<b>56%</b>	<b>0.51</b>	<b>67%</b>	<b>0.62</b>	<b>10.25%</b>	<b>0.11</b>

The inclusion of ancillary data in the form of a DSM increased the overall accuracy and kappa score in all situations, though not always by a large amount as the improvement varied between 2% and 28% in terms of overall accuracy and 0.03 and 0.3 in terms of kappa.

The average improvement in overall accuracy was 10.25%, while kappa scores were improved by 0.11. In simple terms, this means that on average the OBIA process had an additional 10.25% probability of correctly classifying a given surface and avoided 11% more of the errors that would have been caused by a purely random classification.

Tables 4.2 and 4.3 present the results of the LME model applied in R to test for the effects of all the co-variates on Overall Accuracy and Kappa, respectively.

**Table 4.2: Analysis of deviance of LME for the effect of ancillary DSM data and Season on Overall Accuracy (n = 24 values from Table 4.1)**

<b>Factor</b>	<b>Chi-squared</b>	<b>df</b>	<b>Significance<sup>13</sup></b>
<b>Ancillary DSM data</b>	15.031	1	0.00011 ***
<b>Season</b>	2.370	3	0.499

<sup>13</sup> The number of asterisks indicates the degree of significance:

\* = < 0.05 'Significant'

\*\* = < 0.01 'Highly Significant'

\*\*\* = < 0.001 'Extremely Significant'

This applies to all tables in this chapter

**Table 4.3: Analysis of deviance of LME for the effect of ancillary DSM data and Season on Overall Kappa (n = 24 values from Table 4.1)**

Factor	Chi-squared	df	Significance
Ancillary data (DSM)	16.854	1	0.00004 ***
Season	2.074	3	0.557

The results of these tests provide further confirmation that the addition of a DSM to the classifier had an extremely significant improving effect on both Overall Accuracy and Kappa. Meanwhile, the season the imagery was captured in only had a minor, non-significant effect on both measures of accuracy.

#### 4.1.2 Class-Specific Results

Table 4.4 breaks down the accuracy measurements for each of the 28 classes. Here two different measures of accuracy are used as Overall Accuracy and Kappa are measures of accuracy on the level of the entire map, not the component classes.

User's accuracy indicates the level of agreement between the reference data and the classified map. It is generally used to indicate the map's reliability from the point of view of the end-user, as it measures the probability that an area classified as a given type of land cover on the classified map represents that type of land cover in the field (Campbell & Whyne, 2011). User's accuracy is calculated as:

$$User's\ Accuracy_{class(x)} = \frac{Correctly\ classified\ points\ for\ class(x)}{Total\ number\ of\ points\ classified\ as\ class(x)}$$

Producer's accuracy indicates the proportion of reference points for a given class that were correctly classified. This is used to quantify how often features on the ground were assigned their correct class by the image classifier, and thus the level of accuracy on the part of the producer of the map (Campbell & Whyne, 2011). The calculation for this measurement is:

$$Producer's\ Accuracy_{class(x)} = \frac{Correctly\ classified\ points\ for\ class(x)}{Number\ of\ reference\ points\ representing\ class(x)}$$

Table 4.4: Per Class Accuracy

Class Name:	Type:	Accuracy	Accuracy w/DSM	Change	n <sup>14</sup> .	Significant Improvement?
<b>Water</b>	UA	0.944	0.967	0.023	<b>12</b>	<i>Yes (p=0.0267)*</i>
	PA	0.903	0.959	0.056		<i>No (p=0.0779)</i>
<b>Mixed Grasses</b>	UA	0.681	0.788	0.108	<b>12</b>	<i>Yes (p=0.0223)*</i>
	PA	0.423	0.522	0.099		<i>Yes (p=0.0110)*</i>
<b>Brown Grass</b>	UA	0.453	0.788	0.335	<b>4</b>	<i>Yes (p=0.0308)*</i>
	PA	0.293	0.403	0.110		<i>No (p=0.3118)</i>
<b>Isolepis</b>	UA	0.800	0.827	0.027	<b>12</b>	<i>Yes (p=0.0475)*</i>
	PA	0.523	0.648	0.124		<i>Yes (p=0.0221)*</i>
<b>Yellow Isolepis</b>	UA	0.900	0.870	-0.030	<b>1</b>	<i>Too Few Observations</i>
	PA	0.590	0.810	0.220		
<b>Reeds</b>	UA	0.399	0.459	0.060	<b>12</b>	<i>No (p=0.1870)</i>
	PA	0.476	0.538	0.062		<i>No (p=0.2578)</i>
<b>Rush</b>	UA	0.295	0.358	0.063	<b>4</b>	<i>No (p=0.4366)</i>
	PA	0.338	0.598	0.260		<i>No (p=0.0562)</i>
<b>Sedge</b>	UA	0.163	0.198	0.036	<b>12</b>	<i>Yes (p=0.0115)*</i>
	PA	0.437	0.588	0.151		<i>Yes (p=0.0052)**</i>
<b>Flax</b>	UA	0.508	0.630	0.123	<b>12</b>	<i>Yes (p=0.0225)*</i>
	PA	0.581	0.660	0.079		<i>Yes (p=0.0053)**</i>
<b>Toetoe</b>	UA	0.238	0.325	0.087	<b>6</b>	<i>No (p=0.1102)</i>
	PA	0.298	0.472	0.173		<i>No (p=0.0770)</i>
<b>Cabbage Tree</b>	UA	0.275	0.433	0.158	<b>12</b>	<i>Yes (p=0.0191)*</i>
	PA	0.699	0.747	0.048		<i>No (p=0.3073)</i>
<b>Manuka</b>	UA	0.161	0.308	0.147	<b>12</b>	<i>Yes (p=0.0020)**</i>
	PA	0.556	0.763	0.208		<i>Yes (p=0.0068)**</i>
<b>Kahikatea</b>	UA	0.154	0.398	0.243	<b>12</b>	<i>Yes (p=0.0088)**</i>
	PA	0.528	0.823	0.295		<i>Yes (p=0.0028)**</i>

<sup>14</sup> Here 'n' represents the number of accuracy measurements for each class.

<b>Other Tree 1</b>	UA	0.199	0.431	0.232	<b>12</b>	<i>Yes (p=0.0327)*</i>
	PA	0.330	0.649	0.319		<i>Yes (p=0.0092)**</i>
<b>Other Tree 2</b>	UA	0.070	0.505	0.435	<b>4</b>	<i>No (p=0.0858)</i>
	PA	0.163	0.518	0.355		<i>No (p=0.1235)</i>
<b>Other Tree 3</b>	UA	0.110	0.147	0.037	<b>3</b>	<i>No (p=0.5172)</i>
	PA	0.350	0.320	-0.030		<i>No (p=0.4226)</i>
<b>Azolla</b>	UA	0.866	0.873	0.008	<b>9</b>	<i>No (p=0.7770)</i>
	PA	0.718	0.808	0.090		<i>Yes (p=0.0042)**</i>
<b>Green Algae</b>	UA	0.698	0.767	0.069	<b>9</b>	<i>No (p=0.0606)</i>
	PA	0.321	0.484	0.163		<i>Yes (p=0.0088)**</i>
<b>Mixed Algae</b>	UA	0.185	0.725	0.540	<b>2</b>	<i>No (p=0.3743)</i>
	PA	0.205	0.325	0.120		<i>No (p=0.5000)</i>
<b>Yellow Algae</b>	UA	0.630	0.820	0.190	<b>1</b>	<i>Too few observations</i>
	PA	0.670	0.600	-0.070		
<b>Blackberry</b>	UA	0.223	0.265	0.043	<b>8</b>	<i>No (p=0.1929)</i>
	PA	0.474	0.606	0.133		<i>Yes (p=0.0247)*</i>
<b>Bidens</b>	UA	0.646	0.754	0.109	<b>7</b>	<i>No (p=0.0859)</i>
	PA	0.471	0.651	0.180		<i>No (p=0.1013)</i>
<b>Dry Bidens</b>	UA	0.62	0.79	0.170	<b>1</b>	<i>Too few observations</i>
	PA	0.62	0.69	0.07	<b>1</b>	
<b>Dry Vegetation</b>	UA	0.733	0.861	0.128	<b>12</b>	<i>Yes (p=0.0180)*</i>
	PA	0.315	0.375	0.060		<i>No (p=0.0815)</i>
<b>Dormant Tree</b>	UA	0.250	0.410	0.160	<b>9</b>	<i>No (p=0.2169)</i>
	PA	0.644	0.613	-0.031		<i>No (p=0.8456)</i>
<b>Waterlogged Grass</b>	UA	0.640	0.716	0.076	<b>7</b>	<i>No (p=0.1241)</i>
	PA	0.451	0.619	0.167		<i>Yes (p=0.0090)**</i>
<b>Mud</b>	UA	0.920	0.963	0.043	<b>3</b>	<i>No (p=0.1859)</i>
	PA	0.573	0.723	0.150		<i>No (p=0.2730)</i>
<b>Shadow</b>	UA	0.815	0.917	0.102	<b>11</b>	<i>Yes (p=0.0294)*</i>
	PA	0.624	0.761	0.137		<i>No (p=0.1033)</i>

Of the 28 classes observed, 23 displayed an improvement in both user's and producer's accuracy upon application of the DSM, the remaining four only displayed improvement in one or the other

measure. 16 out of 28 displayed a statistically significant improvement in their either their user or producer accuracy and seven of these exhibited statistically significant improvement in both measures. The remainder did not display significant improvement in either accuracy measure, of which two classes were not observed enough times to enter their data into the t-test, which requires a minimum of two pairs of means to compare.

Based on this data, the average improvement in user accuracy when a DSM was included was 13.1%, while for producer accuracy the average improvement was 13.4%, which shows that the addition of the DSM has improved both the ability of the classifier to distinguish between classes and the reliability of the map for the eventual user.

### 4.1.3 Multispectral Imagery Tests

This set of tests was conducted as an independent case study and the classified imagery produced from it was not included in the change detection analysis as it was only available for a single season. The objective of this set of tests was to determine whether the extra layers of ancillary data improved the classification accuracy to a sufficiently significant degree that would justify the additional expense and logistics inherent in acquiring and deploying a multispectral sensor.

**Table 4.5: Overall Accuracy and Kappa with different combinations of ancillary data**

Stage	<i>RGB Only</i>		<i>RGB + DSM</i>		<i>RGB + Multispectral</i>		<i>RGB + Multispectral &amp; DSM Combined</i>	
	<i>Overall Accuracy</i>	<i>Kappa</i>	<i>Overall Accuracy</i>	<i>Kappa</i>	<i>Overall Accuracy</i>	<i>Kappa</i>	<i>Overall Accuracy</i>	<i>Kappa</i>
<b>One</b>	54%	0.48	53%	0.47	59%	0.54	61%	0.56
<b>Two</b>	72%	0.62	71%	0.62	77%	0.70	80%	0.73
<b>Three</b>	50%	0.43	51%	0.44	63%	0.57	64%	0.58
<b>Average:</b>	59%	0.51	58%	0.51	66%	0.6	68%	0.62

When examining the results presented in table 4.5, we can see that including Near-Infrared and Red-Edge imagery has a clear ameliorating effect over the baseline accuracy figures acquired from an RGB-only classification, as the two additional layers of ancillary information provided an average improvement of 9.33% overall accuracy and 0.11 kappa.

Of special note is that there was only minimal difference between the ‘multispectral only’ classifications and those which included the full range of ancillary data. Equally, adding a DSM to the base RGB data does not appear to have had any noticeable effect on classification accuracy. The LME model’s results (table 4.6 and 4.9 below) confirm these trends.

These two tables show that there was no significant interaction between the DSM and Multispectral datasets in terms of their effects on accuracy, and that there was no synergistic improvement or antagonistic deterioration in accuracy when including both datasets.

**Table 4.6: Analysis of deviance of LME for the effect of ancillary data in the form of a DSM and/or multispectral infrared on Overall Accuracy assessed in late Summer (n = 12 values from Table 4.5)**

Factor	Chi-squared	df	Significance
DSM	0.034	1	0.855
Multispectral	17.732	1	0.00003***
DSM + Multispectral	0.603	1	0.437

**Table 4.7: Analysis of deviance of LME for the effect of ancillary data in the form of a DSM and/or multispectral infrared on Overall Kappa assessed in late Summer (n = 12 values from Table 4.5)**

Factor	Chi-squared	df	Significance
DSM	0.000	1	1.000
Multispectral	32.441	1	<0.00001 ***
DSM + Multispectral	0.745	1	0.388

#### 4.1.4 Class-Specific Results

Owing to the reduced resolution and general image quality of the true-colour imagery produced by the RedEdge sensor, it was only possible to reliably identify 17 distinct classes. Except for the 'Other Tree – Dark' class which now incorporates the previously distinct 'Manuka' class, all classes in the table below represent the same surface types as in table 4.8 below.

**Table 4.8: Class-Specific Accuracy (Multispectral Camera)**

Class Name:	Type:	Accuracy	Accuracy w/All Ancillaries	Change	n.	Significant Improvement?
<b>Water</b>	UA	0.913	0.987	0.073	<b>3</b>	<i>No (p=0.0904)</i>
	PA	0.910	0.953	0.043		<i>No (p=0.3178)</i>
<b>Mixed Grasses</b>	UA	0.640	0.780	0.140	<b>3</b>	<i>No (p=0.2315)</i>
	PA	0.537	0.663	0.127		<i>No (p=0.0849)</i>
<b>Isolepis</b>	UA	0.903	0.903	0.000	<b>3</b>	<i>No (p=1)</i>
	PA	0.550	0.557	0.007		<i>No (p=0.9719)</i>
<b>Reeds</b>	UA	0.453	0.447	-0.007	<b>3</b>	<i>No (p=0.9432)</i>
	PA	0.487	0.710	0.223		<i>Yes (p=0.0286)*</i>
<b>Sedge</b>	UA	0.130	0.267	0.137	<b>3</b>	<i>Yes (p=0.0058)**</i>
	PA	0.297	0.400	0.103		<i>No (p=0.6050)</i>
<b>Flax</b>	UA	0.533	0.533	0.000	<b>3</b>	<i>No (p=1)</i>
	PA	0.557	0.703	0.147		<i>No (p=0.1754)</i>
<b>Toetoe</b>	UA	0.300	0.200	-0.100	<b>1</b>	<i>Too few observations</i>
	PA	0.160	0.480	0.320		
<b>Cabbage Tree</b>	UA	0.153	0.370	0.217	<b>3</b>	<i>No (p=0.0668)</i>
	PA	0.257	0.533	0.277		<i>No (p=0.1527)</i>
<b>Kahikatea</b>	UA	0.020	0.030	-0.010	<b>1</b>	<i>Too few observations</i>
	PA	0.170	0.420	-0.250		
<b>Other Tree 1</b>	UA	0.200	0.210	0.010	<b>3</b>	<i>No (p=0.9504)</i>
	PA	0.523	0.600	0.077		<i>No (p=0.6758)</i>
<b>Other Tree 3</b>	UA	0.285	0.420	0.135	<b>2</b>	<i>No (p=0.6411)</i>
	PA	0.115	0.345	0.230		<i>Yes (p=0.0009)***</i>
<b>Green Algae</b>	UA	0.915	0.915	0.000	<b>2</b>	<i>No (p=1)</i>
	PA	0.250	0.710	0.460		<i>No (p=0.0527)</i>
<b>Blackberry</b>	UA	0.135	0.250	0.115	<b>2</b>	<i>Yes (p=0.0442)*</i>
	PA	0.665	0.725	0.060		<i>No (p=0.7536)</i>
<b>Bidens</b>	UA	0.437	0.797	0.360	<b>3</b>	<i>No (p=0.2417)</i>
	PA	0.263	0.590	0.327		<i>No (p=0.2416)</i>

<b>Dry Vegetation</b>	UA	0.833	0.900	0.067	<b>3</b>	<i>No (p=0.1789)</i>
	PA	0.320	0.390	0.070		<i>Yes (p=0.0317)*</i>
<b>Dormant Tree</b>	UA	0.210	0.240	0.030	<b>3</b>	<i>No (p=0.8771)</i>
	PA	0.343	0.453	0.110		<i>No (p=0.7396)</i>
<b>Shadow</b>	UA	1.000	1.000	0.000	<b>3</b>	<i>No (p=1)</i>
	PA	0.375	0.915	0.540		<i>Yes (p=0.0303)*</i>

While the majority of the improvements in accuracy were not statistically significant, it should be noted that these figures are drawn from only three observations at most, compared to up to 12 for the seasonal flights. Two results is the bare minimum needed to run a t-test, so more data could refine these results and perhaps indicate some significant differences. Taking all results into account, the average improvement in user accuracy was 8.9%, while producer accuracy increased by 16.9% but this is based on primarily statistically insignificant results, so should be considered with caution.

## 4.2 Change Detection

### 4.2.1 Land / Water Change by Surface Area

<b>Stage:</b>	<b><i>Permanent Open Water</i></b>	<b><i>Maximum Flood Coverage</i></b>	<b><i>Permanent Dry Land</i></b>
Stage One	11,260m <sup>2</sup>	32,460m <sup>2</sup>	27,790m <sup>2</sup>
Stage Two	16,570m <sup>2</sup>	46,520m <sup>2</sup>	11,390m <sup>2</sup>
Stage Three	1,170m <sup>2</sup>	26,500m <sup>2</sup>	19,560m <sup>2</sup>

Stage three featured the greatest levels of change in water levels, expressed in terms of surface area. The 25,300m<sup>2</sup> difference between the area of water coverage at the lowest and highest levels amounts to an increase of 2164.96%. Stage one's water coverage increased by a similar area of 21,200m<sup>2</sup>, though this only equates to a percentage increase of 188.228%. Stage two's coverage area differs by 29,950m<sup>2</sup> – a percent change of 180.75%.

Stage three may exhibit the most dramatic difference in coverage area as the flooded areas may be at a lower elevation relative to the lowest water level, thus a small increase in water levels has the potential to 'spill' further than at other sites. Stage one features a raised berm running around the edge of the local body of water, which is probably serving as a stopbank preventing water from spreading in certain directions, resulting in the water becoming deeper instead. This is demonstrated

by the ring-like patterns of 'occasionally flooded' area around the islands in figure 9 (see below). Stage two has no earthworks, the only limitation to the spread of water is that the areas that remain dry are high enough above the water table to remain dry.

#### 4.2.2 Change Visualisation

In the maps below, the areas which remained open water are shown in blue, while areas that were either temporarily covered by floodwater or feature vegetation types that grow in water, sodden soil or in areas cleared by retreating water (for instance, Azolla, Isolepis or Raupō) are marked in orange. All other areas remained dry land and featured terrestrial vegetation for the full course of the project.

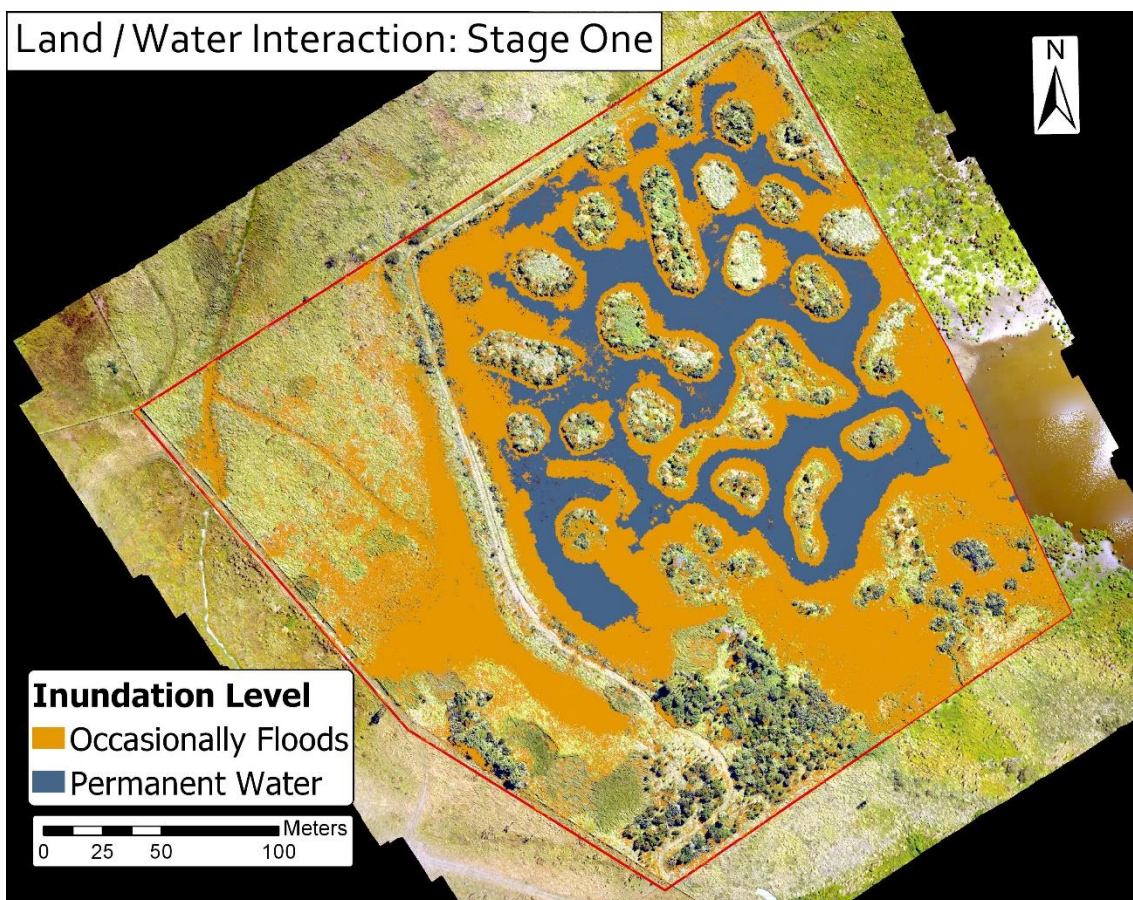


Figure 9: Land/Water Change in Stage One

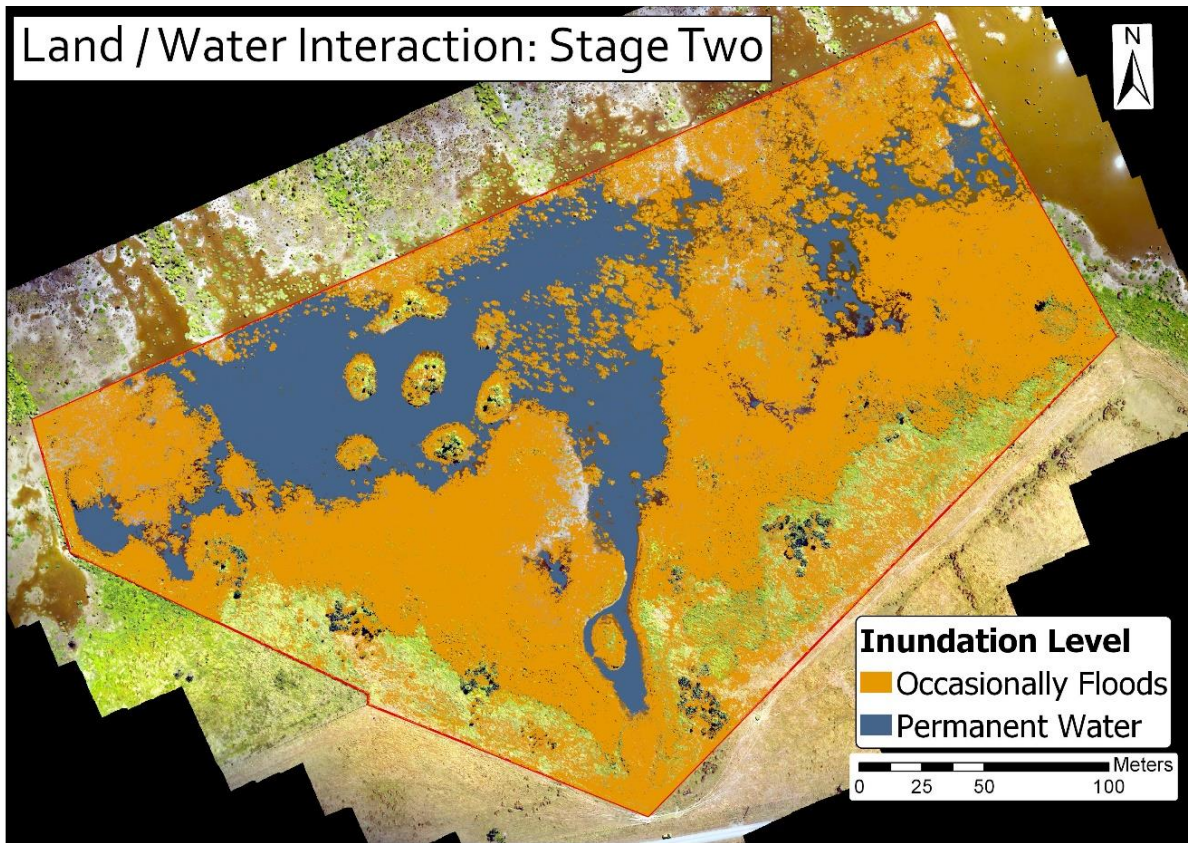


Figure 10: Land/Water Change in Stage Two

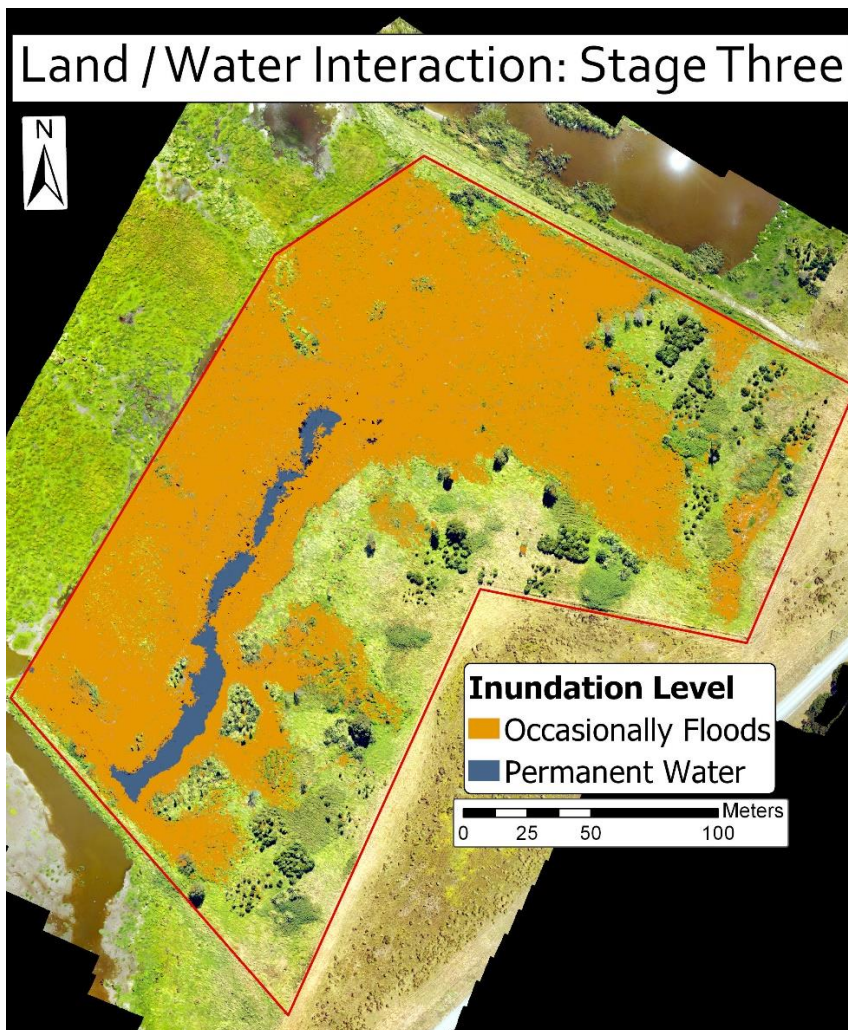


Figure 11: Land/Water Change in Stage Three

### 4.2.3 Descriptive

#### Stage One

The terrestrial portion of stage one remained largely unchanged over the course of the year in terms of vegetation coverage, but the aquatic section displayed significant change. Between June and October, the water level across the entire wetland rose considerably. In stage one, this manifested in lower-lying areas of the south-eastern section of the stage flooding, and the water level rose high enough to encroach on several of the flax & toetoe plantations on the raised islands. Based on the prevalence of *Isolepis*, I infer this may be a regular occurrence on the grounds that *Isolepis* prefers the damp conditions associated with poor drainage or regular flooding. The increase in water level and the increase in sunlight during the transition into summer coincided with the appearance of floating plants in the stage such as Red Azolla. By January 2019, this species was prevalent across a wide area of the open water in the stage but had mostly died back by March. The quantity of Raupō increased noticeably between June 2018 and January 2019, as the existing banks of the reed increased in both their apparent density and coverage area. *Bidens* became evident in January 2019,

(coinciding with the gradual retreat of the water level) and remained present at the conclusion of the survey flights.

### *Stage Two*

The rise in water level between winter and spring was especially noticeable in stage 2. Of note is that the water level increased to cover areas of land which appear not to have been previously inundated. This was evident as prior to flooding, the areas contained terrestrial grasses which are not known to survive flooding and do not spread fast enough to have become as established as they had been in the few months between flood periods. Azolla and other unidentified aquatic plants became evident on the surface of open areas of water in spring and remained in evidence until after January 2019. The water level receded somewhat by this time, and the areas of land exposed by the retreating water now featured a predominance of *Isolepis* in the place of the previous exotic grasses, though it appears that *Bidens* was once again able to quickly recolonise these areas. By March 2019, the water had retreated still further, exposing bare sediment beneath.

### *Stage Three*

Stage three also experienced a dramatic change in water coverage between Winter and Spring, but unlike stage one, the water levels did not subside to their previous level at the same rate, since several areas that were dry land as of the start of the project in June 2018 remained flooded as of January 2019. A side-effect of the flooding is that the clusters of *Bidens* that were detected in June 2018 were eliminated, as their positions were inundated and the plants no longer distinguishable by eye in subsequent orthomaps and were not present in subsequent on-foot surveys of their location. However, *Bidens* did in fact outlast the flooding and re-established itself, becoming clearly observable by April 2019. The water levels eventually receded to an approximation of their previous levels by March 2019, revealing bare sediment in several places. As was the case in stage one, the flooded areas were previously covered in *Isolepis*, which would lend weight to the inference that the change in water level across the wetland is a regular seasonal pattern, rather than a one-off event caused by an unusually rainy period<sup>15</sup>. Red Azolla and green algae appeared in stage three later than the other sites, not being apparent until the summer flights. Several blackberry patches in the site appear to have expanded over time and their position on relatively high ground has protected them

---

<sup>15</sup> Monthly rainfall data from MetService shows that the study period (in particular, the months in which imagery was captured) was actually drier than the historical norm, as were the 12 months preceding the start of the project (Meteorological Service of New Zealand, 2019). However, the rainfall for November and December 2018 was more than double the historical average for these months, which could account for stage three appearing to retain water levels longer.

from flooding for some time. Anecdotal reports suggest these patches have been extant for some time and are reportedly much larger now than their first observation a couple of years ago<sup>16</sup>.

#### **4.2.4 Comparative Maps**

The maps below serve as side-by-side comparisons of the seasonal imagery to illustrate the changes discussed in the section above. Full page versions of each image may be found at Annex C.

---

<sup>16</sup> Personal conversation with Dr Stephen Hartley, my supervisor and regular visitor to the Wairio block.

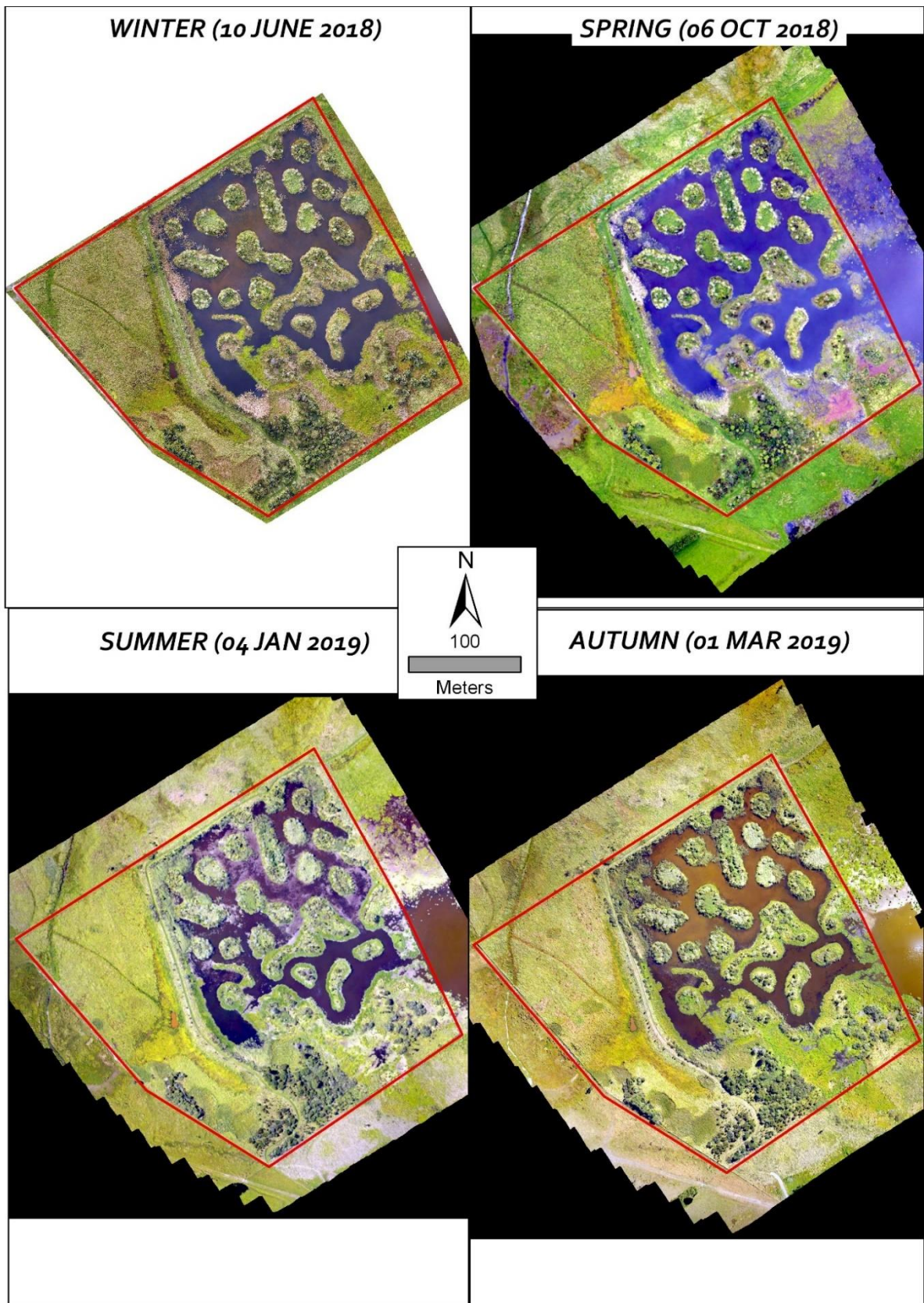


Figure 12: Stage One - changes over time

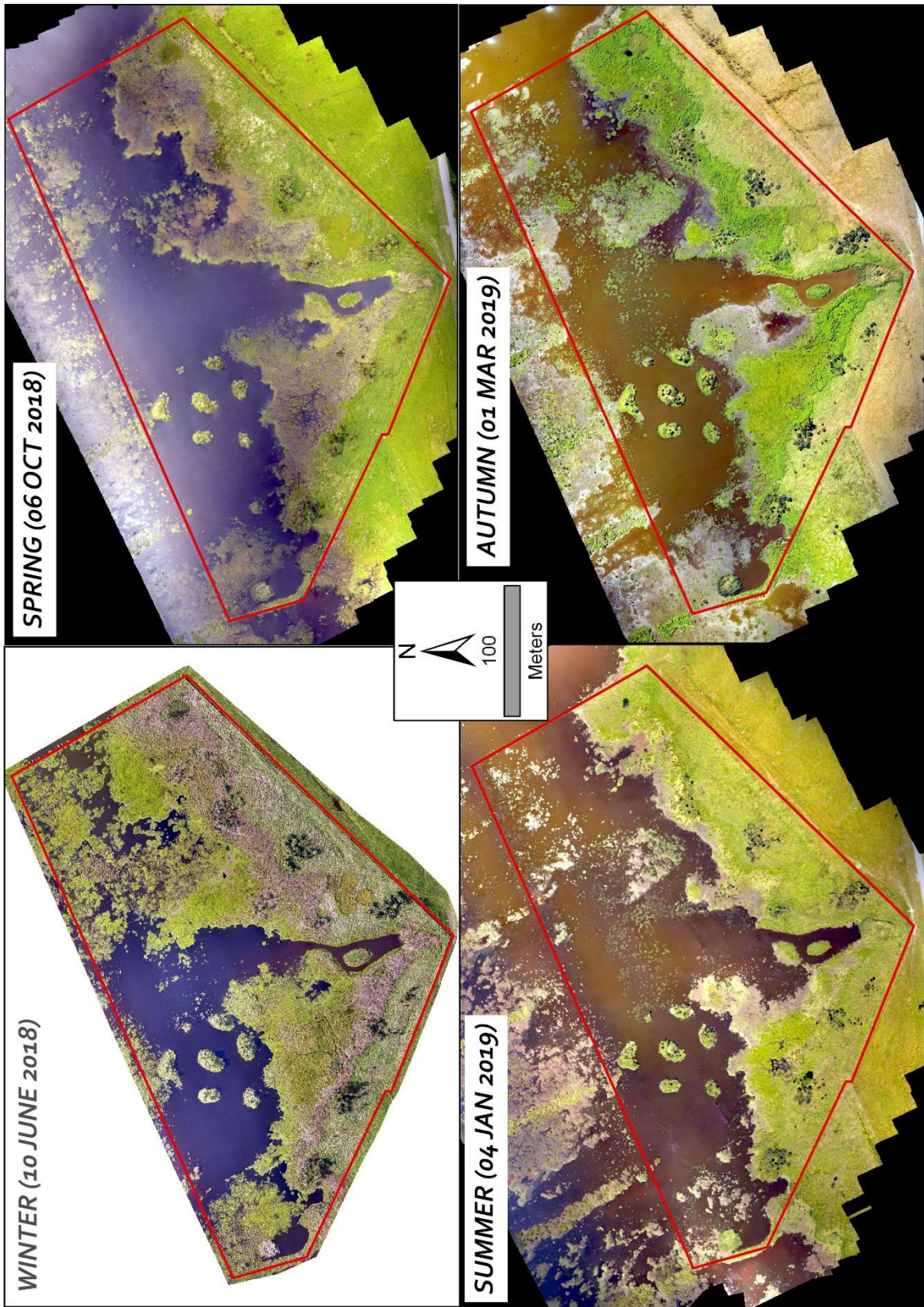


Figure 13: Stage Two - changes over time

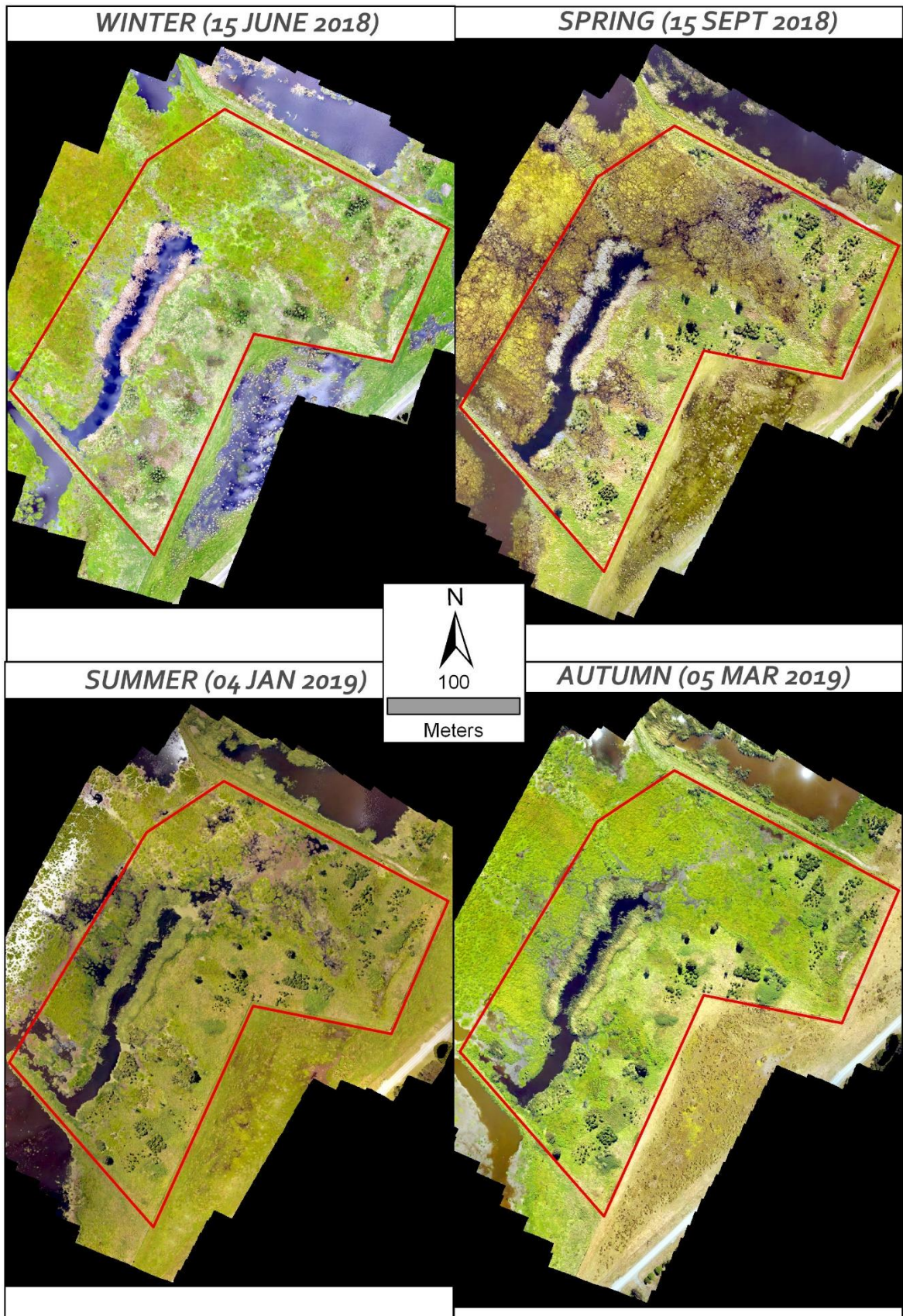


Figure 14: Stage Three - changes over time

# Chapter 5

## Discussion & Evaluation

Two research questions were defined at the outset of this project:

1. Test the proposition that UAVs can provide accurate and convenient assessment of changes in vegetation and water coverage over time, using a recovering wetland area as a case study.
2. To what extent is the accuracy of the image classification process improved with the addition of ancillary data, such as digital surface models or near infrared imagery?

Guided by these questions, I sought to test the ability of an OBIA process to distinguish a range of different land cover classes to determine what land cover types common to a wetland environment were easiest to classify and to demonstrate how OBIA can be improved with the addition of a range of ancillary data sources. Concurrently, I evaluated how current UAV technology, remote sensing techniques and image processing software could enable a research team or management unit with limited skills, budget and time to gather and process data with much greater levels of detail than might otherwise be available without recourse to contracting professional UAV operators or GIS technicians. An additional focus of this line of investigation was an investigation into whether multispectral (NIR and RE band) ancillary data could offer equal or greater improvements in classification accuracy to those offered using a DSM.

### 5.1 Classification Accuracy

In this section, I cover the accuracy of the classifications produced from the UAV imagery sets, in line with research question one.

Regrettably, the average overall accuracy (67%) and kappa (0.62) of the classifications derived from the DSM-informed seasonal flights are not high enough to regard the maps as having a fully reliable degree of *overall* accuracy. Nonetheless, it is worth noting that there is no universally observed criteria for what constitutes a desirable degree of accuracy, whether measured by percent agreement or kappa (Bakeman, Quera, McArthur, & Robinson, 1997). For example, Landis & Koch (1977) held that the bracket for 'substantial agreement' as indicated by kappa values was between 0.61-0.8, a bracket which most of the classifications in this study fall into. Meanwhile, Fleiss (1981) posited that a score between 0.4 and 0.75 was 'fair to good'.

'Overall Accuracy' (OA) is a weighted measure obtained from the accuracy for each class in the confusion matrix. Therefore, a few low scores will have reduced the overall measure in every case. As a result, it may be more appropriate to evaluate the results based on the class-specific accuracy

scores. When these are examined, it becomes clear there is a great deal of variability in how accurately the classification program was able to deal with different types of vegetation and surfaces. For the purposes of this section, I have created an ‘overall class-specific accuracy’ measurement by taking the average of the user and producer accuracies for each class in the DSM-inclusive (the ‘best case’) tests to provide a combined measure of the level of commission and omission error for each class, and used this measure to rank the accuracy of each class (Table 5.1).

**Table 5.1: Classes Ranked by Overall Accuracy (OA)**

*UA = User’s Accuracy    PA = Producer’s Accuracy*

<b>Class:</b>	<b>UA</b>	<b>PA</b>	<b>OA</b>	<b>UA Rank</b>	<b>PA Rank</b>	<b>OA Rank</b>
<b>Water</b>	0.967	0.959	0.963	<b>1</b>	<b>1</b>	<b>1</b>
<b>Mud</b>	0.963	0.723	0.843	<b>2</b>	<b>8</b>	<b>2</b>
<b>Azolla</b>	0.873	0.808	0.841	<b>4</b>	<b>4</b>	<b>3</b>
<b>Yellow Isolepis</b>	0.870	0.810	0.840	<b>5</b>	<b>3</b>	<b>4</b>
<b>Shadow</b>	0.917	0.761	0.839	<b>3</b>	<b>6</b>	<b>5</b>
<b>Dry <i>Bidens</i></b>	0.790	0.690	0.740	<b>9</b>	<b>9</b>	<b>6</b>
<b>Isolepis</b>	0.827	0.648	0.738	<b>7</b>	<b>13</b>	<b>7</b>
<b>Yellow Algae</b>	0.820	0.600	0.710	<b>8</b>	<b>17</b>	<b>8</b>
<b><i>Bidens</i></b>	0.754	0.651	0.703	<b>13</b>	<b>11</b>	<b>9</b>
<b>Waterlogged Grass</b>	0.716	0.619	0.668	<b>15</b>	<b>14</b>	<b>10</b>
<b>Mixed Grasses</b>	0.788	0.522	0.655	<b>10</b>	<b>21</b>	<b>11</b>
<b>Flax</b>	0.630	0.660	0.645	<b>16</b>	<b>10</b>	<b>12</b>
<b>Green Algae</b>	0.767	0.484	0.626	<b>12</b>	<b>23</b>	<b>13</b>
<b>Dry Vegetation</b>	0.861	0.375	0.618	<b>6</b>	<b>26</b>	<b>14</b>
<b>Kahikatea</b>	0.398	0.823	0.611	<b>22</b>	<b>2</b>	<b>15</b>
<b>Brown Grass</b>	0.788	0.403	0.596	<b>11</b>	<b>25</b>	<b>16</b>
<b>Cabbage Tree</b>	0.433	0.747	0.590	<b>19</b>	<b>7</b>	<b>17</b>
<b>Other Tree (Dark Green)</b>	0.431	0.649	0.540	<b>20</b>	<b>12</b>	<b>18</b>
<b>Manuka</b>	0.308	0.763	0.536	<b>25</b>	<b>5</b>	<b>19</b>
<b>Mixed Algae</b>	0.725	0.325	0.525	<b>14</b>	<b>27</b>	<b>20</b>
<b>Other Tree (Brown)</b>	0.505	0.518	0.512	<b>17</b>	<b>22</b>	<b>21</b>
<b>Dormant Tree</b>	0.410	0.613	0.512	<b>21</b>	<b>15</b>	<b>22</b>
<b>Reed</b>	0.459	0.538	0.499	<b>18</b>	<b>20</b>	<b>23</b>
<b>Rush</b>	0.358	0.598	0.478	<b>23</b>	<b>18</b>	<b>24</b>
<b>Blackberry</b>	0.265	0.606	0.436	<b>26</b>	<b>16</b>	<b>25</b>
<b>Toetoe</b>	0.325	0.472	0.399	<b>24</b>	<b>24</b>	<b>26</b>
<b>Sedge</b>	0.198	0.588	0.393	<b>27</b>	<b>19</b>	<b>27</b>
<b>Other Tree (Light Green)</b>	0.147	0.320	0.234	<b>28</b>	<b>28</b>	<b>28</b>

### 5.1.1 Higher-Accuracy Classifications (OA: >70%)

A common factor among the nine classes with OA greater than 70% is that each appears as a fairly smooth surface with consistent colouration. These classes are:

1. Water
2. Mud
3. Azolla
4. Yellow Isolepis
5. Shadow
6. Dry *Bidens*
7. Isolepis
8. Yellow Algae
9. *Bidens*

The exception to this rule is *Bidens* which is rougher, but its distinctive brown colouration may be acting as a unique identifier preventing confusion with other surface types. Azolla and potentially Water, Shadow and Yellow Isolepis may also benefit from their unique colouration (red, light to dark blue, black, or very dark green and yellow respectively) as these colours are not found in other surface types. Consistency of colouration and smooth surface texture lead to increased accuracy for two reasons. Firstly, this means that one segment of a given class will be fairly similar to all other segments representing that class throughout the image, so fewer areas will differ sufficiently from the training data to be treated as something else. Secondly, the similarity in these factors will have increased the probability that adjacent segments representing that class will have merged into one during the segmentation process. This reduces the number of individual segments for that class, which in turn reduces the possibility for error as there are fewer segments that could be subject to classification error.

### 5.1.2 Moderate Accuracy (OA: 60%-69%)

10. Waterlogged Grass
11. Mixed Grasses
12. Flax
13. Green Algae
14. Dry Vegetation
15. Kahikatea

As accuracy levels drop, rates of confusion between spectrally similar classes increase to the point that clear trends can be observed in the confusion matrices (Annex B). For example, 'Mixed Grasses' was commonly confused for the 'Sedge' classes and vice versa, the result of which was reduced accuracy for all classes. Regular confusion between classes such as this is a strong argument in favour of reducing the number of classes in the classification scheme by incorporating the two species into a single class. Most of these classes (with the exclusion of green algae) featured a rougher texture or

less consistent colouration, so were more segmented than the higher accuracy classes, which may have reduced their accuracy to a small degree.

### **5.1.3 Poor Accuracy (OA: <60%)**

16. Brown Grass
17. Cabbage Tree
18. Other Tree (Dark Green)
19. Manuka
20. Mixed Algae
21. Other Tree (Brown)
22. Dormant Tree
23. Reed
24. Rush
25. Blackberry
26. Toetoe
27. Sedge
28. Other Tree (Light Green)

In these cases, the reduced accuracy was generally due to a higher rate of confusion between classes (see the confusion matrices at annex B). For instance, 'Toetoe' features a similar coloration to many of the longer exotic grasses, meaning it was occasionally difficult to distinguish them manually and thus the higher rate of confusion is understandable. In other cases, the low accuracy was due to a combination of over-segmentation of the objects representing the class and the texture and colour of the object. A good example of this effect are blackberry bushes, which are segmented into very small parts and can display a range of colours across a single bush, from light green to near black and occasionally yellow as leaves die off in autumn and winter. Since the small segments had such a degree of variance in their properties, other small segments with similar spectral properties – often areas of scrub around fence lines or patches of short, rough grass - were misclassified as blackberry.

### **5.1.4 Confusions**

Table 5.2 lists the common confusions for each class. The complete set of confusion matrices can be found at Annex B. Some interesting patterns in the types of confusions that occurred can be seen here. First, larger vegetation classes were most often confused with ground cover when a DSM was not present (for instance, Kahikatea/Mixed Grass confusion) and when a DSM was present, the larger classes were usually only confused with other large vegetation varieties. A similar pattern exists for ground cover, which was normally only mistaken for other ground cover. This pattern supports the hypothesis that including a DSM would allow for better separation between classes based on their physical properties, rather than relying on spectral separability. This also suggests that a simpler classification scheme that combined all ground cover classes into a single class and did likewise for

larger vegetation types, might show significantly less confusion with a higher rate of accuracy obtained. This is discussed further in section 5.6.2.

**Table 5.2: Classes and their Common Conclusions**

<b>Class:</b>	<b>OA Rank</b>	<b>Most commonly confused with:</b>
<b>Water</b>	<b>1</b>	Shadow ( <i>darker coloured water only</i> )
<b>Mud</b>	<b>2</b>	Waterlogged Grass
<b>Azolla</b>	<b>3</b>	Water, Green Algae
<b>Yellow Isolepis</b>	<b>4</b>	Isolepis, Brown Grass
<b>Shadow</b>	<b>5</b>	Water, various vegetation types ( <i>if shadow is weak</i> )
<b>Dry Bidens</b>	<b>6</b>	<i>Bidens</i> , Dry Vegetation
<b>Isolepis</b>	<b>7</b>	Mixed Grass, Sedge
<b>Yellow Algae</b>	<b>8</b>	Green Algae, Waterlogged grass
<b>Bidens</b>	<b>9</b>	Isolepis (while green) Dry <i>Bidens</i> , Dry Vegetation (while brown/dormant)
<b>Waterlogged Grass</b>	<b>10</b>	Water, Mixed Grass, Sedge. <i>Kahikatea (Stage 3 only and when no DSM was present)</i>
<b>Mixed Grasses</b>	<b>11</b>	Sedge, Toetoe. <i>Various Tree Classes - when no DSM present</i>
<b>Flax</b>	<b>12</b>	Reeds ( <i>while they are green: Spring-Autumn</i> ). Cabbage Tree
<b>Green Algae</b>	<b>13</b>	Mixed Grass, Waterlogged Grass
<b>Dry Vegetation</b>	<b>14</b>	Reeds, Sedge ( <i>when these are dry/dormant and appear lighter brown: Winter-Spring</i> ). Toetoe, Bidens
<b>Kahikatea</b>	<b>15</b>	Mixed Grass ( <i>without DSM</i> ). Manuka, dry vegetation ( <i>bare branches</i> )
<b>Brown Grass</b>	<b>16</b>	Sedge, Mixed Grass, Dry Vegetation. <i>When no DSM Present: Manuka, Other Tree (Brown)</i>
<b>Cabbage Tree</b>	<b>17</b>	Flax, Other Tree (Dark Green)
<b>Other Tree (Dark Green)</b>	<b>18</b>	Mixed Grass,
<b>Manuka</b>	<b>19</b>	Kahikatea ( <i>confusion rate reduces with DSM</i> ) Other Tree (dark green)
<b>Mixed Algae</b>	<b>20</b>	Azolla, Waterlogged Grass
<b>Other Tree (Brown)</b>	<b>21</b>	Brown Grass, Mixed Grass
<b>Dormant Tree</b>	<b>22</b>	Dry Vegetation, <i>Bidens</i>
<b>Reed</b>	<b>23</b>	Flax, Dry Vegetation, Mixed Grass
<b>Rush</b>	<b>24</b>	Flax, Mixed Grass, Dry Vegetation
<b>Blackberry</b>	<b>25</b>	Mixed Grass, Brown Grass, Waterlogged Grass
<b>Toetoe</b>	<b>26</b>	Mixed Grass, Dry Vegetation
<b>Sedge</b>	<b>27</b>	Mixed Grass, Dry vegetation (when brown)
<b>Other Tree (Light Green)</b>	<b>28</b>	Mixed Grass, Other Tree (dark green)

### 5.1.5 Implications of Accuracy

Though 19 out of 28 classes were not classified with a 'high' level of accuracy, there are encouraging conclusions to be drawn from the results. The classes with accuracies of around 70% or better are among the most common classes in the wetland and represent the majority of land cover by area. More interestingly, two of the high-accuracy classes: *Bidens* and *Azolla* are invasive species, so the classifier's ability to reliably locate these plants could be leveraged in more targeted applications to track just these species, as their spectral uniqueness allows them to be easily separated from their surrounds. This would be advantageous for anyone wishing to monitor the pest species, but without the need of a complete land cover inventory. Meanwhile, high accuracy for *Isolepis* is also a good result, as this species can be used as an indicator of the water retention of soil, (New Zealand Plant Conservation Network, 2019) which is important information as wetlands, by definition, must retain water. A sudden reduction in the prevalence of *Isolepis* could serve as an early indication that the wetland was drying out, even if surface water levels appeared unchanged.

High levels of user accuracy for the various algae classes are also encouraging but would be more so if complemented by equal measures of producer accuracy. Algae often create the foundation for the food chain in aquatic ecosystems, so the presence of algae in reasonable amount is a good indicator of environmental health (Kislik, Dronova, & Kelly, 2018). However, algal blooms in lakes, rivers, oceans and wetlands can be disruptive to the local system and in some cases can be toxic (Ministry for Primary Industries, 2019). Prevention of the spread of harmful algae blooms as *Didymosphenia geminata* is a real and current concern of New Zealand's environmental protection services (Feltham, 2006). Proper control programmes require early detection and reliable intelligence as to the exact distribution of the algae. Since algae commonly manifest as distinctly coloured patches under or on the water's surface, image analysis techniques that can reliably detect these would be a boon to researchers looking to monitor a waterway for the spread of unwanted algae. The use of a UAV would also be advisable here, as a UAV affords the researcher cost-effective aerial survey capability and improved temporal and spatial resolutions compared to large airborne or space-based systems leveraged in this project and elsewhere (Kislik, Dronova, & Kelly, 2018).

### 5.1.6 Accuracy vs. Usability

Low classification accuracy for a given class does not necessarily equate to the classified image not being of use in detecting the presence of a targeted species. In April 2019, a contractor working for the wetland restoration team travelled to Wairio to carry out weed control, one objective was to spray herbicide on blackberry bushes throughout the wetland. To assist them in locating the blackberry bushes, they were provided with extracts (Figure 15) from the full set of classified images for stage three, showing the location of all detected blackberry patches.

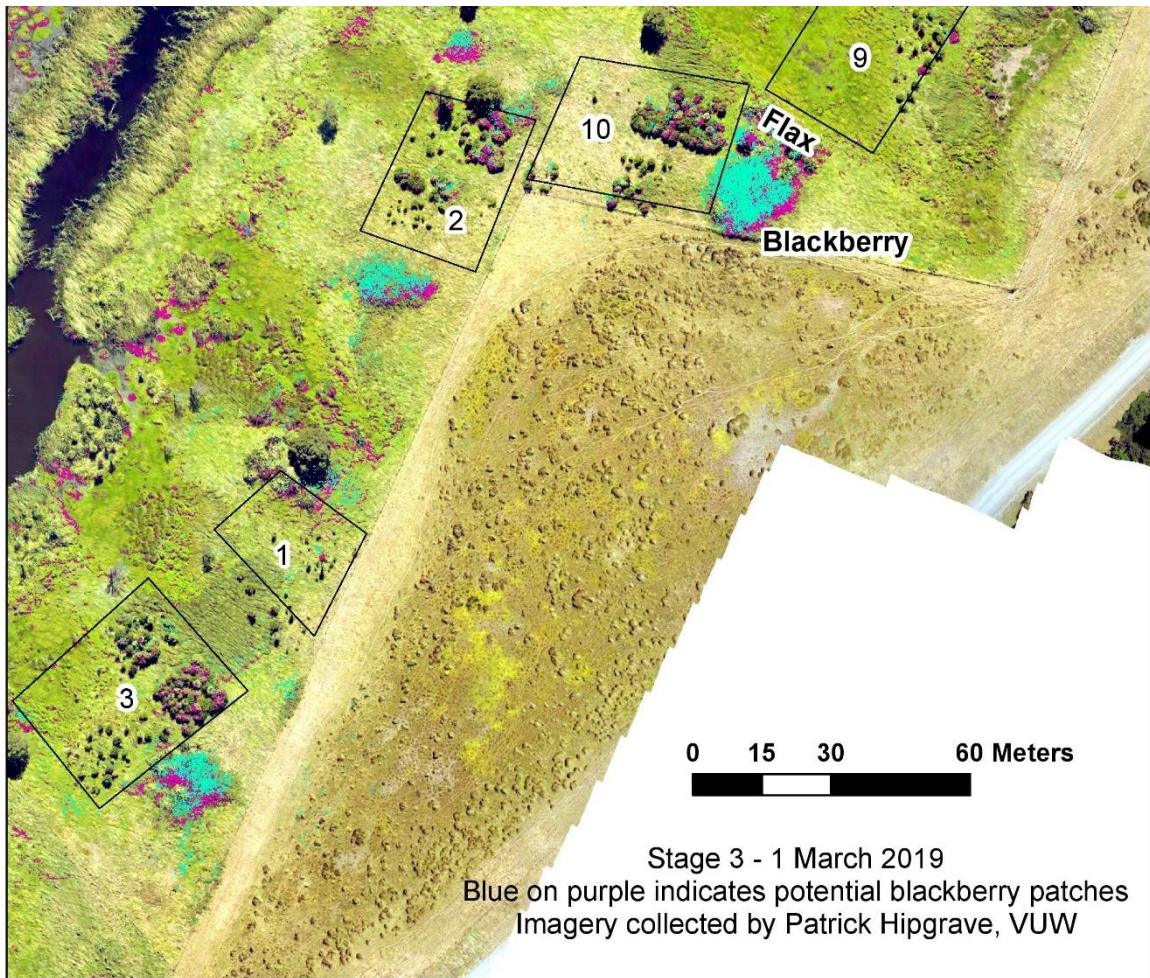


**Figure 15 : Example of the Blackberry Patch maps given to the contractor. Extracted from a Map created by Stephen Hartley (2019). Blue patches represented blackberry detected in one season, purple indicates the same, but in a different season. Overlapping areas are therefore the most likely locations for blackberry patches.**

They were positive about the use of the vegetation maps produced:

*“I think the overview photo has got them [the blackberry patches] nailed pretty well. I had a good look over much of Stage 3 and the areas I saw correspond exactly with the blue patches. I am planning on doing the spraying next week so the map will be very useful.”*

In spite of the poor reported user accuracy of the ‘blackberry’ class, a common-sense interpretation of the map still allows for the class to be useful for practical purposes. This usefulness is present despite the class’s low accuracy as even though certain parts of the image that should have been classed as blackberry were not (and some that were should not have been), a high concentration of contiguous ‘blackberry’ pixels in the classified image is a reliable indicator of the presence of a blackberry bush in that location. Meanwhile, occasional scattered ‘blackberry’ pixels can be easily discounted by the end-user as probable error. While contiguous clusters of pixels may not accurately capture the dimensions of the plant, many practical applications do not require this level of

precision. In this case, only the general location of a plant was required, the exact dimensions could be determined once on site.

The high resolution of the UAV images could be grounds to skip the image classification process entirely as once the user learns to recognise blackberry bushes. These bushes are easily distinguished by manually interpreting the raw photo. In this case, providing the weed sprayer with a high-resolution photo on which all blackberry bushes were highlighted may have been of equal use. Being able to remove the specialised process of image classification from the workflow could be useful to the amateur monitor, as they are likely sufficiently familiar with the plant species to reliably identify them from an aerial photograph. This alleviates the need for additional software and experience with classifying images. One drawback to this approach is that it is still possible for the interpreter to miss plants of smaller size, whereas the classifier is perhaps more likely to catch smaller plants represented by only a few pixels the human would miss. This could limit the effectiveness of approaches that benefit from detecting a species in the early stages of growth, for instance, detecting and eliminating weed species before they have a chance to become established. Conversely, early detection of newly-emergent plant species that are desirable in the local environment would help quantify the rate of recovery of the wetland and help target vegetation modification schemes to support the plants as they established themselves.

Another drawback is that depending on the application, errors of commission may be less of a concern than errors of omission. For example, false positive results can result in weed control programmes being targeted at areas that do not require them, resulting in a greater financial cost than is truly necessary. However, false negatives can result in areas that do require attention being overlooked, leading to an environmental cost through the uncontrolled spread of invasive species and an additional financial cost in the future when trying to control the plants not detected in the initial survey (Psaltopoulos, et al., 2017).

## **5.2 Potential Causes of Error**

### *Segmentation*

Proper segmentation of the objects in the aerial photograph is essential to accurate object-based classifications (Haralick & Shapiro, 1985). While the segmentation settings were tested and adjusted for the best results (see 3.4.2), it was not possible to find settings that were well-suited to all classes. As a consequence, some classes were represented by many thousands of small ( $<0.1\text{m}^2$ ) segments, while others were represented by only a few larger segments of several tens of square meters. A drawback of smaller segments is that they do not always cover enough area to give the classification algorithm a representative set of textural or spectral data (Zhou & Lam, 2008). As an example, an

area of only a few square meters of mixed grass would typically contain several hundred segments, while an area of *Isolepis* might only contain a dozen. This indicates that in instances where species-specific classification is desired, the segmentation approach should be tailored to individual species, rather than pursuing a 'one size fits all' approach.

Another challenge inherent in accurate segmentation is having the borders between segments representing different classes correctly align with the actual divide between each class on the ground (Dronova, Gong, & Wang, 2011). However, these divides are rarely distinct lines as different types of vegetation overlap one another, and so appear to blend into one another. This effect was exacerbated by the high resolution of the images, meaning the merging areas are represented by enough pixels to be treated as independent objects and it proved difficult, sometimes impossible, to adequately adjust the segmentation process. The end result of this was that areas of incorrect classification can often be seen around the edges of areas of certain types of vegetation, such as in figure 16 below where the core of a patch of *Isolepis* has been correctly classified (light green), but the edges of the patch have been mis-identified as belonging to the 'Mixed Grass' (dark green) class.

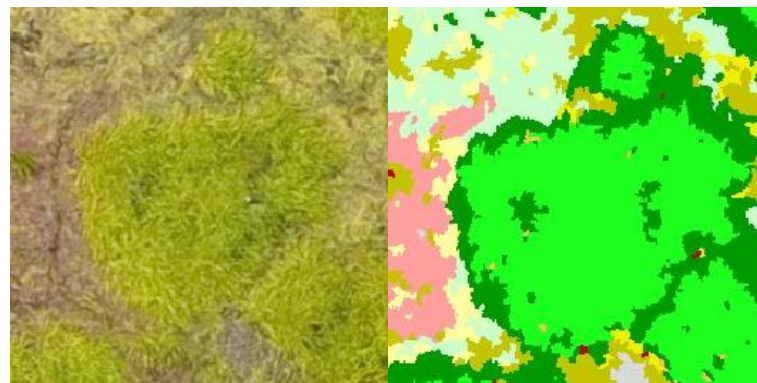


**Figure 16: Demonstration of edge effects in the classified imagery (Stage two, October 2018)**

While it was possible to reduce this 'edge effect' by including samples of segments representing these border areas in the training data, to fully eliminate the issue would have required the addition of multiple subclasses representing only borderline areas and across all possible combinations of neighbouring classes. Alternatively, post-processing of the image, replacing cells based on the majority values in their neighbourhood (such as with the 'majority filter' tool in ArcGIS) could have eliminated some of this effect, but could also have caused error-free areas of the raster to change values unnecessarily.

### *Class Similarity*

As the class roster includes a mix of generic classes representing several species and single-species classes, it is possible that the wider range of spectral and textural properties of the generic classes

includes data values that either match, or are sufficiently close to the narrower range of values representing the single-species class. A higher than expected degree of similarity between the segments representing different classes may be responsible for several of the low accuracy rates for certain classes, especially the high frequency of sedges being mis-classified as 'mixed grass'. While patches of sedge and mixed grass are easily distinguishable by an observer familiar with both types when viewing the aerial photographs, the purely numerical properties that the feature extraction module uses to segment and classify them may be close enough to overlap, leading some areas of exotic grasses to be classified as sedge, and vice versa.

### *Training Data*

While care was taken to ensure that training sites were properly distributed and only contained examples of the land cover class they were meant to (see section 3.5.2), the possibility that the range of acceptable values used to denote certain classes may have overlapped suggests that the selection of training sites is a likely source of error. Adding subclasses to cover variations in colour and texture within classes helped to eliminate some of this type of error. Additionally, subclasses were occasionally used to represent land cover classes in different locations. For instance, the 'Island Mixed Grass' subclass created to account for the higher elevation and longer leaves of the grass on the islands in stage one relative to the rest of the stage. Without this subclass, the classifier identified a significant proportion of the mixed grass across the whole image as 'Toetoe'<sup>17</sup> regardless of whether a DSM was applied. This subclass prevented the properties of grass in one specific location from affecting the values used to classify the remainder of the exotic grasses in the stage. However, in cases where two classes (or subclasses) were not easily separable based on the available data, it is unlikely that creating more subclasses would have been an effective strategy without additional information or insight into the properties of each class to separate the two.

The choice of mixing generic and species-specific classes could also have reduced the overall accuracy of the map. Consider the 'Manuka' and 'Other Tree (Dark Green) and (Brown)' classes. While Manuka trees have a single, fairly recognisable shade of green, the 'Other Tree' classes are trained on a variety of species which, while excluding Manuka, do include several species with not dissimilar heights and textures, as well as providing a wide bracket of spectral values which Manuka's own spectral properties fall into. This resulted in the classes being conflated with one another on occasion, thus reducing the accuracy of all of them. A sensible solution to the latter confusion would have been to include Manuka in one or the other of the 'Other Tree' class, however Manuka was

---

<sup>17</sup> Most of the Toetoe in stage one is concentrated on the raised islands.

kept separate as a test of the Feature Extraction Module's ability to pick a single species out from a variety of not dissimilar types.

#### *Accuracy Assessment Method*

While the method used to assess the accuracy of the classified images was a standard procedure, two factors relating to it may mean that the overall and class-specific accuracies may not be a true reflection of the accuracy of the classifications. Firstly, the accuracy assessment points were distributed according to a stratified random model, with the locations of the points based on the results of the classification process, not the actual locations of the target species for each class. There is a distinct possibility that rarer examples of vegetation types that do not occur often in the image, (such as 'dormant tree') which might only be represented by two or three individuals in the field, or types with many individual examples but only a small area visible in the images, (like Cabbage Trees) are disadvantaged by this approach. The random placement of accuracy points and number of points assigned to each class combining to mean few of the points were located on actual examples of a tree species, especially if many areas in the classified image were wrongly assigned to that class. Considering that user's accuracy should in principle shed light on the rate at which points representing a class were correctly classified, if there are only a dozen or fewer such points, this measure loses some of its statistical weight (Campbell & Whyne, 2011).

To overcome this, manually adding a small number of points in addition to those created by the random process would improve the representation of classes with a small presence in the field. Though care would need to be taken not to introduce bias by unintentionally distributing points in a way that stacked the accuracy assessment calculation in favour of a positive result. For instance, adding many points to represent a few examples of a class, rather than distributing an equal number of points around as many examples of the class as possible.

Additionally, using a method of accuracy assessment that considers the rate at which pixels were correctly classified seems out of step with a classification process that was otherwise focused on classifying whole objects, or portions of them. Since the results of the segmentation process often broke objects into several segments, there were several occasions where some of the segments representing a single object were correctly classified, while the others were not. If by chance an accuracy assessment point was located within the borders of this object, and within one of the incorrectly classified segments, then according to the confusion matrix the whole object would seem to have been incorrectly classified, when in truth only a portion of it was.

### **5.3 Convenience of UAV Mapping**

In this section, I describe the potential of UAV platform to offer convenient mapping solutions for a wetland environment, in line with research question one.

Over the course of this project, I have had the opportunity to use and evaluate two UAV platforms which are in common use worldwide and which are representative examples of two subtypes of quadrotor UAVs. Here I present my observations as to the convenience of using a UAV for a long-term wetland monitoring programme, with particular reference to the advantages afforded a volunteer or untrained monitor.

Here, 'convenience' is assessed through five qualitative measures:

- The logistics involved in deploying and operating the UAV
- The skill level required of the operator
- The operational capability of the UAV
- The capacity of the UAV to be used without disrupting the environment in which it operates
- The ease with which captured imagery may be converted into useful results.

Though my appraisal cannot apply to all the varieties of UAV, the prevalence of quadcopter types of similar size and capability to the DJI Phantom and Matrice models allows for the points raised here to apply to a sufficiently broad range of platforms.

#### **5.3.1 UAV Logistics & Ease of Use**

##### *Portability*

The Wairio wetland is not an unusual example of a New Zealand backcountry site. The launch points for each of the three stages were roughly five minutes' walk from the access road and reaching them required porting all necessary equipment over at least one fence or through a gate and walking over uneven ground. The proximity of the launch points to the access road is an advantage not shared by many backcountry locations, which might require longer periods of on-foot travel to reach and in such cases the operator may also need to carry other equipment, including food or water. Therefore, the portability of a UAV platform, determined by its size and weight, could be a deciding factor in whether that platform can be used for monitoring a remote site. Given that UAVs are now being deployed locations which have historically been inaccessible, and remain difficult to access such as the Antarctic (Bollard-Breen, Brooks, & Jones, 2015) post-earthquake cities (Baiocchi, Dominici, &

Mormile, 2013) and volcanic environments (Amici, Turci, Giammanco, Spampinato, & Giulietti, 2013), the ability of a platform of a certain size or weight to be transported in or around difficult locations is an important concern.

Not all wetlands are in the backcountry, and many can be found on farms or in areas with good vehicle access. However, the ease of transporting the UAV within a location is to ensure the UAV is launched from a location that makes the most efficient use of its limited battery. Since this location may not be the access point to the wetland, or the nearest road, the portability of a UAV platform when travelling on foot is a valid consideration.

The low weight (1.4kg) and small size (290mm x 290mm x 200mm) of the Phantom makes it easy to transport both to and within the survey location. The Phantom can be carried in a backpack-style case, making transporting the UAV to the designated launch point easy, even when getting there requires crossing fences or trekking over difficult terrain. This degree of portability is not shared by the Matrice. While the platform's weight (3.8kg) is not an issue of itself, its size (720mm x 220mm x 240mm while folded, 890mm x 890 x 380mm when rigged for flight) presents more of a challenge when trying to transport the UAV. The Matrice used in this project was provided with a protective case roughly the size of a suitcase, which proved cumbersome to carry (weighing 5kg when fully loaded). While such a case can be carried by one person relatively easily, doing so over longer distances becomes tiring, and the carrier loses a free hand with which they might otherwise operate gates, steady themselves or carry other equipment. Consequently, the Matrice, and UAVs of equivalent size are perhaps not best suited for use in backcountry sites not accessible by vehicle.

### *Ease of Use*

Flight planning requires a basic understanding of the principles of aerial photography. Since DroneDeploy and equivalent apps are compatible with most smartphones and tablets, making use of the app and its web browser-based counterpart should not be beyond the capability of the amateur operator.

Since the flight plan automates the entire flight from take-off to landing, operating the UAV in flight also requires little specialist knowledge. Nevertheless, the ability to manually fly the UAV in the event of emergencies is desirable. The method of control input for quadcopter UAVs is standardised across most models, regardless of manufacturer. Therefore, an operator who has flown one such UAV should have all the experience they need to operate a different model.

The automatic position holding system and collision avoidance sensors which are becoming increasingly common features of commercially-available models combine to make it easy to fly even

for inexperienced operators and greatly reduce the risk of accident through collision with the ground or obstacles, which proved useful when trying to land the UAV in a confined space of open ground little larger than the UAV itself.

### **5.3.2 Operational Capability**

#### *Endurance*

The battery life and comparatively short range of small quadcopter UAVs compared to fixed-wing varieties or conventional aircraft represent two significant limitations to the usefulness of such types for monitoring larger areas. While it is probable that the natural development of the technology over time will eventually reduce this restriction (Anderson & Gaston, 2013), it was clear that survey flights covering areas of around 8 hectares and with the high spatial resolution desired are comfortably within the capability of the UAV to perform. By tailoring the survey flight's desired levels of overlap, altitude and flight speed, I estimate that with the present development level of camera and battery technology, areas at least twice this size could be surveyed on a single battery without a significant loss of resolution or accuracy in the final classified image.

However, the regulations concerning line-of-sight operation can limit the range over which a UAV may be operated just as much as the battery capacity. Based on my experience in the field, a UAV of size equivalent to the Phantom remains visible up to around 300 metres from the observer, though this would vary based on individual eyesight, and the UAV's colour in contrast to the sky. Therefore, a single operator is limited to surveying small sites equivalent to the stages at Wairio unless they are supported by additional observers, or gain a qualification that permits beyond-line-of-sight operation.

#### *Vulnerability to Weather*

Unfavourable weather only prevented the completion of survey flights on two occasions, this can be ascribed to good advance planning rather than the UAV's resistance to weather conditions. In order for the UAV to follow the desired flight path, the wind must not to push the UAV off course. While UAVs of equivalent weight to the Phantom can hold their course in crosswinds of up to approximately 10 knots, in the event the UAV is blown off-track, it will halt in place and attempt to regain the correct line of flight before continuing. Alternatively, a strong headwind can prevent the UAV from making way in a certain direction as it must maintain a constant forward speed to keep the same amount of forward overlap between images. Therefore, winds close to or greater than the programmed flight speed can prevent it making any headway. Interference by wind can therefore cause the survey flight to take much longer than planned, which can prove problematic in the event

that spare charged batteries are not available. Meanwhile, especially strong gusts may blow the UAV into trees, resulting in the craft becoming damaged or stuck.

As a result, flights of the type conducted in this project might be difficult to perform successfully in locations that are more exposed to prevailing winds or are generally windier than the normally calm conditions in the Wairarapa.

### **5.3.3 Non-Disruptive Operation**

A small UAV would be unlikely to cause major damage to local vegetation in the event of a crash. Being lightweight limits the force of any impact with either trees or ground cover, and the fragility of smaller models means that a collision with a solid object like a tree trunk is more likely to damage the UAV than the plant.

An important consideration during the design of this project and during UAV operations was how the UAV might disrupt wildlife in the survey area. This is of importance from both an ethical and legal standpoint, as the Wairio block is home to a number of protected bird species which the Wildlife Act of 1953 prohibits disturbing or harming, whether deliberately or by accident (Department of Conservation, 2019). While UAVs have been used in close proximity to birds in previous studies without incident (Chabot & Bird, 2011), DOC guidelines and 'best practice' recommendations from the scientific community (Gonzalez & Johnson, 2017; Cowie, et al., 2018) recommend bringing flights to an immediate halt in the event of an alarmed or aggressive response to the UAV by local bird life. There is a growing field of study into the possibility of using UAVs as aerial scarecrows, exploiting their disruptive potential for the purpose of repelling birds from agricultural sites (Wang, Lucas, Wong, & Charmitoff, 2017), the opposite of the intent of this project.

The rotors of quadcopter UAVs spin at several thousand revolutions per minute and can cause serious injury on contact, especially to smaller birds. Meanwhile the noise of the UAV is known to cause distress to some birds and animals (Gonzalez & Johnson, 2017; LaFrance, 2016), and the UAV flying over nest sites could provoke a defensive or alarmed response from nesting birds mistaking the silhouette of the UAV overhead for a predator (Cowie, et al., 2018). Additionally, several of the species present at Wairio and commonly found in wetlands nationwide are either large enough to do a UAV serious harm in the event of a collision or known to mob assumed predators in defence of nests. Consequently, the potential for an unintended interaction between bird and drone causing harm to either party was a valid concern that needed to be minimised if possible.

While the resident bird life demonstrated a range of reactions to the UAV, none appeared to be unduly disturbed by its presence and none demonstrated aggressive (or defensive) behaviour towards it. Australasian harriers, which I assumed would pose the most risk to the flight by virtue of

their size and position as the dominant predator in the location, appeared to have little interest in the UAV. Water birds, such as swans and pukeko, were never observed to be startled by the UAV flying overhead, and several can be observed at rest or nesting in some of the orthomosaics. Small birds (typically swifts) occasionally circled the UAV at a safe distance for less than a minute, but never flew towards it as if to engage a predator, so I attribute this behaviour to curiosity rather than aggression. This is not to suggest that care need not be taken while operating near birds, but does lend credence to the possibility of using UAVs for monitoring bird life, after Chabot & Bird (2011) and shows that UAVs can operate in areas populated by protected wildlife without unduly disrupting said wildlife, as long as the operator uses caution and common sense.

### **5.3.4 Post-Flight Processes**

While learning to operate a UAV is not difficult, processing geospatial data is a specialised task and the typical monitoring volunteer may not be able to gain competence. However, there are still options for data processing that are relatively accessible to the untrained individual. Processing raw photos into orthomosaics by uploading them to a cloud-based system is a straightforward process that is not much more complex than uploading photos to a social media account. While such cloud-based systems require no additional software or training on the end-user's part, this method sacrifices a degree of control over the finished product that would be retained if the user processed their own data through a programme such as Pix4D.

Classifying imagery requires direct involvement on the part of the user. Unlike orthomosaic creation, classification requires the user to acquire and familiarise themselves with a geoprocessing software suite capable of object-based image analysis. Several options are available, ranging from specialised programmes to all-purpose suites. Cost-wise, the user has a choice of paid programmes or free and open source software. Despite this, it must be acknowledged that the average person may not be proficient in GIS programmes or 'tech-savvy' enough to become so under their own training. If performing a simple classification with only half a dozen classes is beyond the user's capability, regardless of whether the limiting factor is their skill or the software available to them, it may be that producing an orthophoto is all that is needed. Depending on the requirements of the end-user, a suitably detailed orthophoto may suffice for the identification of certain land cover classes. For instance, consider the case of the weed control contractor described in section 5.1.6.

In this instance, a user with sufficient familiarity with the appearance of blackberry plants would have no difficulty in picking these out and indicating their general location with enough precision for the contractor to locate the plants in the field. This task does not require the precise delineation of the borders of the blackberry patch that image classification would provide, as the contractor can determine these themselves in the field. The time saved by providing the contractor with a

photographic map rather than having them search the wetland on foot for individual plants would significantly reduce the contractor's operating costs, and therefore save the restoration team money which could then be redirected to other ends.

#### **5.4 Improving Effects of the DSM**

Sections 5.4 and 5.5 relate the effects of including different combinations of ancillary data in image classifications, with a focus on the impact on the accuracy of the classification process. These sections address research question two.

When a DSM was included in the classification process, both the overall accuracy of the entire classification and that of each class contained within improved. The classes that experienced improvements of the greatest magnitude were primarily those that represented larger vegetation types, such as Kahikatea. As increases in overall accuracy and kappa on the application of the DSM were both present and statistically significant, there are grounds to accept the hypothesis that the DSM allows the classification process to distinguish between low-lying ground cover and larger plants, even if they were visually similar. This confirms the findings of the studies that argue in favour of the use of topographic data in image classification (Cao, et al., 2018; Kim, Madden, & Xu, 2010; and Corcoran, et al., 2012).

In certain circumstances, smaller Kahikatea trees were not readily visible in the aerial photographs as they feature a very similar colouration to the ground cover beneath them (as in figure 17 below), thus the vertical perspective of the photo meant the trees blended into the background. In some cases, the presence of a tree was only given away by the shadow it cast. As a result, the 'Kahikatea' class returned low classification accuracy rates in the RGB-only tests, with a high instance of confusion with ground cover classes, or with other tree-type classes in images where the Kahikatea was distinguishable. With the addition of the DSM, the rate of confusion between Kahikatea and other trees dropped significantly as even the smaller Kahikatea were several metres taller than all other trees nearby, and so the DSM values were able to provide a point of difference when spectral values could not. This is a similar trend to that observed by Cao, et al., (2018) when trying to distinguish mangrove species with similar spectral properties, but significant differences in size.



**Figure 17: Two Kahikatea trees in stage one blend into the background in the leftmost image (Winter, 2018), but are clearly visible in the image to the right (Spring, 2018).**

The improvements were less pronounced for classes that do not have a significant vertical presence, such as 'water' or '*Isolepis*', but were still present. This small improvement may be due to the DSM providing additional information about the texture or roughness of the surface, helping to increase the rate at which individual segments were merged or providing an extra characteristic to allow the classification algorithm to differentiate otherwise similar segments. In figures 18 and 18b, extracts from the classified imagery for stage two in June 2018 are compared, to illustrate the effect of including a DSM.

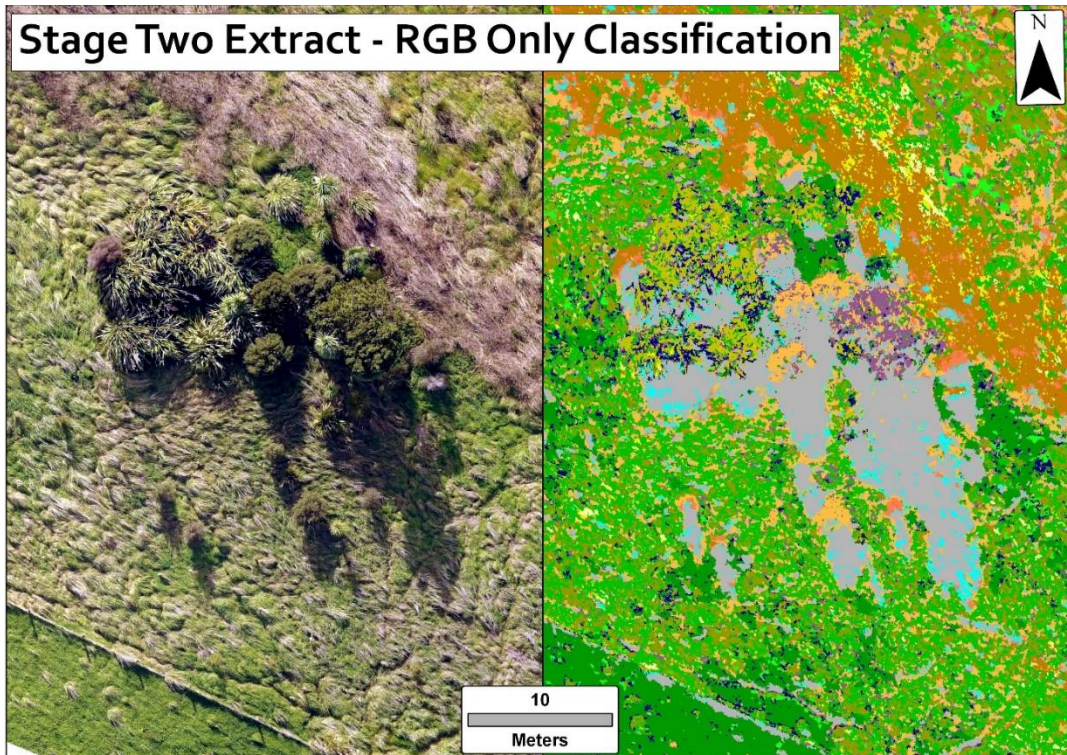
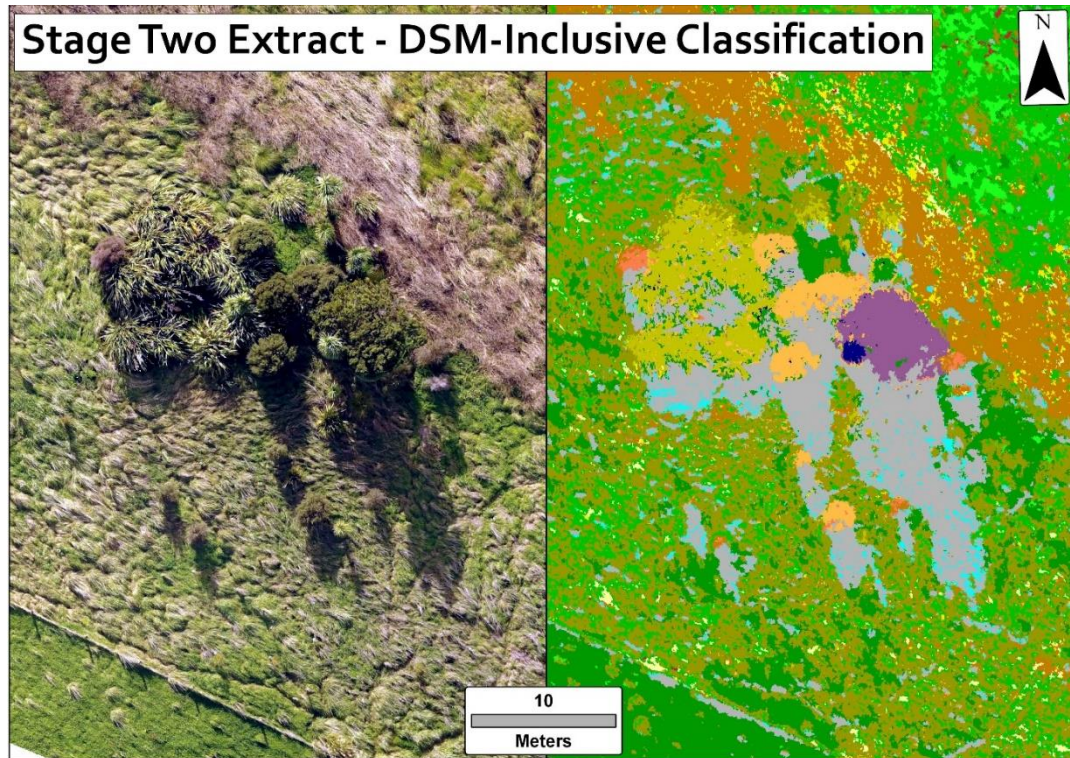


Figure 18a & 18b: Comparing RGB-Only (above) and DSM-Inclusive Classifications (below) of stage



Since a DSM must be produced as a precursor to the creation of a proper orthomosaic, it requires no extra effort on the part of the user to produce. Because of this, the DSM is effectively a free source of ancillary data, as there is no cost to its production and use other than a small increase in processing time during the classification phase. Therefore, given the ease of DSM creation and the fact that DSMs have been proven to increase accuracy in measurable and statistically significant amounts, it is unclear why a DSM should ever not be used, if the option to employ ancillary data exists.

## 5.5 Multispectral Camera Imagery Tests

Despite the lower spatial resolution of the imagery (approximately 4cm/pixel), the accuracy levels of the classifications produced with the RedEdge multispectral camera are equivalent to those

produced from the true-colour imagery from the Phantom's stock camera. However, despite the additional sources of ancillary data produced by the RedEdge, combining all of these datasets did not result in a greater degree of accuracy than was attained with the Phantom camera's products. Nevertheless, the inclusion of the multispectral ancillary data did produce a significant improvement in classification accuracy.

### 5.5.1 Data Quality Issues

Three problems with the raw imagery may have prevented the accuracy of the final classifications of the RedEdge-sourced imagery exceeding the bar set by the Phantom imagery. The first and most prevalent are areas in the orthomosaic that appear out-of-focus compared to the rest of the image (Figure 19).



**Figure 19: Extract from Stage One Orthomosaic (April 2019) showing the blurred areas.**

Why this should have happened was initially unclear, though vibration and movement of the camera is a probable cause (Wigmore, pers. Comm. 2019). The attachment that connects the RedEdge camera to the Matrice is a fixed type (figure 20), which cannot automatically adjust for pitch and roll as motorised gimbals can. Most importantly, the fixed mount offers no dampening of the high frequency vibrations of the UAV's motor, which pass directly from the UAV's fuselage and into the camera. The frequency of this vibration is high enough that even extremely high shutter speeds offered by global shutters such as that fitted to the RedEdge cannot always eliminate blurring caused by the camera moving as the image is recorded. The Matrice does have three vibration dampers fitted to the camera mounting point, but it appears these were not enough to reduce vibration to manageable levels. Possibly the attachment between the camera itself and the mounting adapter was not secure enough to prevent vibration. In addition to the UAV's own motion, strong wind gusts

on the day of capture may have contributed additional movement to the camera during the exposure windows.



**Figure 20: The mounting arrangement for the RedEdge Camera**

This phenomenon of movement-induced distortion is quite common in cheaper multispectral cameras (Wigmore, pers. Comm. 2019), which feature rolling shutters as opposed to high-speed mechanical ones. Cameras fitted with this type of shutter begin scanning an image from one edge of the frame, rather than by taking a snapshot of the whole frame at once, so if the camera moves while the shutter rolls, then parts of the image may be distorted. While such distortion is less common in cameras with global shutters (Rengarajan, Rajagopalan, Aravind, & Seetharaman, 2016), it is not the case that it never occurs. Vibration-induced blur can have a marked negative effect on a program's ability to detect tie points between a pair of images. Sieberth, Wackrow and Chandler (2015) tested the effect that vibrations of different magnitude had on this aspect of photogrammetry and experimented with overlapping a single sharp image and a single blurred image, with the blur induced by vibrating the camera while the image was captured. Once displacement during exposure windows increased beyond around 0.25mm, the rate of correct tie point registration declined rapidly. Displacement of as little as 0.377mm reduced the number of detected tie points by 28%, and the number of correctly referenced points by 83% - from a total of 12,214 possible ties, only 1,524 were matched correctly. At a displacement of 1.028mm, the number of correctly registered points was only 47 (Sieberth, Wackrow, & Chandler, 2015). While the amount of vibration affecting the RedEdge camera in flight cannot be known, it is clear that not much movement is necessary to induce blur. Considering that the camera is already in motion regardless of any vibration, blur induced by the camera being displaced in the interval that the camera's shutter is open is the most likely cause of the blurred areas in the orthomosaic.

The effect of motion blur may be compounded by the fact that the RedEdge camera takes five separate images to represent the five spectral bands it can detect. These five images are all offset from each other owing to the layout of the camera's lenses and must be overlaid with one another to form a single multiband raster image, which is then used to create the final orthomosaic. Therefore, motion blur has the potential to distort imagery on two occasions when precise detection of tie points is needed: first when the five image bands are composited and again when the composite images are overlaid.

Two options to counter this blurring in future uses of the camera are recommended, both of which are applicable to all deployments of sensitive imaging sensors. Either ensure the mounting kit is fitted with strong vibration dampers and confirm that the camera is as securely fastened to the mount as is possible, or edit the finished orthomosaic to remove distorted raw images. However, while the latter option is offered by paid software suites such as AgiSoft Photoscan, it is not offered by PrecisionMapper, so this represents a drawback to processing images in a closed system where the user forfeits control for the sake of convenience. While removing distorted photos before they were uploaded is possible, either by deleting them or applying blur correction algorithms, it would also be very time-consuming in this case, as the RedEdge camera captured in the region of 3000 images per stage.

Another workaround for this issue would be to increase the altitude at which images were taken. The increased relief between the camera lens and the photographed surface would reduce the distortion, while at the same time also reducing the spatial resolution of the images. Given that a high level of spatial resolution is needed for reliably identifying training areas for species specific classification, such a workaround could make identifying some land cover classes difficult. Reducing the UAV's flight speed to reduce the amount of camera movement during exposures would also be effective.

The total area of each image affected by distortion was around 10% of the total area of each map. However, as the dominant land cover type in the blurred areas was still identifiable, I opted to keep the data and used subclasses in the training dataset to represent land cover in the blurred areas and so reduce the rate of classification errors.

The second issue in the orthomosaics concerns high levels of overexposure, this may be attributed to the sun briefly breaking through the cloud cover and the camera not adjusting its exposure settings in time. This only occurred in stage two and affects around 0.0005% of the total area of the stage, so this is a very minor issue. Additionally, the only land cover class affected are the already light-coloured dry vegetation types, which are difficult to make out in the over-exposed areas. This issue was countered by created an 'over-exposed' subclass for the land cover classes in these areas.

A final issue appears to have been caused by a GPS tagging error. Partway through the flights over stages two and three, the GPS module used to geotag the photographs seems to have lost its position fix. As a result, some images were marked as being in a different location to their actual position. Consequently, a section of each orthomosaic is missing, as without correct GPS data these images could not be properly overlapped with the other images in the mosaic. However, a smaller area to classify should not have any effect on the resulting classification accuracy scores. Stage two lost an area of 0.43ha, around 5% of its total area, but the remaining classifiable area was still larger than either of the other stages, so I believe the results to be still be meaningful. Meanwhile stage 3 only lost 0.07ha (approx. 1% of the total area), meaning the loss of data here was negligible.

### **5.5.2 Benefits of additional ancillary data**

As expected, the addition of near-infrared and red edge imagery provided measurable and significant improvements in classification accuracy. However, it is curious that the inclusion or exclusion of a DSM appears to have had little effect on the accuracy of this set of imagery. In theory, the addition of just the DSM to the base RGB imagery should have increased the overall accuracy and kappa score, but this increase was not evident. Likewise, only a small improvement was evident when the DSM was included alongside multispectral ancillary data.

The inclusion of DSMs as ancillary datasets is not always effective in all applications (Campbell & Whyne, 2011; Puzinas, 2017). However, it is not clear why it should not have been so in this instance, as the RGB and DSM datasets from the Phantom and RedEdge cameras are of comparable resolution and the classifier was trained on the same objects. The DSM produced by the RedEdge-M images was of slightly lower resolution (Figure 21b), but still picked out the same areas of larger vegetation as the DSM produced from the Phantom's camera. Therefore, the three-dimensional information provided by the DSM should have increased the user and producer accuracy of certain classes, and thus a noticeable difference in overall accuracy and kappa. It is not impossible that the lack of improvement could be grounded in user error, for instance if the segmentation and classification process were not configured to include the DSM, then no effect would be evident. However, as three separate iterations of an RGB + DSM classification were run, it is unlikely that such an error would have recurred on three occasions. The distortion effects in the base RGB dataset could have offset improvements in accuracy – but as these were kept isolated by training data subclasses and only affected a small portion of each image in any case, increases in classification accuracy throughout the rest of the image should still have been present.

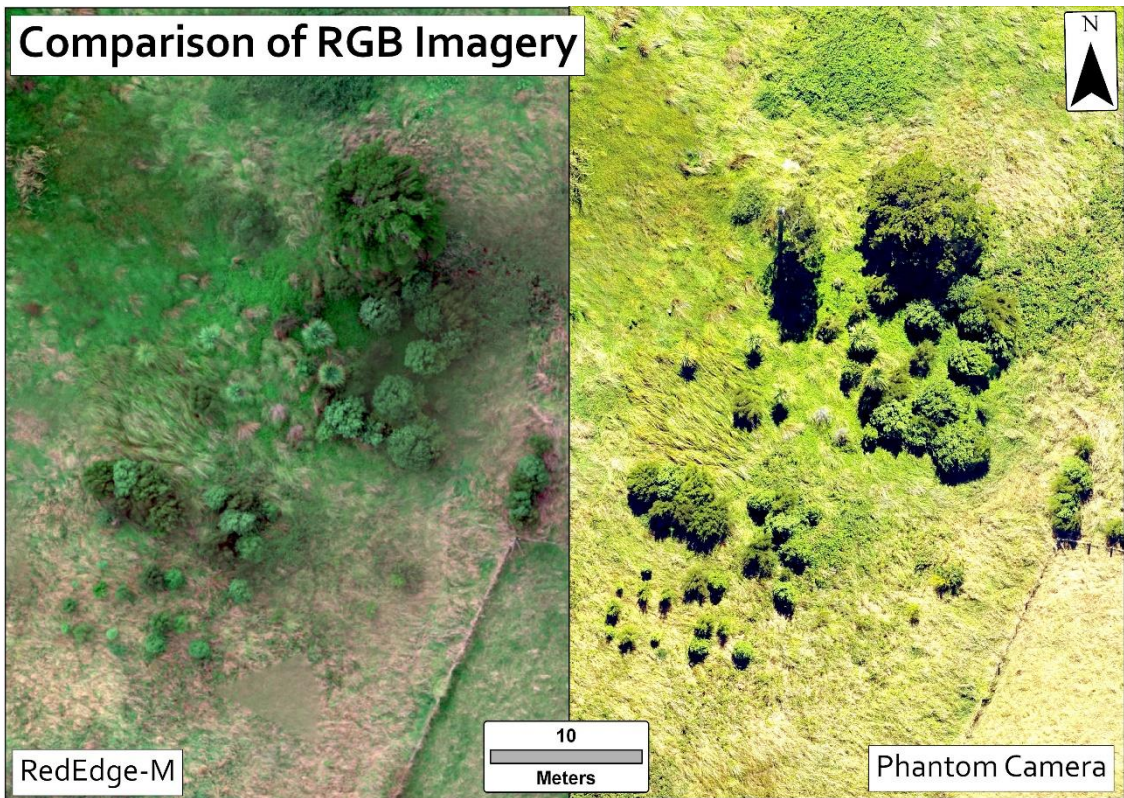
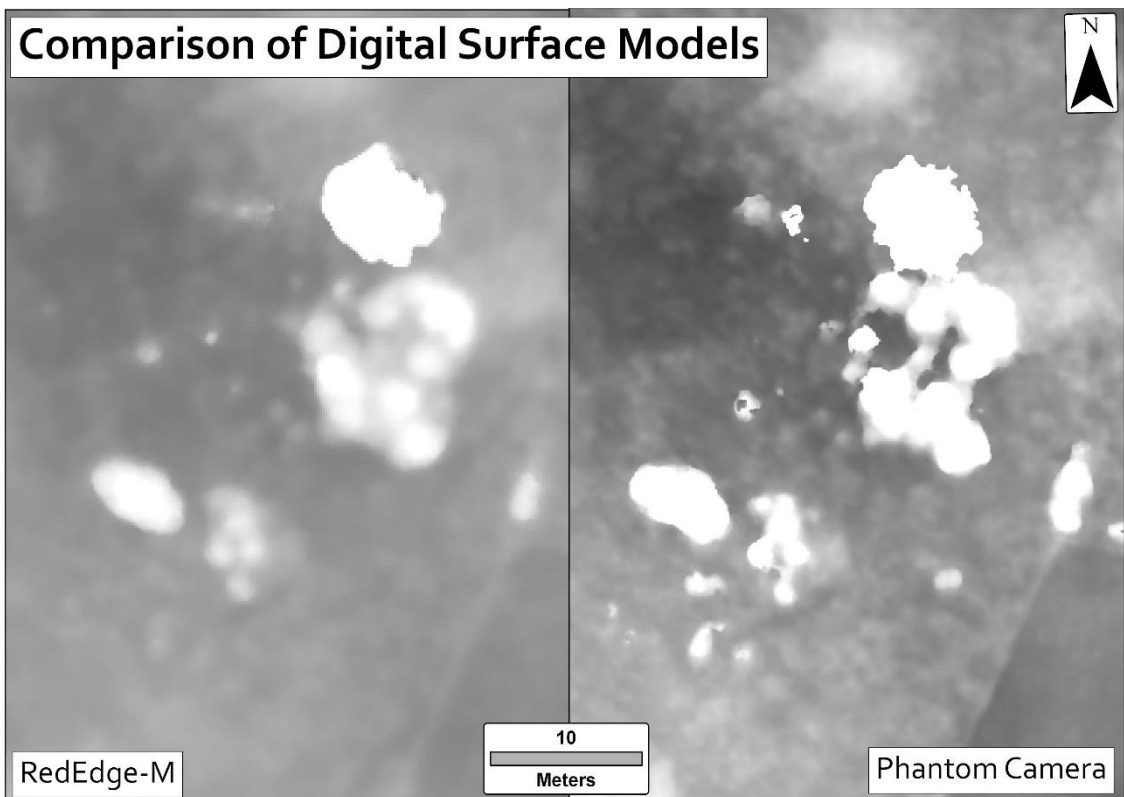


Figure 21a & 21b: Comparison of base orthomosaics (above) and DSM resolution (below) between the two cameras. The area shown is an extract of stage three, as surveyed on the 5<sup>th</sup> of March (Phantom) and 4<sup>th</sup> April 2019 (RedEdge-M)



However, inclusion of multispectral (NIR and RE) data did have a pronounced positive effect on classification accuracy and did so with an extremely high level of statistical significance (see tables 4.6 and 4.7). Here, the increase in accuracy stems from the additional data improving the classifier's ability to distinguish between classes on spectral grounds, rather than adding a topographic element to act as a unique identifier. The bulk of the improvement is probably due to the inclusion of the NIR band as opposed to the RE band, as the former band is considered to offer the greatest degree of spectral separability between otherwise similar vegetation classes (Everitt, Yang, Fletcher, & DeLoach, 2008).

## **5.6 Evaluation**

### **5.6.1 Survey Flights**

In keeping with the principle of 'bad data in = bad data out', faults in the methodology of the survey flights would have led to unsatisfactory results in either the creation of the aerial imagery datasets or the classification result drawn from them. However, I can state with confidence that the flights were conducted in accordance with accepted best practice methods and produced results that were of satisfactory quality. Given time to familiarise myself with the RedEdge-M, the flaws in the images captured with this camera could have been eliminated. As discussed in section 5.5.1 however, I do not believe they will have resulted in a significant drop in accuracy as I was able to introduce measures to work around them, such as the introduction of subclasses to represent example of land cover types that were overexposed or blurred.

Given the intent of this project to explore the capabilities of multispectral mapping, conducting additional flights to capture this type of data would have been desirable. This was not done for two reasons, the first of which was financial. Conducting multispectral mapping at seasonal intervals in tandem with the other survey flights would have given me a great deal more data to work with and thus might have allowed me to produce more statistically significant results to inform my conclusions about the usefulness of multispectral imagery for identifying individual land cover classes. However, the RedEdge camera was not available from the outset of this project, so acquiring multispectral imagery would have required contracting a professional operator on multiple occasions. The budget was not available for this project.

While the UAV was easily acquired, unforeseen delays in modifying it to be compatible with the RedEdge camera's mounting kit meant the combined set of equipment was not ready for use until late March 2019, too late to align with any of the seasonal imagery.

## 5.6.2 Image Processing

Given that several classes were not accurately classified, a revised approach to the image segmentation or classification process might have been desirable. It may be that the number of classes I sought to classify was too ambitious, as image classification typically becomes less precise as more classes are introduced, creating more opportunities for error (Campbell & Whyne, 2011). To avoid this issue a classification scheme with only a few generic classes (as was used for the change detection tests) could have been employed. Exploratory classifications of the seasonal imagery from March 2019 using the change detection classes defined in section 3.6 produced overall accuracy levels as shown in table 5.3 below, demonstrating a clear improvement in all cases:

**Table 5.3: Contrasting Classification Accuracy between schemes with many and few classes based on March 2019 imagery**

Stage:	Overall Accuracy: Original Classification Scheme	Overall Accuracy: Five Classes	Difference
Stage One	53% (19 Classes)	63%	10%
Stage Two	68% (14 Classes)	83%	15%
Stage Three	57% (18 classes)	78%	21%

While this would have been less useful for the purposes of identifying and locating specific species of plant, it would still have provided a much more detailed documentation of the surface cover at Wairio than is currently available. The New Zealand Land Cover Database (Landcare Research New Zealand Ltd - Informatics Team, 2018) only lists two land cover classes in the survey area: ‘Herbaceous Freshwater Vegetation’ and ‘Low Producing Grassland’, and ignores all areas of water and larger vegetation. Alternatively, a more rigorous approach to image segmentation, employing multiple levels of segmentation for different surface types (after Pande-Chhetri *et al* (2017)) and merging the results into a single classified image rather than trying to tailor a single setting to best suit all surfaces could have reduced some of the loss in accuracy for the classes that were typically broken into very small segments.

## Chapter 6

### Conclusions

#### 6.1 Research Question One

*Test the proposition that UAVs can provide accurate and convenient assessment of changes in vegetation and water coverage over time, using a recovering wetland area as a case study.*

The use of the UAV to gather the data for this project allowed for total avoidance of environmental damage and was not observed to disrupt local fauna, both of which are highly desirable in fragile or protected environments such as wetlands. The large degree of automation in the data capture and initial image processing allows for this type of project to be conducted by anyone with access to the required equipment, regardless of prior experience or training, although the process of classifying images may remain beyond the reach of the amateur for the moment. The resolution of the orthomaps produced (~2cm/pixel) was more than sufficient for reliable visual identification of many different species of vegetation in the area, and such high-resolution imagery can be advantageous to end-users of the imagery even without being run through an image classifier. Consequently, this project demonstrated that the use of UAVs can provide small and inexperienced operators with a convenient, non-disruptive and user-friendly option for remote sensing of fragile or difficult to access areas.

Using object-based methods to classify vegetation and other surface types at the Wairio wetland block proved difficult to perform with a consistently high level of accuracy. This was partly due to the level of variability within classes, partly to too little variation between classes used for training the classifier and partly due to the difficulty in finding segmentation settings that allowed for the best representation of all classes. Despite this, the classifier showed a promising ability to detect certain individual land cover classes which are more easily distinguished from their surroundings by virtue of their spectral properties and the high spatial resolution of the UAV-sourced imagery. This proves that the OBIA process would be well-suited to more targeted applications where tracking a single class (for instance *Bidens frondosa*) was desired.

Though the initial classification scheme developed to inventory local land cover resulted in only a moderate level of accuracy, this did not prevent the use of a modified, more generic version of the classification scheme being used for accurate mapping of the changing water levels within the wetland over the course of the year. Neither did the limited accuracy of the classified maps prevent them being employed by a third party with limited GIS knowledge to good effect. This should not be considered a challenge to the idea that higher levels of classification accuracy are always desirable.

However, this project does serve as an example of how a high level of accuracy is not always necessary to provide a useful finished product. This is because an interpretation of a classified image based on the user's own knowledge and common sense can overcome inaccuracies by filtering out false results. Therefore, I propose that classification processes that do not feature high accuracy levels of overall accuracy should not be immediately dismissed as invalid or being of no use.

## 6.2 Research Question Two

*To what extent is the accuracy of the image classification process improved with the addition of ancillary data, such as digital surface models or near infrared imagery?*

With respect to the beneficial effects of ancillary datasets for image classification; the inclusion of a DSM to the classifier produced a clear improvement in accuracy in the majority of cases and was particularly effective when used to distinguish taller vegetation types (such as trees) from ground cover. In terms of overall accuracy, the DSM's inclusion in the classification process resulted in an average increase of 10.25% OA and 0.11 kappa. The average magnitude of improvement on a class-specific basis was around 13% in terms of user's and producer's accuracy, with a maximum improvement of 43.5% and above average improvements were exhibited vegetation types of larger size than ground cover. As no extra effort was required to produce the DSM and the resulting improvements have the potential to be significant in terms of both magnitude and statistical meaning, these findings represent a strong case for the inclusion of topographic data in all such classifications.

Likewise, the inclusion of multispectral ancillary data resulted in a pronounced and extremely statistically significant improvement in overall accuracy (averaging 9.33%) and kappa (averaging 0.11) in all cases. In this case, improvements were more evenly distributed across all classes, and particularly strong improvement such as those provided to large vegetation types by a DSM were not evident. However, a statistically meaningful measurement of the average improvement in class-specific accuracy could not be obtained, which was partly due to a smaller set of results to draw conclusions from. What results were obtained suggest that producer's accuracy was especially improved by the inclusion of multispectral data, as the average increase in this metric (16%) was double that of user's accuracy (8%).

Contrary to expectations, an approach that combined a DSM with multispectral imagery only exhibited a negligible synergistic improvement in accuracy – the difference amounted to an average of only 2% OA and 0.02 kappa. Therefore, I cannot conclusively determine whether the two data sources could be combined to offer superior accuracy levels in contrast to those derived from only a consumer-grade true-colour camera with a higher spatial resolution. Nevertheless, the beneficial

effect of the inclusion of multispectral data itself was clearly shown, even in a small dataset. With refinements to the process by which this data was gathered, and the classification process itself, a strong synergistic improvement through the inclusion of both topographic and multispectral ancillary data could be proved possible.

### **6.3 Future Research Opportunities**

#### *Synergistic Improvement from Ancillary Data Sources*

In the tests which involved the digital surface model produced from the RedEdge, no improvement in classification accuracy was evident when the DSM was added to the classification process. This was not the expected outcome and a reason was not established. It may be that the source of the error lies in the resolution of either the DSM or the base RGB imagery. It would be of interest to test whether an approach which combined higher-resolution RGB imagery and DSMs from a true-colour-only camera mounted to a UAV with multispectral data from space-based, aerial or UAV mounted sensors could leverage the respective strengths of the two sensor types to provide a stronger synergistic improvement.

#### *Land Cover as Ancillary Data*

A second premise worth investigation would be whether historical land cover classifications can be used as ancillary data to enhance the accuracy of future classifications of the same area, a topic which is not yet well addressed in the existing literature. Theoretically, certain classes should remain constant over long periods, for instance, trees or larger vegetation. In the context of Wairio, a Manuka tree present in one year is likely to be present in the same location a year or more in the future, so it appears logical that knowing that an object was previously classified as 'manuka' would greatly increase the chance of that object still being a manuka tree. However, it is not clear whether this logic would hold in the case of land cover classes that frequently supplant one another, which is much more likely with lower-lying ground cover classes.

An additional line of investigation would be whether land cover representing one season could be used to improve classifications for a different season. For instance, does knowing that a certain site was floodwater in winter increase the classifier's ability to correctly classify emergent *Bidens frondosa* when the water retreats from those sites? Other points of interest would be the necessary level of classification accuracy and specificity (i.e. the number of distinct classes) needed to reliably improve results. If historical land cover can serve as a reliable predictor of future land cover, this would be a useful, if perhaps situational tool to improve classifications of areas that exhibit pronounced seasonal variation, or that may feature significant change over long periods, such as recovering wetlands.

## Bibliography

- Amici, S., Turci, M., Giammanco, S., Spampinato, L., & Giulietti, F. (2013). UAV Thermal Infrared Remote Sensing of an Italian Mud Volcano. *Advances in Remote Sensing*, 2, 358-364.
- Anderson, K., & Gaston, K. (2013). Lightweight unmanned aerial vehicles will revolutionize spatial ecology. *Frontiers in Ecology and the Environment*, 138-146.
- Ausseil, A., Gerbeaux, P., Chadderton, W., Stephens, T., Brown, D., & Leathwick, J. (2008). *Wetland ecosystems of national importance for biodiversity: Criteria, methods and candidate list of nationally important inland wetlands*. Landcare Research.
- Avery, T., & Berlin, G. (1992). *Fundamentals of Remote Sensing and Airphoto Interpretation* (5th ed.). Prentice Hall.
- Baiocchi, V., Dominici, D., & Mormile, M. (2013). UAV Application in Post-Seismic Environment. *International Archives of the Photogrammetry, Remote Sensing and Spatial Information Sciences*, 40(1), 21-25.
- Bakeman, R., Quera, V., McArthur, D., & Robinson, B. F. (1997). Detecting sequential patterns and determining their reliability with fallible observers. *Psychological Methods*, 2(4), 357-370.
- Berhane, T. M., Lane, C. R., Wu, Q., Autrey, B. C., Anenkhonov, O. A., Chepinoga, V. V., & Liu, H. (2018). Decision-Tree, Rule-Based, and Random Forest Classification of High-Resolution Multispectral Imagery for Wetland Mapping and Inventory. *Remote Sensing*, 10(4), 580.
- Bhatt, A. (2019). *A review of change detection techniques*. Retrieved February 21, 2019, from <http://aves.ktu.edu.tr/ImageOfByte.aspx?Resim=8&SSNO=29&USER=3847>
- Blaschke, T. (2010, January). Object based image analysis for remote sensing. *ISPRS Journal of Photogrammetry and Remote Sensing*, 65(1), 2-16.
- Bollard-Breen, B., Brooks, J. D., & Jones, M. R. (2015). Application of an unmanned aerial vehicle in spatial mapping of terrestrial biology and human disturbance in the McMurdo Dry Valleys, East Antarctica. *Polar Biology*, 38(4), 573-578.
- Campbell, J. B., & Whyne, R. H. (2011). Image Classification. In *Introduction to Remote Sensing (5th ed)*. New York: Guilford Press.
- Campbell, J., & Whyne, R. H. (2011). Accuracy Assesment. In *Introduction to Remote Sensing (5th Ed.)* (pp. 408-419). New York: Guilford Press.
- Cao, J., Leng, W., Liu, K., Liu, L., He, Z., & Zhu, Y. (2018). Object-Based Mangrove Species Classification Using Unmanned Aerial Vehicle Hyperspectral Images and Digital Surface Models. *Remote Sensing*, 10(1), 89.
- Chabot, D., & Bird, D. M. (2011). Evaluation of an off-the-shelf Unmanned Aircraft System for Surveying Flocks of Geese. *Waterbirds*, 35(1), 170-174.
- Chisholm, R. A., Jinqiang, C., Lum, S., & Chen, B. M. (2013). UAV LiDAR for below-canopy forest surveys. *Journal of Unmanned Vehicle Systems*, 1(1), 61-68.
- Civil Aviation Authority (NZ). (2017, October). *RPAS, UAV, UAS, Drones and Model Aircraft*. Retrieved October 7, 2017, from Civil Aviation Authority of New Zealand: <https://www.caa.govt.nz/rpas/>
- Civil Aviation Authority of New Zealand. (2018, December). *Part 101 - CAA Consolidation*. Retrieved January 16, 2019, from Civil Aviation Rules: [https://www.caa.govt.nz/assets/legacy/rules/Rule\\_Consolidations/Part\\_101\\_Consolidation.pdf](https://www.caa.govt.nz/assets/legacy/rules/Rule_Consolidations/Part_101_Consolidation.pdf)
- Congalton, R., & Green, K. (2008). *Assessing the Accuracy of Remotely Sensed Data: Principles and Practices* (2nd ed.). Taylor & Francis Group, LLC.
- Corcoran, J., Knight, J., Brisco, B., Kaya, S., Cull, A., & Murnaghan, K. (2012). The integration of optical, topographic, and radar data for wetland mapping in northern Minnesota. *Canadian Journal of Remote Sensing*, 37(5), 564-582.
- Cordeiro, C., & Rossetti, D. (2015). Mapping vegetation in a late Quaternary landform of the Amazonian wetlands using object-based image analysis and decision tree classification. *International Journal of Remote Sensing*, 36(13), 3397-3422.

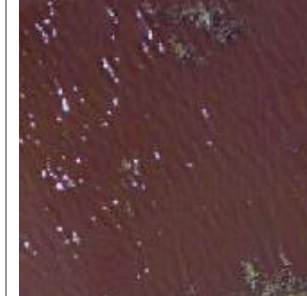
- Cowie, N., Swinfield, T., Humpidge, R., Williams, J., Bridge, D., Casey, C., . . . Morris, D. (2018). *Drones for GIS - Best Practice*. Royal Society for the Protection of Birds.
- Dandois, J. P., Olano, M., & Ellis, E. C. (2015). Optimal Altitude, Overlap, and Weather Conditions for Computer Vision UAV Estimates of Forest Structure. *Remote Sensing*, 13895-13920.
- Department of Conservation. (2019). *Flying drones near birds*. Retrieved May 10, 2019, from Drone use on Conservation land: <https://www.doc.govt.nz/get-involved/apply-for-permits/drone-use-on-conservation-land/flying-drones-near-birds/>
- DigitalGlobe. (2014, June 11). *U.S. Department of Commerce Relaxes Resolution Restrictions, DigitalGlobe Extends Lead in Image Quality (press release)*. Retrieved October 25, 2018, from <http://investor.digitalglobe.com/phoenix.zhtml?c=70788&p=irol-newsArticle&ID=1939027>
- DigitalGlobe. (2017, June 28). *WorldView-4 Data Sheet*. Retrieved October 26, 2017, from [https://dg-cms-uploads-production.s3.amazonaws.com/uploads/document/file/196/DG2017\\_WorldView-4\\_DS.pdf](https://dg-cms-uploads-production.s3.amazonaws.com/uploads/document/file/196/DG2017_WorldView-4_DS.pdf)
- Dronova, I., Gong, P., & Wang, L. (2011). Object-based analysis and change detection of major wetland cover types and their classification uncertainty during the low water period at Poyang Lake, China. *Remote Sensing of Environment*, 115(12), 3220-3236.
- Dronova, I., Gong, P., E, C. N., Fu, W., Qi, S., Liu, Y., & Wang, L. (2012). Landscape analysis of wetland plant functional types: the effects of image segmentation scale, vegetation classes and classification methods. *Remote Sensing of Environment*, 127, 357-369.
- Ducks Unlimited. (2016, March). *Wairio Wetland Restoration Strategic Plan 2016-2020*. Retrieved January 19, 2019, from Ducks Unlimited New Zealand: [https://www.ducks.org.nz/images/PDF/Wairio\\_Wetland\\_Restoration\\_2016.pdf](https://www.ducks.org.nz/images/PDF/Wairio_Wetland_Restoration_2016.pdf)
- Everitt, J. H., Yang, C., Fletcher, R., & Deloach, C. J. (2008). Comparison of QuickBird and SPOT 5 Satellite Imagery for Mapping Giant Reed. *Journal of Aquatic Plant Management*, 46, 77-82.
- Feltham, C. (2006). *Didymosphenia geminata (Didymo) in New Zealand*. Wellington: Parliamentary Library of New Zealand.
- Fleiss, J. L. (1981). *Statistical methods for rates and proportions*. New York: John Wiley.
- Gelasca, E. D., Ebrahimi, T., Farias, M., Carli, M., & Mitra, S. (2004). Towards perceptually driven segmentation evaluation metrics. *Conference on Computer Vision and Pattern Recognition Work*, 4.
- Giles, D. K., & Billing, R. (2014). Unmanned aerial platforms for spraying: deployment and performance. *Aspects of Applied Biology*, 122, 63-69.
- Goldbergs, G., Maier, S. W., Levick, S. R., & Edwards, A. (2018). Efficiency of Individual Tree Detection Approaches Based on Light-Weight and Low-Cost UAS Imagery in Australian Savannas. *Remote Sensing*, 10(2), 161.
- Gonzalez, F., & Johnson, S. (2017). Standard operating procedures for UAV or drone based monitoring of wildlife. *Proceedings of UAS4RS 2017 (Unmanned Aircraft Systems for Remote Sensing)*. Brisbane: Queensland University of Technology.
- Graaf, C., Koster, A., Vincken, K., & Viergever, M. (1994). Validation of the interleaved pyramid for the segmentation of 3d vector images. *Pattern Recognition Letters*, 15, 467-475.
- Green, D. R., & Hartley, S. (2000). Integrating Photointerpretation and GIS for Vegetation Mapping: Some Issues of Error. In R. Alexander, & A. C. Millington, *Vegetation Mapping* (pp. 103-134). Chichester: John Wiley & Sons.
- Hansford, D. (2010, January). *Wetlands*. Retrieved February 26, 2019, from New Zealand Geographic: <https://www.nzgeo.com/stories/wetlands/>
- Haralick, R., & Shapiro, L. (1985). Survey: image segmentation techniques. *Computer Vision, Graphics and Image Processing*, 29, 100-132.
- Hinchliffe, G. (2017, October 12). *Mapping Threatened Landscapes with UAVs (lecture slides)*. Retrieved October 13, 2017, from <http://learn.canterbury.ac.nz/mod/resource/view.php?id=643976>
- Hirano, A., Madden, M., & Welch, R. (2003, June). Hyperspectral image data for mapping wetland vegetation. *Wetlands*, 23(2), 436-448.

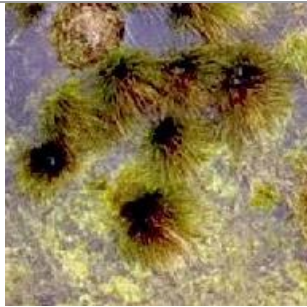
- Inzamul, H., & Basak, R. (2017). Land cover change detection using GIS and remote sensing techniques: A spatio-temporal study on Tanguar Haor, Sunamganj, Bangladesh. *The Egyptian Journal of Remote Sensing and Space Science*, 20(2), 251-263.
- ITT Visual Information Solutions. (2008). *ENVI Feature Extraction Module User's Guide*.
- Johnson-Roberson, M., Murphy, R. J., & Bongiorno, D. (2013). Kite Aerial Photography for Low-Cost, Ultra-high Spatial Resolution Multi-Spectral Mapping of Intertidal Landscapes. *PLoS ONE*, 8(9).
- Kavzoglu, T. (2017). Chapter 33 - Object-Oriented Random Forest for High Resolution Land Cover Mapping Using Quickbird-2 Imagery. In P. Samui, S. Sekhar, & V. E. Balas (Eds.), *Handbook of Neural Computation* (pp. 607-619). Academic Press.
- Kim, M., Madden, M., & Xu, B. (2010). GEOIBA vegetation mapping in Great Smoky Mountains National Park with spectral and non-spectral ancillary information. *Photogrammetric Engineering & Remote Sensing*, 76(2), 137-149.
- Kiser, J. D., & Paine, D. P. (2003). *Aerial Photography and Image Interpretation*. John Wiley & Sons.
- Kislík, C., Dronova, I., & Kelly, M. (2018). UAVs in Support of Algal Bloom Research: A Review of Current Applications and Future Opportunities. *Drones*, 2(4), 35.
- Kumar, R. (1997). *Tactical Reconnaissance: UAVS Versus Manned Aircraft*. Fort Belvoir: Defence Technical Information Centre.
- LaFrance, A. (2016, May 9). *Why Drones Make Elephants Go Berserk*. Retrieved October 9, 2017, from The Atlantic: <https://www.theatlantic.com/technology/archive/2016/05/elephant-vs-drone/481701/>
- Landcare Research New Zealand Ltd - Informatics Team. (2018, November 29). *LCDB v4.1 - Land Cover Database version 4.1, Mainland New Zealand*. Retrieved January 6, 2019, from LRIS Portal: <https://iris.scinfo.org.nz/layer/48423-lcdb-v41-land-cover-database-version-41-mainland-new-zealand/>
- Landis, J. R., & Koch, G. G. (1977). The measurement of observer agreement for categorical data. *Biometrics*, 33(1), 159-174.
- Lawrence, G. ( ). *Using satellite imagery and novel low altitude aerial imagery to classify coastal wetland vegetation for change detection at Whatipu Scientific Reserve, Auckland, NZ*. Auckland: Auckland University of Technology.
- Lechner, A., Fletcher, A., Johansen, K., & Erskine, P. (2012). Characterising upland swamps using object-based classification methods and hyper-spatial resolution imagery derived from an unmanned aerial vehicle. *Proceedings of the XXII ISPRS Annals of the Photogrammetry, Remote Sensing and Spatial Information Sciences*, 4, 101-106.
- Li, J., & Chen, W. (2005). A rule-based method for mapping Canada's wetlands using optical, radar and DEM data. *International Journal of Remote Sensing*, 26(22), 5051-5069.
- Lillesand, T., Kiefer, R. W., & Chipman, J. (2004). *Remote sensing and image interpretation*. John Wiley & Sons.
- Lin, J., Wang, M., Ma, M., & Lin, Y. (2018). Aboveground Tree Biomass Estimation of Sparse Subalpine Coniferous Forest with UAV Oblique Photography. *Remote Sensing*, 10(11), Article No: 1849.
- Lu, D., Mausel, P., Brondizio, E., & Moran, E. (2005). Change detection techniques. *International Journal of Remote Sensing*, 25(12), 2365-2401.
- Ma, L., Li, M., Ma, X., Cheng, L., Du, P., & Liu, Y. (2017, August). A review of supervised object-based land-cover image classification. *ISPRS Journal of Photogrammetry and Remote Sensing*, 130, 277-293.
- Mahlangu, P., Mathieu, R., Wessels, K., Naidoo, L., Verstraete, M., Asner, G., & Main, R. (2018). Indirect Estimation of Structural Parameters in South African Forests Using MISR-HR and LiDAR Remote Sensing Data. *Remote Sensing*, 10(10), 1537.
- Melgani, F., & Bruzzone, L. (2004, August). Classification of hyperspectral remote sensing images with support vector machines. *IEEE Transactions on Geoscience and Remote Sensing*, 42(8), 1778-1790.
- Meteorological Service of New Zealand. (2019, May 15). *Wairarapa Weather*. Retrieved May 15, 2019, from MetService Rural Forecasts: <https://www.metservice.com/rural/wairarapa#!/martinborough>

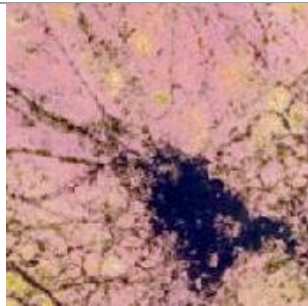
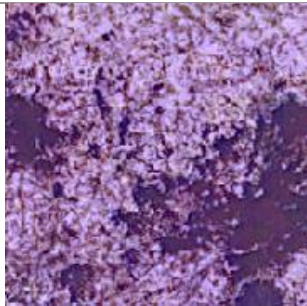
- MicaSense Inc. (2017). *RedEdge-M User Manual*.
- Ministry for Primary Industries. (2019, May 8). *Toxic algal blooms*. Retrieved May 22 22, 2019, from New Zealand Food Safety: <https://www.mpi.govt.nz/travel-and-recreation/fishing/shellfish-biotoxin-alerts/toxic-algal-blooms/>
- Moore, L. B., & Edgar, E. (1970). *Flora of New Zealand (vol. 2)*. Wellington: Government Printer. Retrieved from New Zealand Plant Conservation Network.
- Morgan, J. L., Gergel, S. E., & Coops, N. C. (2010, January). Aerial Photography: A Rapidly Evolving Tool for Ecological Management. *BioScience*, *60*(1), 47-59.
- Munyati, C. (2000). Wetland change detection on the Kafue Flats, Zambia, by classification of a multitemporal remote sensing image dataset. *International Journal of Remote Sensing*, *21*, 1787-1806.
- New Zealand Plant Conservation Network. (2019, January 30). *Isolepis Prolifera*. Retrieved March 20, 2019, from New Zealand Plant Conservation Network: [http://www.nzpcn.org.nz/flora\\_details.aspx?ID=2035](http://www.nzpcn.org.nz/flora_details.aspx?ID=2035)
- Ozesmi, S. L., & Bauer, M. E. (2002, October). Satellite remote sensing of wetlands. *Wetlands Ecology and Management*, *10*(5), 381-402.
- Pal, M., & Mather, M. (2005). Support vector machines for classification in remote sensing. *International Journal of Remote Sensing*, *26*(5), 1007-1011.
- Pande-Chhetri, R., Abd-Elrahman, A., Liu, T., Morton, J., & Wilhelm, V. (2017). Object-based classification of wetland vegetation using very high-resolution unmanned air system imagery. *European Journal of Remote Sensing*, *50*(1), 574-576.
- Panigrahy, R., Kale, M., Dutta, U., Mishra, A., Banerjee, B., & Singh, S. (2010). Forest cover change detection of Western Ghats of Maharashtra using satellite remote sensing based visual interpretation technique. *Current Science*, *98*(5), 657-664.
- Peña, J., Torres-Sánchez, J., Serrano-Pérez, A., de Castro, A., & López-Granados, F. (2015). Quantifying Efficacy and Limits of Unmanned Aerial Vehicle (UAV) Technology for Weed Seedling Detection as Affected by Sensor Resolution. *Sensors*, *15*(3), 5609-5626.
- PrecisionMapper Support. (2018, December 8). *Mission Settings*. Retrieved February 6, 2019, from PrecisionMapper Support: <https://support.precisionmapper.com/support/solutions/articles/6000185648-mission-settings>
- Psaltopoulos, D., Wade, A., Skuras, D., Kernan, M., Tyllianakis, E., & Erlandsson, M. (2017). False positive and false negative errors in the design and implementation of agri-environmental policies: a case study on water quality and agricultural nutrients. *Science of the Total Environment*, *575*, 1087-1099.
- Puzinas, J. (2017). *Land Cover Classification Using Satellite Imagery and LiDAR*. Copenhagen: Aalborg University .
- Ramsey, E. W., & Laine, S. C. (1997). Comparison of Landsat Thematic Mapper and High Resolution Photography to Identify Change in Complex Coastal Wetlands. *Journal of Coastal Research*, *12*(2), 281-292.
- Rengarajan, V., Rajagopalan, A. N., Aravind, R., & Seetharaman, G. (2016). Image Registration and Change Detection under Rolling Shutter Motion Blur. *IEEE Transactions on Pattern Analysis and Machine Intelligence*, *39*(10), 1959 - 1972.
- Ruwaimana, M., Satyanarayana, B., Otero, V., Muslim, A., Syafiq, M., Ibrahim, S., . . . Dahdouh-Guebas, F. (2018, July 18). *The advantages of using drones over space-borne imagery in the mapping of mangrove forests*. Retrieved February 15, 2019, from PLoS ONE: <https://doi.org/10.1371/journal.pone.0200288>
- Shelley, A. V. (2018). A Framework for Counter-Unmanned Aircraft System Regulation in New Zealand. *Policy Quarterly*, *14*(3), 74-80.
- Sieberth, T., Wackrow, R., & Chandler, J. H. (2015). UAV Image Blur - Its Influence and Ways to Correct it. *International Archives of the Photogrammetry, Remote Sensing and Spatial Information Sciences*, *40*(1), 33-39.
- Skylogic Research. (2018, September). *2018 Drone Market Sector Report*. Retrieved May 9, 2019, from Drone Girl: <http://thedronegirl.com/2018/09/18/dji-market-share/>

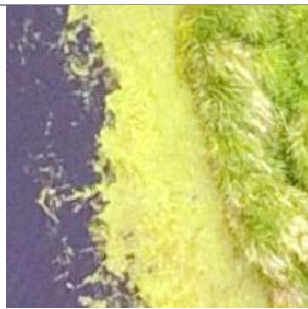
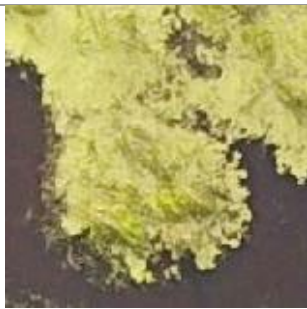
- Turner, W., Spector, S., Gardiner, N., & Fladeland, M. (2003). Remote sensing for biodiversity science and conservation. *Trends in Ecology and Evolution*, 306-314.
- Wang, Z., Lucas, A., Wong, K. C., & Charmitoff, G. (2017). Biomimetic design for pest bird control UAVs: A survey. *17th Australian International Aerospace Congress* (pp. 469-476). Royal Aeronautical Society.
- Waser, L., Baltsavias, E., Ecker, K., Eisenbeiss, H., Feldmeyer-Criste, E., Ginzler, C., . . . Zhang, L. (2008). Assessing changes of forest area and shrub encroachment in a mire ecosystem using digital surface models and CIR aerial images. *Remote Sensing of Environment*, 112(5), 1956-1968.
- Wigmore, O. (2019, May 29). Personal Communication.
- Wulder, M. (1998). Optical remote sensing techniques for the assessment of forest inventory and biophysical parameters. *Progress in Physical Geography*, 22, 449-476.
- Yamazaki, F., Yano, Y., & Matsuoka, M. (2005). Visual Damage Interpretation of Buildings in Bam City Using QuickBird Images Following the 2003 Bam, Iran, Earthquake. *Earthquake Spectra*, 21(1), 329-336.
- Zhang, H., Fritts, J., & Goldman, S. (2008). Image segmentation evaluation: a survey of unsupervised methods. *Computer Vision and Image Understanding*, 110(2), 260-280.
- Zhou, G., & Lam, N. (2008). Reducing Edge Effects in the Classification of High Resolution Imagery. *Photogrammetric Engineering & Remote Sensing*, 74(4), 431-441.

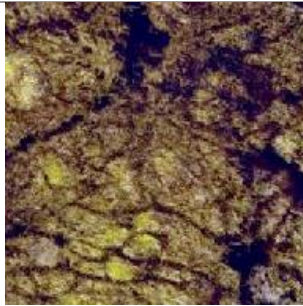
## Appendix A: Class Example Images

Class Name:	Example Images		
<b>Water</b>			
<b>Mixed Grasses</b>			
<b>Brown Grass</b>			
<b>Isolepis</b>			
<b>Yellow Isolepis</b>			

<p><b>Reeds</b></p>			
<p><b>Rush</b></p>			
<p><b>Sedge</b></p>			
<p><b>Flax</b></p>			
<p><b>Toetoe</b></p>			
<p><b>Cabbage Tree</b></p>			

<p><b>Manuka</b></p>			
<p><b>Kahikatea</b></p>			
<p><b>Other Tree (Dark Green)</b></p>			
<p><b>Other Tree (Brown)</b></p>			
<p><b>Other Tree (Light Green)</b></p>			
<p><b>Azolla</b></p>			

<b>Green Algae</b>			
<b>Mixed Algae</b>			
<b>Yellow Algae</b>			
<b>Blackberry</b>			
<b>Bidens</b>			
<b>Dry Bidens</b>			

<p><b>Dry Vegetation</b></p>			
<p><b>Dormant Tree</b></p>			
<p><b>Waterlogged Grass</b></p>			
<p><b>Mud</b></p>			
<p><b>Shadow</b></p>			

## Appendix B: Confusion Matrices

### Stage One – Winter

RGB ONLY

ClassValue:	Water	Isolepis	Mixed Grass	Reed	Toetoe	Bidens	Cabbage Tree	Flax	Blackberry	Other Tree (Dark)	Shadow	Kahikatea	Other Tree (Brown)	Dormant Tree	Manuka	Sedge	Dry Vegetation	Brown Grass	Total	U Accuracy	Kappa
Water	210	0	0	1	0	0	0	0	0	0	0	0	0	0	0	0	0	0	211	1.00	0
Isolepis	0	18	2	0	0	0	0	0	0	0	0	0	0	0	0	0	0	0	20	0.90	0
Mixed Grass	0	37	68	0	0	0	1	0	0	2	2	2	3	0	2	0	1	4	122	0.56	0
Reed	0	0	2	21	4	1	0	2	1	0	0	0	0	0	0	1	13	2	47	0.45	0
Toetoe	1	0	11	1	10	0	0	1	0	0	0	1	0	1	0	0	2	0	28	0.36	0
Bidens	0	0	0	2	0	2	0	0	0	0	0	0	0	0	0	1	3	1	9	0.22	0
Cabbage Tree	0	0	3	0	0	0	3	4	1	0	0	0	2	0	0	0	0	0	13	0.23	0
Flax	3	5	1	11	3	2	2	32	1	2	3	0	0	0	1	0	1	1	68	0.47	0
Blackberry	0	3	17	4	7	0	1	7	1	0	0	0	1	0	2	3	6	3	55	0.02	0
Other Tree (Dark)	0	2	20	0	1	0	4	3	0	3	0	0	1	0	1	1	0	0	36	0.08	0
Shadow	2	0	0	0	0	0	0	1	0	0	5	0	0	0	0	0	0	0	8	0.63	0
Kahikatea	0	1	14	0	7	3	0	0	0	0	0	3	1	4	0	0	20	16	69	0.04	0
Other Tree (Brown)	0	2	14	0	2	0	1	1	0	0	0	0	2	0	0	0	0	0	22	0.09	0
Dormant Tree	1	3	0	0	0	5	0	0	0	0	0	0	0	3	0	0	10	7	29	0.10	0
Manuka	1	10	78	0	0	1	1	2	0	1	0	3	1	0	2	2	2	12	116	0.02	0
Sedge	1	4	46	0	2	2	0	0	0	1	0	1	2	0	3	8	18	17	105	0.08	0
Dry Vegetation	0	0	0	5	1	7	0	0	1	0	0	1	0	2	0	1	26	4	48	0.54	0
Brown Grass	0	0	1	0	0	2	0	0	0	0	0	0	0	0	0	0	17	7	27	0.26	0
<b>Total</b>	<b>219</b>	<b>85</b>	<b>277</b>	<b>45</b>	<b>37</b>	<b>25</b>	<b>13</b>	<b>53</b>	<b>5</b>	<b>9</b>	<b>10</b>	<b>11</b>	<b>13</b>	<b>10</b>	<b>11</b>	<b>17</b>	<b>119</b>	<b>74</b>	<b>1033</b>	<b>0.00</b>	<b>0</b>
<b>P_Accuracy</b>	<b>0.96</b>	<b>0.21</b>	<b>0.25</b>	<b>0.47</b>	<b>0.27</b>	<b>0.08</b>	<b>0.23</b>	<b>0.60</b>	<b>0.20</b>	<b>0.33</b>	<b>0.50</b>	<b>0.27</b>	<b>0.15</b>	<b>0.30</b>	<b>0.18</b>	<b>0.47</b>	<b>0.22</b>	<b>0.09</b>	<b>0.00</b>	<b>0.41</b>	<b>0.00</b>
<b>Kappa</b>	<b>0</b>	<b>0</b>	<b>0</b>	<b>0</b>	<b>0</b>	<b>0</b>	<b>0</b>	<b>0</b>	<b>0</b>	<b>0</b>	<b>0</b>	<b>0</b>	<b>0</b>	<b>0</b>	<b>0.35</b>						

DSM

ClassValue:	Water	Isolepis	Mixed Grass	Reed	Toetoe	Bidens	Cabbage Tree	Flax	Blackberry	Other Tree (Dark)	Shadow	Kahikatea	Other Tree (Brown)	Dormant Tree	Manuka	Sedge	Dry Vegetation	Brown Grass	Total	U Accuracy	Kappa
Water	218	0	0	0	0	0	0	0	0	0	0	0	0	0	0	0	0	0	218	1.00	0
Isolepis	0	61	1	0	0	0	0	0	0	0	0	0	0	0	0	0	0	0	62	0.98	0
Mixed Grass	0	11	170	0	3	0	1	0	0	1	0	0	0	0	0	2	0	7	195	0.87	0
Reed	0	2	0	38	2	0	0	1	0	0	0	0	0	1	0	0	3	0	47	0.81	0
Toetoe	0	0	3	1	14	0	0	2	0	0	0	0	0	0	0	0	1	1	22	0.64	0
Bidens	0	0	0	2	0	19	0	0	0	0	0	0	0	0	0	0	7	3	31	0.61	0
Cabbage Tree	0	0	1	0	0	0	3	3	1	0	0	0	0	0	1	0	0	1	10	0.30	0
Flax	0	1	1	1	3	1	0	35	0	2	0	0	1	0	2	0	0	0	47	0.74	0
Blackberry	0	0	13	1	5	3	1	8	3	0	0	0	1	0	4	0	5	1	45	0.07	0
Other Tree (Dark)	0	0	0	0	0	0	5	0	0	5	0	0	0	0	0	0	0	0	10	0.50	0
Shadow	1	0	0	0	0	0	0	0	0	0	10	0	0	0	0	0	0	0	11	0.91	0
Kahikatea	0	0	0	0	0	0	0	0	0	0	0	10	0	0	0	0	0	0	10	1.00	0
Other Tree (Brown)	0	0	0	0	1	0	0	0	0	0	0	0	9	0	0	0	0	0	10	0.90	0
Dormant Tree	0	0	0	0	0	0	0	0	0	0	0	1	0	9	0	0	0	0	10	0.90	0
Manuka	0	0	0	0	0	0	1	1	0	0	0	0	2	0	4	0	1	1	10	0.40	0
Sedge	0	8	88	1	9	1	2	3	1	1	0	0	0	0	0	15	23	33	185	0.08	0
Dry Vegetation	0	2	0	1	0	1	0	0	0	0	0	0	0	0	0	0	70	3	77	0.91	0
Brown Grass	0	0	0	0	0	0	0	0	0	0	0	0	0	0	0	0	9	24	33	0.73	0
<b>Total</b>	<b>219</b>	<b>85</b>	<b>277</b>	<b>45</b>	<b>37</b>	<b>25</b>	<b>13</b>	<b>53</b>	<b>5</b>	<b>9</b>	<b>10</b>	<b>11</b>	<b>13</b>	<b>10</b>	<b>11</b>	<b>17</b>	<b>119</b>	<b>74</b>	<b>1033</b>	<b>0.00</b>	<b>0</b>
<b>P_Accuracy</b>	<b>1.00</b>	<b>0.72</b>	<b>0.61</b>	<b>0.84</b>	<b>0.38</b>	<b>0.76</b>	<b>0.23</b>	<b>0.66</b>	<b>0.60</b>	<b>0.56</b>	<b>1.00</b>	<b>0.91</b>	<b>0.69</b>	<b>0.90</b>	<b>0.36</b>	<b>0.88</b>	<b>0.59</b>	<b>0.32</b>	<b>0.00</b>	<b>0.69</b>	<b>0.00</b>
<b>Kappa</b>	<b>0</b>	<b>0</b>	<b>0</b>	<b>0</b>	<b>0</b>	<b>0</b>	<b>0</b>	<b>0</b>	<b>0</b>	<b>0</b>	<b>0</b>	<b>0</b>	<b>0</b>	<b>0</b>	<b>0.65</b>						

# Stage One – Spring

RGB ONLY

Class/Value:	Water	Mixed Grass	Isolepis	Yellow Isolepis	Brown Grass	Dry Vegetation	Shadow	Reed	Other Tree (Dark)	Other Tree (Brown)	Manuka	Blackberry	Flax	Sedge	Dormant Tree	Other Tree (Light)	Waterlogged Grass	Azolla	Green Algae	Toetoe	Rush	Cabbage Tree	Kahikatea	Total	U_Accuracy	Kappa
Water	209	0	0	0	0	0	0	0	0	0	0	0	0	0	0	0	17	1	0	0	0	0	0	227	0.92	0
Mixed Grass	0	194	3	1	0	7	0	0	2	0	1	0	0	3	0	0	4	0	0	0	0	1	0	216	0.90	0
Isolepis	0	2	8	2	0	0	0	0	0	0	0	0	0	0	0	0	0	0	0	0	0	0	0	12	0.67	0
Yellow Isolepis	0	0	1	19	1	0	0	0	0	0	0	0	0	0	0	0	0	0	0	0	0	0	0	21	0.90	0
Brown Grass	0	0	0	1	6	0	0	0	0	0	1	0	0	0	0	0	0	0	0	0	0	0	0	8	0.75	0
Dry Vegetation	0	0	0	0	0	12	0	1	0	0	0	0	1	0	0	0	2	0	0	1	0	0	0	17	0.71	0
Shadow	0	0	0	0	0	0	6	0	0	0	0	0	0	0	0	0	0	0	0	0	0	0	0	6	1.00	0
Reed	0	0	0	0	0	3	0	11	0	0	0	0	0	1	0	0	1	0	0	2	0	0	0	18	0.61	0
Other Tree (Dark)	0	1	0	0	0	0	0	0	4	1	0	0	1	0	0	0	0	0	0	0	0	0	0	7	0.57	0
Other Tree (Brown)	0	34	3	2	8	1	0	0	2	1	0	1	2	0	1	0	0	0	1	0	0	0	0	56	0.64	0
Manuka	0	25	2	0	8	0	6	1	0	3	21	0	3	0	1	0	9	0	0	2	3	0	0	84	0.25	0
Blackberry	0	3	0	0	0	0	1	0	6	2	1	2	4	1	0	0	0	0	0	0	0	0	0	20	0.10	0
Flax	0	1	0	0	0	3	1	3	2	0	0	0	31	0	0	0	1	0	0	2	5	0	0	49	0.63	0
Sedge	0	3	0	2	6	1	0	0	0	0	0	0	0	1	0	0	4	1	0	2	0	0	1	21	0.05	0
Dormant Tree	3	0	0	0	0	5	0	0	0	0	0	0	0	3	0	0	26	2	0	0	1	0	0	40	0.08	0
Other Tree (Light)	0	13	2	3	0	0	0	0	0	0	0	0	0	1	0	3	0	0	0	1	0	6	0	29	0.10	0
Waterlogged Grass	3	0	0	0	3	2	0	0	0	0	0	0	0	0	2	0	50	1	0	0	1	0	0	62	0.81	0
Azolla	0	0	0	0	0	0	0	0	0	0	0	0	0	0	0	0	0	8	0	0	0	0	0	8	1.00	0
Green Algae	0	0	0	0	0	3	0	0	0	0	0	0	1	0	0	0	0	0	0	1	0	0	0	5	0.00	0
Toetoe	0	8	1	0	0	11	0	4	0	0	0	0	3	0	0	2	0	0	15	4	1	0	0	49	0.31	0
Rush	0	0	0	0	0	0	0	0	0	0	0	0	0	0	0	0	0	0	0	0	0	0	0	0	0.00	0
Cabbage Tree	0	17	0	0	0	0	0	0	0	0	0	0	7	0	0	1	0	0	0	2	3	5	1	36	0.14	0
Kahikatea	0	5	1	2	1	13	0	0	0	0	0	0	1	0	0	0	0	0	0	3	0	1	3	30	0.10	0
<b>Total</b>	<b>215</b>	<b>306</b>	<b>21</b>	<b>32</b>	<b>33</b>	<b>61</b>	<b>14</b>	<b>20</b>	<b>14</b>	<b>8</b>	<b>25</b>	<b>2</b>	<b>53</b>	<b>9</b>	<b>6</b>	<b>5</b>	<b>116</b>	<b>13</b>	<b>0</b>	<b>32</b>	<b>17</b>	<b>14</b>	<b>5</b>	<b>1021</b>	<b>0.00</b>	<b>0</b>
<b>P_Accuracy</b>	<b>0.97</b>	<b>0.63</b>	<b>0.38</b>	<b>0.59</b>	<b>0.18</b>	<b>0.20</b>	<b>0.43</b>	<b>0.55</b>	<b>0.29</b>	<b>0.25</b>	<b>0.84</b>	<b>1.00</b>	<b>0.58</b>	<b>0.11</b>	<b>0.50</b>	<b>0.60</b>	<b>0.43</b>	<b>0.62</b>	<b>0.00</b>	<b>0.47</b>	<b>0.00</b>	<b>0.36</b>	<b>0.60</b>	<b>0.00</b>	<b>0.60</b>	<b>0.00</b>
<b>Kappa</b>	<b>0</b>	<b>0</b>	<b>0</b>	<b>0</b>	<b>0</b>	<b>0</b>	<b>0</b>	<b>0</b>	<b>0</b>	<b>0</b>	<b>0</b>	<b>0</b>	<b>0</b>	<b>0</b>	<b>0</b>	<b>0</b>	<b>0</b>	<b>0</b>	<b>0</b>	<b>0</b>	<b>0</b>	<b>0</b>	<b>0</b>	<b>0</b>	<b>0</b>	<b>0.54</b>

# DSM

Class/Value:	Water	Mixed Grass	Isolepis	Yellow Isolepis	Brown Grass	Dry Vegetation	Shadow	Reed	Other Tree (Dark)	Other Tree (Brown)	Manuka	Blackberry	Flax	Sedge	Dormant Tree	Other Tree (Light)	Waterlogged Grass	Azolla	Green Algae	Toetoe	Rush	Cabbage Tree	Kahikatea	Total	U_Accuracy	Kappa	
Water	209	0	0	0	0	0	0	0	0	0	0	0	0	0	0	0	19	2	0	0	0	0	0	230	0.91	0	
Mixed Grass	0	242	3	0	0	3	0	0	1	1	0	0	3	5	0	0	2	0	0	0	0	0	0	0	260	0.93	0
Isolepis	0	1	10	4	0	0	0	0	0	0	0	0	0	0	0	0	0	0	0	0	0	0	0	15	0.67	0	
Yellow Isolepis	0	0	0	26	4	0	0	0	0	0	0	0	0	0	0	0	0	0	0	0	0	0	0	30	0.87	0	
Brown Grass	0	0	0	0	12	0	0	0	0	0	0	0	0	0	0	0	1	0	0	0	0	0	0	13	0.92	0	
Dry Vegetation	0	0	0	0	0	12	0	9	0	0	0	0	0	0	0	0	1	1	0	2	0	0	0	25	0.48	0	
Shadow	0	0	0	0	0	0	10	0	0	0	0	0	0	0	0	0	0	0	0	0	0	0	0	10	1.00	0	
Reed	0	0	0	0	0	5	0	5	0	0	0	0	1	1	0	0	0	0	0	1	0	0	0	13	0.38	0	
Other Tree (Dark)	0	1	0	0	0	0	0	0	9	0	0	0	0	0	0	0	0	0	0	0	0	0	0	10	0.90	0	
Other Tree (Brown)	0	3	0	0	0	0	0	0	4	0	0	1	0	0	1	0	0	0	0	1	0	1	0	11	0.36	0	
Manuka	0	14	1	0	5	1	4	2	0	2	24	0	3	0	1	0	3	0	0	3	0	0	0	63	0.38	0	
Blackberry	0	7	0	0	0	0	0	0	3	1	1	2	1	0	0	0	0	0	0	1	0	0	0	16	0.13	0	
Flax	0	2	0	0	0	2	0	1	1	0	0	0	40	0	0	0	0	0	0	2	2	0	0	50	0.80	0	
Sedge	0	19	2	2	8	6	0	0	0	0	0	0	0	3	0	0	2	0	0	3	3	0	0	48	0.06	0	
Dormant Tree	0	0	0	0	0	2	0	0	0	0	0	0	0	0	5	0	0	2	0	0	0	0	0	9	0.56	0	
Other Tree (Light)	0	5	1	0	0	2	0	0	0	0	0	0	0	0	3	0	0	0	0	0	0	2	0	13	0.23	0	
Waterlogged Grass	6	1	1	0	4	1	0	0	0	0	0	0	0	0	0	0	83	0	0	0	4	0	0	100	0.83	0	
Azolla	0	0	0	0	0	0	0	0	0	0	0	0	0	0	0	0	0	10	0	0	0	0	0	10	1.00	0	
Green Algae	0	0	0	0	0	4	0	0	0	0	0	0	1	0	0	0	0	0	0	0	4	0	0	9	0.00	0	
Toetoe	0	9	1	0	0	22	0	3	0	0	0	0	2	0	0	0	3	0	0	15	1	0	0	56	0.27	0	
Rush	0	0	2	0	0	1	0	0	0	0	0	0	0	0	0	0	0	0	0	0	0	7	0	10	0.70	0	
Cabbage Tree	0	2	0	0	0	0	0	0	0	0	0	0	1	0	0	1	0	0	0	0	0	7	0	11	0.64	0	
Kahikatea	0	0	0	0	0	0	0	0	0	0	0	0	0	0	0	0	0	0	0	0	0	4	5	9	0.56	0	
<b>Total</b>	<b>215</b>	<b>306</b>	<b>21</b>	<b>32</b>	<b>33</b>	<b>61</b>	<b>14</b>	<b>20</b>	<b>14</b>	<b>8</b>	<b>25</b>	<b>2</b>	<b>53</b>	<b>9</b>	<b>6</b>	<b>5</b>	<b>116</b>	<b>13</b>	<b>0</b>	<b>32</b>	<b>17</b>	<b>14</b>	<b>5</b>	<b>1021</b>	<b>0.00</b>	<b>0</b>	
<b>P_Accuracy</b>	<b>0.97</b>	<b>0.79</b>	<b>0.48</b>	<b>0.81</b>	<b>0.36</b>	<b>0.20</b>	<b>0.71</b>	<b>0.25</b>	<b>0.64</b>	<b>0.50</b>	<b>0.96</b>	<b>1.00</b>	<b>0.75</b>	<b>0.33</b>	<b>0.83</b>	<b>0.60</b>	<b>0.72</b>	<b>0.77</b>	<b>0.00</b>	<b>0.47</b>	<b>0.41</b>	<b>0.50</b>	<b>1.00</b>	<b>0.00</b>	<b>0.73</b>	<b>0.00</b>	
<b>Kappa</b>	<b>0</b>	<b>0</b>	<b>0</b>	<b>0</b>	<b>0</b>	<b>0</b>	<b>0</b>	<b>0</b>	<b>0</b>	<b>0</b>	<b>0</b>	<b>0</b>	<b>0</b>	<b>0</b>	<b>0</b>	<b>0</b>	<b>0</b>	<b>0</b>	<b>0</b>	<b>0</b>	<b>0</b>	<b>0</b>	<b>0</b>	<b>0</b>	<b>0</b>	<b>0.68</b>	

## Stage One – Summer

RGB ONLY

ClassValue:	Water	Isolepis	Shadow	Mixed Grass	Dry Vegetation	Reed	Flax	Azolla	Toetoe	Cabbage Tree	Other Tree (Dark)	Brown Algae	Green Algae	Manuka	Sedge	Other Tree (Light)	Blackberry	Kahikatea	Other Tree (Brown)	Total	U_Accuracy	Kappa
Water	126	0	1	0	0	0	0	5	0	0	0	0	0	0	0	0	0	0	0	132	0.95	0
Isolepis	0	52	0	16	0	0	0	0	0	0	0	1	0	0	3	0	0	0	0	72	0.72	0
Shadow	2	0	16	0	0	0	0	0	0	0	0	0	1	0	0	0	0	0	0	19	0.84	0
Mixed Grass	0	12	0	91	3	2	1	0	0	0	0	2	0	6	0	0	0	0	0	117	0.78	0
Dry Vegetation	0	0	0	8	24	0	0	1	3	0	0	1	5	0	0	0	0	0	0	42	0.57	0
Reed	1	0	0	7	2	7	3	3	3	0	1	0	0	0	1	1	1	0	0	30	0.23	0
Flax	0	0	2	3	1	6	24	0	1	0	0	0	0	0	1	0	0	0	0	38	0.63	0
Azolla	8	0	0	1	2	0	47	0	0	0	0	2	6	0	0	0	0	0	0	66	0.71	0
Toetoe	0	0	0	19	17	6	1	0	10	0	0	2	2	0	3	0	0	0	0	60	0.17	0
Cabbage Tree	0	9	0	54	5	20	13	0	6	5	1	2	2	0	6	1	2	0	0	126	0.04	0
Other Tree (Dark)	0	9	0	8	0	0	0	0	0	0	2	0	0	0	1	0	0	0	0	20	0.10	0
Brown Algae	0	1	0	1	8	0	1	0	1	0	0	7	0	0	0	0	0	0	0	19	0.37	0
Green Algae	0	0	0	0	5	0	0	0	1	0	0	0	6	0	0	0	0	0	0	12	0.50	0
Manuka	0	1	6	8	1	3	6	2	0	0	1	2	0	9	0	1	1	0	0	41	0.22	0
Sedge	0	13	0	34	1	1	2	0	0	1	2	0	0	0	13	0	0	0	0	67	0.19	0
Other Tree (Light)	0	3	0	14	9	3	0	1	0	0	0	0	3	1	1	0	0	0	0	35	0.00	0
Blackberry	0	1	0	1	4	8	6	1	0	2	2	0	1	0	0	0	1	0	0	27	0.04	0
Kahikatea	0	6	0	6	1	3	0	0	1	0	0	3	0	4	4	0	0	5	0	33	0.15	0
Other Tree (Brown)	0	8	0	19	2	0	1	0	1	1	0	0	0	2	3	0	0	2	2	41	0.05	0
<b>Total</b>	<b>137</b>	<b>115</b>	<b>25</b>	<b>289</b>	<b>84</b>	<b>61</b>	<b>58</b>	<b>60</b>	<b>27</b>	<b>9</b>	<b>12</b>	<b>17</b>	<b>27</b>	<b>17</b>	<b>42</b>	<b>3</b>	<b>5</b>	<b>7</b>	<b>2</b>	<b>997</b>	<b>0.00</b>	<b>0</b>
<b>P_Accuracy</b>	<b>0.92</b>	<b>0.45</b>	<b>0.64</b>	<b>0.31</b>	<b>0.29</b>	<b>0.11</b>	<b>0.41</b>	<b>0.78</b>	<b>0.37</b>	<b>0.56</b>	<b>0.17</b>	<b>0.41</b>	<b>0.22</b>	<b>0.53</b>	<b>0.31</b>	<b>0.00</b>	<b>0.20</b>	<b>0.71</b>	<b>1.00</b>	<b>0.00</b>	<b>0.45</b>	<b>0</b>
<b>Kappa</b>	<b>0</b>	<b>0</b>	<b>0</b>	<b>0</b>	<b>0</b>	<b>0</b>	<b>0</b>	<b>0</b>	<b>0</b>	<b>0</b>	<b>0</b>	<b>0</b>	<b>0</b>	<b>0</b>	<b>0</b>	<b>0</b>	<b>0</b>	<b>0</b>	<b>0</b>	<b>0</b>	<b>0.00</b>	<b>0.40</b>

DSM

ClassValue	Water	Isolepis	Shadow	Mixed Grass	Dry Vegetation	Reed	Flax	Azolla	Toetoe	Cabbage Tree	Other Tree (Dark)	Brown Algae	Green Algae	Manuka	Sedge	Other Tree (Light)	Blackberry	Kahikatea	Other Tree (Brown)	Total	U_Accuracy	Kappa
Water	132	0	3	0	0	0	0	0	0	0	0	0	0	0	0	0	0	0	0	135	0.98	0
Isolepis	0	54	0	9	0	0	0	1	0	0	0	1	0	0	1	0	0	0	0	66	0.82	0
Shadow	1	0	16	0	0	0	0	0	0	0	0	0	0	0	0	0	0	0	0	17	0.94	0
Mixed Grass	0	14	0	143	3	4	0	0	1	0	0	0	1	1	7	0	0	0	0	174	0.82	0
Dry Vegetation	0	0	0	0	22	0	0	1	0	0	0	1	4	0	0	0	0	0	0	28	0.79	0
Reed	0	3	0	9	3	18	6	2	5	1	1	0	1	0	2	2	1	0	0	54	0.33	0
Flax	0	0	0	1	0	3	25	1	0	0	0	0	0	0	0	0	0	0	0	30	0.83	0
Azolla	4	0	0	0	1	2	1	52	0	0	0	2	2	0	0	0	0	0	0	64	0.81	0
Toetoe	0	1	0	32	34	9	4	0	18	0	0	0	3	1	7	0	0	0	0	109	0.17	0
Cabbage Tree	0	10	0	37	2	10	6	0	1	6	1	0	2	0	4	0	0	0	0	79	0.08	0
Other Tree (Dark)	0	10	0	5	0	0	0	0	0	1	2	1	0	0	4	0	0	0	0	23	0.09	0
Brown Algae	0	1	0	1	7	0	0	0	0	0	0	11	0	0	0	0	0	0	0	20	0.55	0
Green Algae	0	0	0	0	4	0	0	0	0	0	0	0	10	0	0	0	0	0	0	14	0.71	0
Manuka	0	2	3	3	1	3	5	2	0	0	1	2	0	12	0	1	1	0	0	36	0.33	0
Sedge	0	5	0	26	1	3	1	0	1	0	3	0	0	2	10	0	1	0	0	53	0.19	0
Other Tree (Light)	0	0	0	3	2	0	0	1	0	0	0	0	3	0	1	0	0	0	0	10	0.00	0
Blackberry	0	3	3	3	1	7	8	1	0	1	2	0	1	0	0	0	2	0	0	32	0.06	0
Kahikatea	0	4	0	3	0	2	1	0	0	0	1	0	0	1	2	0	0	6	0	20	0.30	0
Other Tree (Brown)	0	8	0	14	3	0	0	0	1	0	0	0	0	0	4	0	0	1	2	33	0.06	0
<b>Total</b>	<b>137</b>	<b>115</b>	<b>25</b>	<b>289</b>	<b>84</b>	<b>61</b>	<b>58</b>	<b>60</b>	<b>27</b>	<b>9</b>	<b>12</b>	<b>17</b>	<b>27</b>	<b>17</b>	<b>42</b>	<b>3</b>	<b>5</b>	<b>7</b>	<b>2</b>	<b>997</b>	<b>0.00</b>	<b>0</b>
<b>P_Accuracy</b>	<b>0.96</b>	<b>0.47</b>	<b>0.64</b>	<b>0.49</b>	<b>0.26</b>	<b>0.30</b>	<b>0.43</b>	<b>0.87</b>	<b>0.67</b>	<b>0.67</b>	<b>0.17</b>	<b>0.65</b>	<b>0.37</b>	<b>0.71</b>	<b>0.24</b>	<b>0.00</b>	<b>0.40</b>	<b>0.86</b>	<b>1.00</b>	<b>0.00</b>	<b>0.54</b>	<b>0</b>
<b>Kappa</b>	<b>0</b>	<b>0</b>	<b>0</b>	<b>0</b>	<b>0</b>	<b>0</b>	<b>0</b>	<b>0</b>	<b>0</b>	<b>0</b>	<b>0</b>	<b>0</b>	<b>0</b>	<b>0</b>	<b>0</b>	<b>0</b>	<b>0</b>	<b>0</b>	<b>0</b>	<b>0</b>	<b>0.00</b>	<b>0.49</b>

## Stage One – Autumn

RGB ONLY

ClassValue	Water	Azolla	Mixed Grass	Toetoe	Flax	Isolepis	Sedge	Shadow	Dry Vegetation	Other Tree (Light)	Cabbage Tree	Bidens	Reed	Kahikatea	Mud	Blackberry	Other Tree (Dark)	Manuka	Dormant Tree	Total	U_Accuracy	Kappa
Water	148	11	0	0	1	0	0	9	0	0	0	0	0	0	1	0	0	0	0	170	0.87	0
Azolla	4	15	1	0	2	1	0	3	0	0	0	0	2	0	1	0	1	0	0	30	0.50	0
Mixed Grass	0	0	50	0	0	13	4	1	2	0	0	0	0	0	0	0	0	0	0	70	0.71	0
Toetoe	0	0	8	9	1	1	0	0	2	0	1	0	0	0	0	0	0	0	0	22	0.41	0
Flax	0	1	3	4	36	1	5	0	0	1	2	1	17	1	0	1	2	0	0	75	0.48	0
Isolepis	0	0	7	1	0	82	0	0	1	1	0	2	0	0	0	0	0	0	0	94	0.87	0
Sedge	0	0	74	4	4	9	36	0	25	3	1	0	8	0	0	0	2	4	0	170	0.21	0
Shadow	0	0	0	0	0	0	0	11	0	0	0	0	0	0	0	0	0	0	0	11	1.00	0
Dry Vegetation	0	0	1	0	0	0	1	0	38	0	0	0	0	0	1	0	0	0	0	41	0.93	0
Other Tree (Light)	0	0	7	3	0	1	2	0	1	5	0	1	2	0	0	0	0	0	0	22	0.23	0
Cabbage Tree	0	0	1	2	5	5	2	0	0	0	13	4	3	0	0	3	1	0	0	39	0.33	0
Bidens	0	0	0	0	0	6	1	0	0	0	0	11	0	0	0	0	0	0	0	18	0.61	0
Reed	1	1	18	6	7	3	10	0	34	0	0	0	26	0	0	0	1	0	0	107	0.24	0
Kahikatea	0	0	3	2	3	4	1	0	0	0	1	2	6	7	1	0	0	0	0	30	0.23	0
Mud	0	0	0	0	0	0	0	0	0	0	0	0	0	0	9	0	0	0	1	10	0.90	0
Blackberry	0	0	1	0	1	0	0	0	0	0	0	1	0	0	0	2	2	0	0	7	0.29	0
Other Tree (Dark)	0	0	5	1	0	10	0	1	0	0	0	3	1	0	0	0	10	0	0	31	0.32	0
Manuka	5	1	3	0	2	4	4	2	9	1	0	0	1	1	0	0	0	18	0	51	0.35	0
Dormant Tree	0	0	0	0	0	0	0	0	2	0	0	0	0	0	2	0	0	0	5	9	0.56	0
<b>Total</b>	<b>158</b>	<b>29</b>	<b>182</b>	<b>32</b>	<b>62</b>	<b>140</b>	<b>66</b>	<b>27</b>	<b>114</b>	<b>11</b>	<b>18</b>	<b>25</b>	<b>66</b>	<b>9</b>	<b>15</b>	<b>6</b>	<b>19</b>	<b>22</b>	<b>6</b>	<b>1007</b>	<b>0.00</b>	<b>0</b>
<b>P_Accuracy</b>	<b>0.94</b>	<b>0.52</b>	<b>0.27</b>	<b>0.28</b>	<b>0.58</b>	<b>0.59</b>	<b>0.55</b>	<b>0.41</b>	<b>0.33</b>	<b>0.45</b>	<b>0.72</b>	<b>0.44</b>	<b>0.39</b>	<b>0.78</b>	<b>0.60</b>	<b>0.33</b>	<b>0.53</b>	<b>0.82</b>	<b>0.83</b>	<b>0.00</b>	<b>0.53</b>	<b>0</b>
<b>Kappa</b>	<b>0</b>	<b>0</b>	<b>0</b>	<b>0</b>	<b>0</b>	<b>0</b>	<b>0</b>	<b>0</b>	<b>0</b>	<b>0</b>	<b>0</b>	<b>0</b>	<b>0.00</b>	<b>0.48</b>								

DSM

ClassValue	Water	Azolla	Mixed Grass	Toetoe	Flax	Isolepis	Sedge	Shadow	Dry Vegetation	Other Tree (Light)	Cabbage Tree	Bidens	Reed	Kahikatea	Mud	Blackberry	Other Tree (Dark)	Manuka	Dormant Tree	Total	U_Accuracy	Kappa
Water	150	7	0	0	0	0	0	3	0	0	0	0	0	0	1	0	0	0	0	161	0.93	0
Azolla	4	19	2	0	3	1	0	5	0	0	0	0	3	0	1	0	1	0	0	39	0.49	0
Mixed Grass	0	0	54	0	0	13	4	1	1	0	1	0	0	0	0	0	0	0	0	74	0.73	0
Toetoe	0	0	5	10	1	1	0	0	3	0	1	0	0	0	0	0	0	0	0	21	0.48	0
Flax	0	1	3	3	36	1	5	0	0	1	1	0	18	1	0	1	2	0	0	73	0.49	0
Isolepis	0	0	7	1	0	83	0	0	2	1	0	2	0	0	0	0	0	0	0	96	0.86	0
Sedge	0	0	72	5	4	8	40	0	23	4	0	0	8	0	0	0	2	4	0	170	0.24	0
Shadow	0	0	0	0	0	0	0	15	0	0	0	0	0	0	0	0	0	0	0	15	1.00	0
Dry Vegetation	0	0	1	0	0	0	0	0	37	0	0	0	0	0	1	0	0	0	0	39	0.95	0
Other Tree (Light)	0	0	6	2	0	1	1	0	2	4	0	1	2	0	0	0	0	0	0	19	0.21	0
Cabbage Tree	0	0	2	2	5	5	3	0	0	0	14	4	2	0	0	2	1	0	0	40	0.35	0
Bidens	0	0	0	0	0	6	1	0	0	0	0	11	0	0	0	0	0	0	0	18	0.61	0
Reed	1	1	17	6	7	3	9	0	35	0	0	1	26	0	0	0	1	0	0	107	0.24	0
Kahikatea	0	0	4	2	3	3	0	0	0	0	1	1	4	7	1	0	0	0	0	26	0.27	0
Mud	0	0	0	0	0	0	0	0	0	0	0	0	0	0	9	0	0	0	1	10	0.90	0
Blackberry	0	0	1	0	1	1	0	0	0	0	0	1	1	0	0	3	2	0	0	10	0.30	0
Other Tree (Dark)	0	0	5	1	0	9	0	1	0	0	0	3	1	0	0	0	10	0	0	30	0.33	0
Manuka	3	1	3	0	2	5	3	2	8	1	0	1	1	1	0	0	0	18	0	49	0.37	0
Dormant Tree	0	0	0	0	0	0	0	0	3	0	0	0	0	0	2	0	0	0	5	10	0.50	0
<b>Total</b>	<b>158</b>	<b>29</b>	<b>182</b>	<b>32</b>	<b>62</b>	<b>140</b>	<b>66</b>	<b>27</b>	<b>114</b>	<b>11</b>	<b>18</b>	<b>25</b>	<b>66</b>	<b>9</b>	<b>15</b>	<b>6</b>	<b>19</b>	<b>22</b>	<b>6</b>	<b>1007</b>	<b>0.00</b>	<b>0</b>
<b>P_Accuracy</b>	<b>0.95</b>	<b>0.66</b>	<b>0.30</b>	<b>0.31</b>	<b>0.58</b>	<b>0.59</b>	<b>0.61</b>	<b>0.56</b>	<b>0.32</b>	<b>0.36</b>	<b>0.78</b>	<b>0.44</b>	<b>0.39</b>	<b>0.78</b>	<b>0.60</b>	<b>0.50</b>	<b>0.53</b>	<b>0.82</b>	<b>0.83</b>	<b>0.00</b>	<b>0.55</b>	<b>0</b>
<b>Kappa</b>	<b>0</b>	<b>0</b>	<b>0</b>	<b>0</b>	<b>0</b>	<b>0</b>	<b>0</b>	<b>0</b>	<b>0</b>	<b>0</b>	<b>0</b>	<b>0</b>	<b>0.00</b>	<b>0.51</b>								

## Stage Two – Winter

RGB ONLY

Class/Value	Water	Isolepis	Mixed Grass	Bidens	Sedge	Reed	Green Algae	Shadow	Flax	Cabbage Tree	Other Tree (Brown)	Dry Vegetation	Azolla	Rush	Manuka	Kahikatea	Other Tree (Dark)	Waterlogged Grass	Total	U Accuracy	Kappa	
Water	240	0	0	0	0	0	0	0	0	0	0	0	0	0	0	0	0	0	240	1.00	0	
Isolepis	0	86	6	0	0	0	3	0	0	0	0	1	0	0	0	0	0	0	96	0.90	0	
Mixed Grass	0	19	103	10	7	1	7	2	5	3	0	39	2	3	0	2	0	30	233	0.44	0	
Bidens	0	1	2	52	1	0	0	0	0	0	0	6	1	0	0	0	0	1	64	0.81	0	
Sedge	0	14	67	1	6	0	8	0	1	1	0	4	0	1	0	1	0	6	110	0.05	0	
Reed	0	0	0	4	0	4	0	0	0	0	0	1	0	1	0	0	0	0	10	0.40	0	
Green Algae	0	1	0	0	0	0	6	0	0	0	0	0	0	0	0	0	0	0	7	0.86	0	
Shadow	10	0	3	0	0	0	0	19	1	0	1	0	0	0	1	1	0	2	38	0.50	0	
Flax	0	0	1	0	1	0	0	1	6	2	0	0	0	0	0	0	0	1	0	12	0.50	0
Cabbage Tree	0	11	11	0	0	0	0	0	2	4	0	0	0	0	0	1	0	2	31	0.13	0	
Other Tree (Brown)	0	0	6	4	0	0	0	0	0	0	2	1	1	0	0	0	0	4	18	0.11	0	
Dry Vegetation	0	0	0	2	0	0	0	0	0	0	0	7	0	0	0	0	0	0	9	0.78	0	
Azolla	0	0	0	0	0	0	0	0	0	0	0	0	7	0	0	0	0	0	7	1.00	0	
Rush	0	0	0	0	0	0	0	0	0	0	0	1	0	1	0	0	0	0	2	0.50	0	
Manuka	1	8	42	7	3	0	1	3	2	0	1	9	0	0	3	1	0	23	104	0.03	0	
Kahikatea	1	8	10	1	1	0	0	1	1	1	0	0	0	0	0	2	0	4	30	0.07	0	
Other Tree (Dark)	0	1	6	0	0	0	0	0	3	2	0	0	0	0	0	0	0	1	13	0.00	0	
Waterlogged Grass	5	0	1	2	0	0	0	2	4	0	4	2	0	0	0	0	0	19	39	0.49	0	
<b>Total</b>	<b>257</b>	<b>149</b>	<b>258</b>	<b>83</b>	<b>19</b>	<b>5</b>	<b>25</b>	<b>28</b>	<b>25</b>	<b>13</b>	<b>8</b>	<b>71</b>	<b>11</b>	<b>6</b>	<b>4</b>	<b>8</b>	<b>1</b>	<b>92</b>	<b>1063</b>	<b>0.00</b>	<b>0</b>	
<b>P Accuracy</b>	<b>0.93</b>	<b>0.58</b>	<b>0.40</b>	<b>0.63</b>	<b>0.32</b>	<b>0.80</b>	<b>0.24</b>	<b>0.68</b>	<b>0.24</b>	<b>0.31</b>	<b>0.25</b>	<b>0.10</b>	<b>0.64</b>	<b>0.17</b>	<b>0.75</b>	<b>0.25</b>	<b>0.00</b>	<b>0.21</b>	<b>0.00</b>	<b>0.53</b>	<b>0.00</b>	
<b>Kappa</b>	<b>0</b>	<b>0</b>	<b>0</b>	<b>0</b>	<b>0</b>	<b>0</b>	<b>0</b>	<b>0</b>	<b>0</b>	<b>0</b>	<b>0</b>	<b>0.46</b>										

DSM

Class/Value	Water	Isolepis	Mixed Grass	Bidens	Sedge	Reed	Green Algae	Shadow	Flax	Cabbage Tree	Other Tree (Brown)	Dry Vegetation	Azolla	Rush	Manuka	Kahikatea	Other Tree (Dark)	Waterlogged Grass	Total	U Accuracy	Kappa
Water	245	0	0	0	0	0	0	0	0	0	0	0	0	0	0	0	0	0	245	1.00	0
Isolepis	0	111	8	0	0	0	1	0	0	0	0	1	0	0	0	0	0	0	121	0.92	0
Mixed Grass	1	35	150	9	4	1	12	0	1	0	0	38	2	1	0	0	0	57	311	0.48	0
Bidens	0	0	2	63	1	0	0	0	0	0	0	7	0	0	0	0	0	1	74	0.85	0
Sedge	0	2	89	4	14	0	2	0	5	0	1	5	0	0	0	0	0	1	123	0.11	0
Reed	0	0	0	5	0	4	0	0	0	0	0	1	0	1	0	0	0	0	11	0.36	0
Green Algae	0	1	0	0	0	0	9	0	0	0	0	0	0	0	0	0	0	0	10	0.90	0
Shadow	9	0	1	0	0	0	0	24	0	0	0	0	0	0	0	0	0	2	36	0.67	0
Flax	0	0	1	0	0	0	0	0	9	0	0	0	0	0	0	0	0	0	10	0.90	0
Cabbage Tree	0	0	0	0	0	0	0	0	0	10	0	0	0	0	0	0	0	0	10	1.00	0
Other Tree (Brown)	0	0	0	0	0	0	0	2	0	0	7	0	0	0	1	0	0	0	10	0.70	0
Dry Vegetation	0	0	0	1	0	0	0	0	0	0	0	12	0	0	0	0	0	0	13	0.92	0
Azolla	0	0	0	0	0	0	1	0	0	0	0	0	9	0	0	0	0	0	10	0.90	0
Rush	0	0	1	1	0	0	0	0	0	0	0	4	0	4	0	0	0	0	10	0.40	0
Manuka	0	0	2	0	0	0	0	2	2	0	1	0	0	0	3	0	0	0	10	0.30	0
Kahikatea	0	0	0	0	0	0	0	0	0	2	0	0	0	0	0	8	0	0	10	0.80	0
Other Tree (Dark)	0	0	1	0	0	0	0	0	7	1	0	0	0	0	0	0	1	0	10	0.10	0
Waterlogged Grass	2	0	3	0	0	0	0	0	1	0	0	2	0	0	0	0	0	31	39	0.79	0
<b>Total</b>	<b>257</b>	<b>149</b>	<b>258</b>	<b>83</b>	<b>19</b>	<b>5</b>	<b>25</b>	<b>28</b>	<b>25</b>	<b>13</b>	<b>8</b>	<b>71</b>	<b>11</b>	<b>6</b>	<b>4</b>	<b>8</b>	<b>1</b>	<b>92</b>	<b>1063</b>	<b>0.00</b>	<b>0</b>
<b>P Accuracy</b>	<b>0.95</b>	<b>0.74</b>	<b>0.58</b>	<b>0.76</b>	<b>0.74</b>	<b>0.80</b>	<b>0.36</b>	<b>0.86</b>	<b>0.36</b>	<b>0.77</b>	<b>0.88</b>	<b>0.17</b>	<b>0.82</b>	<b>0.67</b>	<b>0.75</b>	<b>1.00</b>	<b>1.00</b>	<b>0.34</b>	<b>0.00</b>	<b>0.67</b>	<b>0.00</b>
<b>Kappa</b>	<b>0</b>	<b>0</b>	<b>0</b>	<b>0</b>	<b>0</b>	<b>0</b>	<b>0</b>	<b>0</b>	<b>0</b>	<b>0</b>	<b>0</b>	<b>0.61</b>									

## Stage Two – Spring

RGB ONLY

Class/Value	Water	Isolepis	Bidens	Sedge	Shadow	Flax	Green Algae	Mixed Grass	Kahikatea	Manuka	Dry Vegetation	Reed	Cabbage Tree	Dormant Tree	Waterlogged Grass	Brown Grass	Azolla	Dry Bidens	Total	U_Accuracy	Kappa
Water	258	0	0	0	3	0	0	0	0	0	0	0	0	0	0	0	0	0	261	0.99	0
Isolepis	0	84	0	0	0	0	0	0	0	1	0	0	0	0	0	0	0	0	85	0.99	0
Bidens	0	0	21	0	0	0	0	1	0	1	3	1	0	0	2	0	0	1	30	0.70	0
Sedge	1	7	1	5	0	2	4	16	0	0	8	4	0	0	2	12	0	1	63	0.08	0
Shadow	13	1	0	0	12	0	0	0	0	0	0	0	0	0	1	0	0	0	27	0.44	0
Flax	0	1	0	1	0	18	4	6	0	0	3	2	1	0	1	0	0	0	37	0.49	0
Green Algae	1	1	0	0	0	0	8	0	0	0	0	0	0	0	0	1	0	0	11	0.73	0
Mixed Grass	2	34	0	2	0	1	11	91	0	2	6	0	0	0	8	12	0	0	169	0.54	0
Kahikatea	0	2	0	1	1	0	0	3	1	1	1	0	0	0	0	1	0	0	11	0.09	0
Manuka	2	2	1	0	3	1	0	5	0	8	0	1	0	0	5	2	0	0	30	0.27	0
Dry Vegetation	0	0	0	0	0	0	0	0	0	0	19	1	0	0	0	0	0	3	23	0.83	0
Reed	0	0	0	0	0	0	0	0	0	0	3	9	0	0	0	1	0	1	14	0.64	0
Cabbage Tree	0	2	0	1	0	1	0	2	1	0	1	0	9	0	1	0	0	0	18	0.50	0
Dormant Tree	0	0	0	0	0	0	0	0	0	0	2	0	0	5	3	0	0	0	10	0.50	0
Waterlogged Grass	1	1	4	0	2	0	0	13	0	2	4	1	0	0	23	5	0	4	60	0.38	0
Brown Grass	1	1	3	2	0	0	4	17	0	1	12	0	0	0	25	20	1	11	98	0.20	0
Azolla	0	0	0	0	0	0	0	0	0	0	0	0	0	0	0	10	0	0	10	1.00	0
Dry Bidens	0	0	10	0	0	0	0	0	0	0	8	1	0	0	0	2	0	34	55	0.62	0
<b>Total</b>	<b>279</b>	<b>136</b>	<b>40</b>	<b>12</b>	<b>21</b>	<b>23</b>	<b>31</b>	<b>154</b>	<b>2</b>	<b>16</b>	<b>70</b>	<b>20</b>	<b>10</b>	<b>5</b>	<b>71</b>	<b>56</b>	<b>11</b>	<b>55</b>	<b>1012</b>	<b>0.00</b>	<b>0</b>
<b>P_Accuracy</b>	<b>0.92</b>	<b>0.62</b>	<b>0.53</b>	<b>0.42</b>	<b>0.57</b>	<b>0.78</b>	<b>0.26</b>	<b>0.59</b>	<b>0.50</b>	<b>0.50</b>	<b>0.27</b>	<b>0.45</b>	<b>0.90</b>	<b>1.00</b>	<b>0.32</b>	<b>0.36</b>	<b>0.91</b>	<b>0.62</b>	<b>0.00</b>	<b>0.63</b>	<b>0</b>
<b>Kappa</b>	<b>0</b>	<b>0</b>	<b>0</b>	<b>0</b>	<b>0</b>	<b>0</b>	<b>0</b>	<b>0</b>	<b>0</b>	<b>0</b>	<b>0.57</b>										

DSM

Class/Value	Water	Isolepis	Bidens	Sedge	Shadow	Flax	Green Algae	Mixed Grass	Kahikatea	Manuka	Dry Vegetation	Reed	Cabbage Tree	Dormant Tree	Waterlogged Grass	Brown Grass	Azolla	Dry Bidens	Total	U_Accuracy	Kappa
Water	266	0	0	0	8	0	0	0	0	0	0	0	0	0	0	0	0	0	274	0.97	0
Isolepis	0	85	0	0	0	0	0	0	0	1	0	0	0	0	0	0	0	0	86	0.99	0
Bidens	0	0	26	0	0	0	0	1	0	1	2	1	0	0	1	0	0	0	32	0.81	0
Sedge	2	9	2	5	0	2	3	23	0	1	9	4	0	0	3	15	0	1	79	0.06	0
Shadow	9	1	0	0	9	0	0	0	0	0	0	0	0	0	1	0	0	0	20	0.45	0
Flax	0	1	0	1	0	18	5	5	0	0	2	1	0	0	1	0	0	0	34	0.53	0
Green Algae	1	1	0	0	0	0	8	0	0	0	0	0	0	0	0	0	0	0	10	0.80	0
Mixed Grass	0	32	0	3	0	1	10	90	0	3	6	0	1	0	7	10	0	0	163	0.55	0
Kahikatea	0	3	0	1	2	0	0	3	1	0	1	0	0	0	0	1	0	0	12	0.08	0
Manuka	1	1	0	0	1	0	0	3	0	9	0	1	0	0	4	1	0	0	21	0.43	0
Dry Vegetation	0	0	0	0	0	0	0	0	0	0	22	1	0	0	0	0	0	3	26	0.85	0
Reed	0	0	0	0	0	0	0	0	0	0	1	8	0	0	0	0	0	1	10	0.80	0
Cabbage Tree	0	1	0	1	0	1	1	2	1	0	1	0	9	0	1	0	0	0	18	0.50	0
Dormant Tree	0	0	0	0	0	0	0	0	0	0	3	0	0	5	5	0	0	0	13	0.38	0
Waterlogged Grass	0	2	10	1	1	1	4	27	0	1	16	1	0	0	48	17	1	10	140	0.34	0
Brown Grass	0	0	1	0	0	0	0	0	0	0	1	1	0	0	0	11	0	2	16	0.69	0
Azolla	0	0	0	0	0	0	0	0	0	0	0	0	0	0	0	0	10	0	10	1.00	0
Dry Bidens	0	0	1	0	0	0	0	0	0	0	6	2	0	0	0	1	0	38	48	0.79	0
<b>Total</b>	<b>279</b>	<b>136</b>	<b>40</b>	<b>12</b>	<b>21</b>	<b>23</b>	<b>31</b>	<b>154</b>	<b>2</b>	<b>16</b>	<b>70</b>	<b>20</b>	<b>10</b>	<b>5</b>	<b>71</b>	<b>56</b>	<b>11</b>	<b>55</b>	<b>1012</b>	<b>0.00</b>	<b>0</b>
<b>P_Accuracy</b>	<b>0.95</b>	<b>0.63</b>	<b>0.65</b>	<b>0.42</b>	<b>0.43</b>	<b>0.78</b>	<b>0.26</b>	<b>0.58</b>	<b>0.50</b>	<b>0.56</b>	<b>0.31</b>	<b>0.40</b>	<b>0.90</b>	<b>1.00</b>	<b>0.68</b>	<b>0.20</b>	<b>0.91</b>	<b>0.69</b>	<b>0.00</b>	<b>0.66</b>	<b>0</b>
<b>Kappa</b>	<b>0</b>	<b>0</b>	<b>0</b>	<b>0</b>	<b>0</b>	<b>0</b>	<b>0</b>	<b>0</b>	<b>0</b>	<b>0</b>	<b>0.61</b>										

## Stage Two – Summer

RGB ONLY

Class/Value	Water	Isoplepis	Sedge	Shadow	Flax	Green Algae	Azolla	Waterlogged Grass	Yellow Algae	Rush	Manuka	Reed	Other Tree (Dark)	Mixed Grass	Dry Vegetation	Cabbage Tree	Dormant Tree	Kahikatea	Mixed Algae	Total	U Accuracy	Kappa
Water	445	0	0	2	1	0	0	22	0	0	0	0	0	0	1	0	0	0	0	471	0.94	0
Isoplepis	0	23	2	0	0	0	0	0	0	1	0	0	0	16	0	0	0	0	0	42	0.55	0
Sedge	0	4	7	0	1	0	0	0	0	2	0	0	0	23	0	0	0	0	0	37	0.19	0
Shadow	1	0	0	8	0	0	0	0	0	0	0	0	0	0	0	0	0	1	0	10	0.80	0
Flax	0	0	1	1	11	0	0	2	1	0	0	0	0	6	4	0	0	0	0	26	0.42	0
Green Algae	0	0	0	0	0	15	2	0	2	0	0	0	0	0	0	0	0	0	2	21	0.71	0
Azolla	0	0	0	0	0	4	35	1	1	0	0	0	0	0	0	3	0	0	9	53	0.66	0
Waterlogged Grass	3	0	0	0	1	0	1	27	0	0	0	0	0	1	6	0	1	0	1	41	0.66	0
Yellow Algae	0	0	0	0	0	2	1	0	10	1	0	0	0	0	1	0	0	0	1	16	0.63	0
Rush	0	2	0	0	0	6	1	4	0	4	0	1	0	6	10	0	0	0	5	39	0.10	0
Manuka	0	1	1	0	0	0	0	8	0	2	1	0	1	2	1	0	0	0	0	17	0.06	0
Reed	0	3	1	0	1	0	0	0	0	0	2	1	4	1	1	0	0	0	0	14	0.14	0
Other Tree (Dark)	0	0	0	0	0	0	0	0	0	1	0	0	3	6	0	0	0	0	0	10	0.30	0
Mixed Grass	0	11	4	0	0	1	0	0	0	7	0	2	1	71	4	1	0	1	0	103	0.69	0
Dry Vegetation	0	0	0	0	1	0	0	4	0	0	0	0	0	1	25	0	0	0	2	33	0.76	0
Cabbage Tree	0	0	1	0	2	0	0	0	0	0	0	0	0	2	0	10	0	0	0	15	0.67	0
Dormant Tree	0	0	0	0	0	0	7	7	0	0	0	0	0	0	0	0	1	0	2	17	0.06	0
Kahikatea	0	2	1	0	2	1	0	6	0	1	0	3	0	11	4	0	0	4	0	35	0.11	0
Mixed Algae	6	0	0	0	0	1	0	2	1	0	0	0	0	0	1	0	0	0	0	11	0.00	0
<b>Total</b>	<b>455</b>	<b>46</b>	<b>18</b>	<b>11</b>	<b>20</b>	<b>30</b>	<b>47</b>	<b>83</b>	<b>15</b>	<b>19</b>	<b>1</b>	<b>8</b>	<b>6</b>	<b>149</b>	<b>61</b>	<b>12</b>	<b>2</b>	<b>6</b>	<b>22</b>	<b>1011</b>	<b>0</b>	<b>0</b>
<b>P Accuracy</b>	<b>0.98</b>	<b>0.50</b>	<b>0.39</b>	<b>0.73</b>	<b>0.55</b>	<b>0.50</b>	<b>0.74</b>	<b>0.33</b>	<b>0.67</b>	<b>0.21</b>	<b>1.00</b>	<b>0.25</b>	<b>0.50</b>	<b>0.48</b>	<b>0.41</b>	<b>0.83</b>	<b>0.50</b>	<b>0.67</b>	<b>0.00</b>	<b>0.00</b>	<b>0.69</b>	<b>0.00</b>
<b>Kappa</b>	<b>0</b>	<b>0</b>	<b>0</b>	<b>0</b>	<b>0</b>	<b>0</b>	<b>0</b>	<b>0</b>	<b>0</b>	<b>0</b>	<b>0</b>	<b>0</b>	<b>0</b>	<b>0</b>	<b>0.60</b>							

DSM

Class/Value	Water	Isoplepis	Sedge	Shadow	Flax	Green Algae	Azolla	Waterlogged Grass	Yellow Algae	Rush	Manuka	Reed	Other Tree (Dark)	Mixed Grass	Dry Vegetation	Cabbage Tree	Dormant Tree	Kahikatea	Mixed Algae	Total	U Accuracy	Kappa
Water	450	0	0	0	0	0	0	6	0	0	0	0	0	0	0	0	0	0	0	456	0.99	0
Isoplepis	0	25	3	0	0	0	0	0	0	1	0	0	0	18	0	0	0	0	0	47	0.53	0
Sedge	0	2	7	0	0	0	0	0	0	2	0	0	0	18	0	0	0	0	1	30	0.23	0
Shadow	0	0	0	10	0	0	0	0	0	0	0	0	0	0	0	0	0	0	0	10	1.00	0
Flax	0	0	1	1	15	0	0	1	1	0	0	0	0	10	4	0	0	1	0	34	0.44	0
Green Algae	0	0	0	0	0	16	1	1	1	0	0	0	0	0	0	0	0	0	0	19	0.84	0
Azolla	0	0	0	0	0	5	37	1	0	0	0	0	0	0	0	0	0	0	3	46	0.80	0
Waterlogged Grass	3	0	0	0	1	1	1	39	2	0	0	0	0	0	7	0	1	0	1	56	0.70	0
Yellow Algae	0	0	0	0	0	0	1	0	9	0	0	0	0	0	1	0	0	0	0	11	0.82	0
Rush	0	4	0	0	0	6	1	3	1	6	0	1	0	10	6	0	0	0	5	43	0.14	0
Manuka	2	1	1	0	0	0	0	15	0	3	1	0	0	1	0	0	0	0	0	24	0.04	0
Reed	0	1	1	0	1	0	0	1	1	0	0	4	0	3	2	1	0	0	0	15	0.27	0
Other Tree (Dark)	0	0	0	0	0	0	0	0	0	0	0	0	5	7	0	0	0	0	0	12	0.42	0
Mixed Grass	0	12	4	0	1	1	0	0	0	4	0	1	1	70	9	1	0	0	0	104	0.67	0
Dry Vegetation	0	0	0	0	2	0	0	2	0	1	0	0	0	0	27	0	0	0	1	33	0.82	0
Cabbage Tree	0	0	1	0	0	0	0	0	0	0	0	0	0	1	0	10	0	0	0	12	0.83	0
Dormant Tree	0	0	0	0	0	0	5	8	0	0	0	0	0	0	1	0	1	0	2	17	0.06	0
Kahikatea	0	1	0	0	0	1	0	6	0	2	0	2	0	11	4	0	0	5	0	32	0.16	0
Mixed Algae	0	0	0	0	0	0	1	0	0	0	0	0	0	0	0	0	0	0	9	10	0.90	0
<b>Total</b>	<b>455</b>	<b>46</b>	<b>18</b>	<b>11</b>	<b>20</b>	<b>30</b>	<b>47</b>	<b>83</b>	<b>15</b>	<b>19</b>	<b>1</b>	<b>8</b>	<b>6</b>	<b>149</b>	<b>61</b>	<b>12</b>	<b>2</b>	<b>6</b>	<b>22</b>	<b>1011</b>	<b>0</b>	<b>0</b>
<b>P Accuracy</b>	<b>0.99</b>	<b>0.54</b>	<b>0.39</b>	<b>0.91</b>	<b>0.75</b>	<b>0.53</b>	<b>0.79</b>	<b>0.47</b>	<b>0.60</b>	<b>0.32</b>	<b>1.00</b>	<b>0.50</b>	<b>0.83</b>	<b>0.47</b>	<b>0.44</b>	<b>0.83</b>	<b>0.50</b>	<b>0.83</b>	<b>0.41</b>	<b>0.00</b>	<b>0.74</b>	<b>0.00</b>
<b>Kappa</b>	<b>0</b>	<b>0</b>	<b>0</b>	<b>0</b>	<b>0</b>	<b>0</b>	<b>0</b>	<b>0</b>	<b>0</b>	<b>0</b>	<b>0</b>	<b>0</b>	<b>0</b>	<b>0</b>	<b>0.66</b>							

## Stage Two – Autumn

RGB ONLY

Class/Value	Water	Mud	Isolepis	Bidens	Mixed Grass	Dry Vegetation	Flax	Shadow	Kahikatea	Manuka	Reed	Sedge	Waterlogged Grass	Cabbage Tree	Total	U_Accuracy	Kappa
Water	326	6	1	0	0	0	0	2	0	0	0	0	14	0	349	0.93	0
Mud	1	71	1	0	0	1	0	0	0	0	0	0	2	0	76	0.93	0
Isolepis	0	0	89	13	3	0	0	0	0	0	0	0	0	0	105	0.85	0
Bidens	0	0	0	52	1	0	0	0	0	0	0	0	0	0	53	0.98	0
Mixed Grass	0	0	11	0	18	0	0	0	0	0	0	0	0	0	29	0.62	0
Dry Vegetation	0	3	0	0	7	28	1	0	0	0	1	0	0	0	40	0.70	0
Flax	0	0	1	1	5	4	15	0	0	0	3	0	1	0	30	0.50	0
Shadow	0	0	0	0	0	0	0	8	0	0	0	0	0	0	8	1.00	0
Kahikatea	0	0	4	3	1	0	0	0	4	0	0	1	0	0	13	0.31	0
Manuka	0	1	16	5	7	0	0	0	4	4	0	2	2	0	41	0.10	0
Reed	0	1	6	2	14	5	6	0	0	0	5	1	9	0	49	0.10	0
Sedge	0	0	8	1	37	3	3	0	0	0	1	11	0	0	64	0.17	0
Waterlogged Grass	7	19	9	0	11	12	1	0	0	4	0	1	51	0	115	0.44	0
Cabbage Tree	0	0	5	11	11	0	2	0	1	0	2	4	2	10	48	0.21	0
<b>Total</b>	<b>334</b>	<b>101</b>	<b>151</b>	<b>88</b>	<b>115</b>	<b>53</b>	<b>28</b>	<b>10</b>	<b>9</b>	<b>8</b>	<b>12</b>	<b>20</b>	<b>81</b>	<b>10</b>	<b>1020</b>	<b>0</b>	<b>0</b>
<b>P_Accuracy</b>	<b>0.98</b>	<b>0.70</b>	<b>0.59</b>	<b>0.59</b>	<b>0.16</b>	<b>0.53</b>	<b>0.54</b>	<b>0.80</b>	<b>0.44</b>	<b>0.50</b>	<b>0.42</b>	<b>0.55</b>	<b>0.63</b>	<b>1.00</b>	<b>0.00</b>	<b>0.68</b>	<b>0.00</b>
<b>Kappa</b>	<b>0</b>	<b>0</b>	<b>0</b>	<b>0</b>	<b>0</b>	<b>0</b>	<b>0</b>	<b>0</b>	<b>0</b>	<b>0</b>	<b>0</b>	<b>0</b>	<b>0</b>	<b>0</b>	<b>0</b>	<b>0</b>	<b>0.62</b>

DSM

Class/Value	Water	Mud	Isolepis	Bidens	Mixed Grass	Dry Vegetation	Flax	Shadow	Kahikatea	Manuka	Reed	Sedge	Waterlogged Grass	Cabbage Tree	Total	U_Accuracy	Kappa
Water	322	1	0	0	0	0	0	0	0	0	0	0	0	0	323	1.00	0
Mud	1	82	0	0	0	0	0	0	0	0	0	0	0	0	83	0.99	0
Isolepis	0	0	85	15	1	0	0	0	0	0	0	0	0	0	101	0.84	0
Bidens	0	0	1	51	1	0	0	0	0	0	0	0	0	0	53	0.96	0
Mixed Grass	0	0	15	0	24	0	0	0	0	0	0	0	0	0	39	0.62	0
Dry Vegetation	0	3	0	0	1	29	0	0	0	0	0	0	0	0	33	0.88	0
Flax	0	0	1	1	3	4	20	0	0	0	3	2	0	0	34	0.59	0
Shadow	0	0	0	0	0	0	0	10	0	0	0	0	0	0	10	1.00	0
Kahikatea	0	0	5	4	5	0	0	0	8	0	0	1	0	0	23	0.35	0
Manuka	1	0	11	5	6	0	0	0	0	8	0	0	4	0	35	0.23	0
Reed	0	1	6	2	10	7	4	0	0	0	5	2	14	0	51	0.10	0
Sedge	0	0	9	2	40	3	1	0	0	0	2	14	0	0	71	0.20	0
Waterlogged Grass	10	14	10	0	14	10	0	0	0	0	1	0	61	0	120	0.51	0
Cabbage Tree	0	0	8	8	10	0	3	0	1	0	1	1	2	10	44	0.23	0
<b>Total</b>	<b>334</b>	<b>101</b>	<b>151</b>	<b>88</b>	<b>115</b>	<b>53</b>	<b>28</b>	<b>10</b>	<b>9</b>	<b>8</b>	<b>12</b>	<b>20</b>	<b>81</b>	<b>10</b>	<b>1020</b>	<b>0</b>	<b>0</b>
<b>P_Accuracy</b>	<b>0.96</b>	<b>0.81</b>	<b>0.56</b>	<b>0.58</b>	<b>0.21</b>	<b>0.55</b>	<b>0.71</b>	<b>1.00</b>	<b>0.89</b>	<b>1.00</b>	<b>0.42</b>	<b>0.70</b>	<b>0.75</b>	<b>1.00</b>	<b>0.00</b>	<b>0.71</b>	<b>0.00</b>
<b>Kappa</b>	<b>0</b>	<b>0</b>	<b>0</b>	<b>0</b>	<b>0</b>	<b>0</b>	<b>0</b>	<b>0</b>	<b>0</b>	<b>0</b>	<b>0</b>	<b>0</b>	<b>0</b>	<b>0</b>	<b>0</b>	<b>0</b>	<b>0.66</b>

### Stage Three – Winter

RGB Only

ClassValue:	Water	Isolepis	Reed	Green Algae	Bidens	Brown Grass	Mixed Grass	Shadow	Manuka	Other Tree (Dark)	Cabbage Tree	Blackberry	Dry Vegetation	Flax	Toetoe	Dormant Tree	Red Algae	Kahikatea	Sedge	Total	U_Accuracy	Kappa
Water	50	0	3	1	0	1	0	0	0	0	0	0	0	0	0	0	0	0	0	55	0.91	0
Isolepis	0	90	0	0	0	19	3	0	0	0	0	0	0	0	0	0	0	0	0	112	0.80	0
Reed	2	0	63	0	1	3	1	0	0	0	0	2	15	0	0	0	0	0	2	89	0.71	0
Green Algae	0	0	0	8	0	0	1	0	0	0	0	0	0	0	0	0	0	0	0	9	0.89	0
Bidens	3	0	2	0	22	7	1	0	2	0	0	0	8	0	0	1	0	0	4	50	0.44	0
Brown Grass	0	23	1	0	1	98	24	0	0	2	0	0	6	0	1	0	0	2	3	161	0.61	0
Mixed Grass	3	30	4	5	2	10	129	0	0	0	0	0	41	0	2	0	0	0	1	227	0.57	0
Shadow	1	0	0	0	0	0	2	5	1	0	0	0	0	0	0	0	0	0	0	9	0.56	0
Manuka	2	8	0	0	0	16	12	0	1	0	0	0	0	0	0	0	0	1	4	44	0.02	0
Other Tree (Dark)	0	0	0	0	0	0	1	0	0	2	0	0	0	1	0	0	0	0	0	4	0.50	0
Cabbage Tree	2	5	2	5	0	1	22	0	0	7	5	0	4	2	3	0	0	0	0	58	0.09	0
Blackberry	2	0	2	0	0	4	2	1	1	1	0	10	1	3	0	0	0	0	1	28	0.36	0
Dry Vegetation	0	0	1	0	4	0	3	0	0	0	0	0	19	0	0	1	0	0	0	28	0.68	0
Flax	0	0	1	0	0	1	1	1	0	0	0	0	0	10	0	0	0	0	0	14	0.71	0
Toetoe	0	0	1	0	0	1	1	0	0	0	0	0	8	0	0	0	0	0	0	11	0.00	0
Dormant Tree	7	0	4	0	8	0	3	0	0	0	0	0	21	0	0	6	0	0	0	49	0.12	0
Red Algae	0	0	0	0	0	0	0	0	0	0	0	0	0	0	0	0	10	0	0	10	1.00	0
Kahikatea	4	0	0	0	2	3	4	1	0	0	0	2	1	0	0	0	0	3	3	23	0.13	0
Sedge	0	0	4	0	5	17	4	0	0	1	0	0	5	0	0	1	0	1	6	44	0.14	0
<b>Total</b>	<b>76</b>	<b>156</b>	<b>88</b>	<b>19</b>	<b>45</b>	<b>181</b>	<b>214</b>	<b>8</b>	<b>5</b>	<b>13</b>	<b>5</b>	<b>14</b>	<b>129</b>	<b>16</b>	<b>6</b>	<b>9</b>	<b>10</b>	<b>7</b>	<b>24</b>	<b>1025</b>	<b>0.00</b>	<b>0</b>
<b>P_Accuracy</b>	<b>0.66</b>	<b>0.58</b>	<b>0.72</b>	<b>0.42</b>	<b>0.49</b>	<b>0.54</b>	<b>0.60</b>	<b>0.63</b>	<b>0.20</b>	<b>0.15</b>	<b>1.00</b>	<b>0.71</b>	<b>0.15</b>	<b>0.63</b>	<b>0.00</b>	<b>0.67</b>	<b>1.00</b>	<b>0.43</b>	<b>0.25</b>	<b>0.00</b>	<b>0.52</b>	<b>0.00</b>
<b>Kappa</b>	<b>0</b>	<b>0</b>	<b>0</b>	<b>0</b>	<b>0</b>	<b>0</b>	<b>0</b>	<b>0</b>	<b>0</b>	<b>0</b>	<b>0</b>	<b>0</b>	<b>0.46</b>									

DSM

ClassValue:	Water	Isolepis	Reed	Green Algae	Bidens	Brown Grass	Mixed Grass	Shadow	Manuka	Other Tree (Dark)	Cabbage Tree	Blackberry	Dry Vegetation	Flax	Toetoe	Dormant Tree	Red Algae	Kahikatea	Sedge	Total	U_Accuracy	Kappa
Water	76	1	0	0	0	0	1	0	0	0	0	0	0	0	0	0	0	0	0	78	0.97	0
Isolepis	0	133	0	2	0	15	0	0	0	0	0	0	0	0	0	0	0	0	0	150	0.89	0
Reed	0	2	82	0	6	2	0	0	0	0	0	0	21	0	0	1	0	0	0	114	0.72	0
Green Algae	0	0	0	16	0	0	0	0	0	0	0	0	0	0	0	0	0	0	0	16	1.00	0
Bidens	0	0	3	1	36	6	0	0	1	0	0	0	7	0	0	3	0	0	2	59	0.61	0
Brown Grass	0	8	0	0	0	132	12	0	0	0	0	1	4	0	0	0	0	0	6	163	0.81	0
Mixed Grass	0	8	1	0	1	6	164	0	0	1	1	0	26	0	2	0	0	0	0	210	0.78	0
Shadow	0	0	0	0	0	0	2	8	0	0	0	0	0	0	0	0	0	0	0	10	0.80	0
Manuka	0	1	0	0	0	5	8	0	4	3	0	1	0	0	0	0	0	0	0	22	0.18	0
Other Tree (Dark)	0	0	0	0	0	0	4	0	0	4	0	0	0	1	1	0	0	0	0	10	0.40	0
Cabbage Tree	0	0	0	0	0	0	3	0	0	1	4	0	0	2	0	0	0	0	0	10	0.40	0
Blackberry	0	0	0	0	0	3	1	0	0	1	0	11	7	0	0	0	0	0	0	23	0.48	0
Dry Vegetation	0	0	0	0	1	0	1	0	0	0	0	0	31	0	0	0	0	0	0	33	0.94	0
Flax	0	0	0	0	0	0	0	0	0	1	0	0	0	11	0	0	0	0	0	12	0.92	0
Toetoe	0	0	2	0	0	2	6	0	0	2	0	0	8	2	3	0	0	0	1	26	0.12	0
Dormant Tree	0	0	0	0	0	0	0	0	0	0	0	0	5	0	0	5	0	0	0	10	0.50	0
Red Algae	0	0	0	0	0	0	0	0	0	0	0	0	0	0	0	0	10	0	0	10	1.00	0
Kahikatea	0	0	0	0	0	1	0	0	0	0	0	0	1	0	0	0	0	7	1	10	0.70	0
Sedge	0	3	0	0	1	9	12	0	0	0	0	1	19	0	0	0	0	0	14	59	0.24	0
<b>Total</b>	<b>76</b>	<b>156</b>	<b>88</b>	<b>19</b>	<b>45</b>	<b>181</b>	<b>214</b>	<b>8</b>	<b>5</b>	<b>13</b>	<b>5</b>	<b>14</b>	<b>129</b>	<b>16</b>	<b>6</b>	<b>9</b>	<b>10</b>	<b>7</b>	<b>24</b>	<b>1025</b>	<b>0.00</b>	<b>0</b>
<b>P_Accuracy</b>	<b>1.00</b>	<b>0.85</b>	<b>0.93</b>	<b>0.84</b>	<b>0.80</b>	<b>0.73</b>	<b>0.77</b>	<b>1.00</b>	<b>0.80</b>	<b>0.31</b>	<b>0.80</b>	<b>0.79</b>	<b>0.24</b>	<b>0.69</b>	<b>0.50</b>	<b>0.56</b>	<b>1.00</b>	<b>1.00</b>	<b>0.58</b>	<b>0.00</b>	<b>0.73</b>	<b>0.00</b>
<b>Kappa</b>	<b>0</b>	<b>0</b>	<b>0</b>	<b>0</b>	<b>0</b>	<b>0</b>	<b>0</b>	<b>0</b>	<b>0</b>	<b>0</b>	<b>0</b>	<b>0</b>	<b>0.70</b>									

### Stage Three – Spring

RGB ONLY

Class/Value	Water	Mixed Grass	Shadow	Dry Vegetation	Waterlogged Grass	Blackberry	Manuka	Other Tree (Dark)	Flax	Cabbage Tree	Kahikatea	Isolepis	Azolla	Reed	Dormant Tree	Sedge	Toetoe	Green Algae	Total	U_Accuracy	Kappa
Water	82	0	5	0	5	0	0	0	0	0	0	0	0	1	0	0	0	0	93	0.88	0
Mixed Grass	0	112	0	1	0	0	0	1	0	2	0	3	0	0	0	0	0	0	119	0.94	0
Shadow	0	0	14	0	0	0	0	0	0	0	0	0	0	0	0	0	0	0	14	1.00	0
Dry Vegetation	0	0	0	3	0	0	0	0	0	0	0	0	0	2	0	0	0	0	5	0.60	0
Waterlogged Grass	13	2	0	0	199	0	1	0	0	0	1	3	3	0	0	1	0	15	238	0.84	0
Blackberry	1	1	0	4	9	4	0	0	0	0	0	0	0	7	0	2	0	6	34	0.12	0
Manuka	0	9	1	1	13	0	4	1	2	0	0	0	0	1	0	0	1	6	39	0.10	0
Other Tree (Dark)	0	9	0	0	0	0	0	5	2	0	0	0	0	0	0	0	0	0	16	0.31	0
Flax	0	1	0	1	0	0	0	0	8	1	2	0	0	1	0	0	1	0	15	0.53	0
Cabbage Tree	0	6	0	1	0	0	0	0	2	9	0	1	0	0	0	0	2	0	21	0.43	0
Kahikatea	2	29	1	14	23	5	1	0	3	2	9	21	0	4	0	0	1	19	134	0.07	0
Isolepis	0	22	0	12	2	0	1	0	0	0	1	46	0	1	0	0	1	1	87	0.53	0
Azolla	0	0	0	0	0	0	0	0	0	0	0	0	7	0	0	0	0	0	7	1.00	0
Reed	0	2	0	23	0	0	0	0	2	0	0	0	0	29	0	5	0	3	64	0.45	0
Dormant Tree	0	0	0	3	0	0	0	0	0	0	0	0	0	1	3	0	0	1	8	0.38	0
Sedge	0	2	0	6	8	3	0	0	0	1	0	5	2	3	1	15	0	0	46	0.33	0
Toetoe	0	6	0	6	0	0	0	0	0	0	0	3	0	1	0	0	4	2	22	0.18	0
Green Algae	0	1	0	11	1	1	0	0	0	0	0	0	1	2	1	0	0	24	42	0.57	0
<b>Total</b>	<b>98</b>	<b>202</b>	<b>21</b>	<b>86</b>	<b>260</b>	<b>13</b>	<b>7</b>	<b>7</b>	<b>19</b>	<b>15</b>	<b>13</b>	<b>82</b>	<b>13</b>	<b>53</b>	<b>5</b>	<b>23</b>	<b>10</b>	<b>77</b>	<b>1004</b>	<b>0</b>	<b>0</b>
<b>P_Accuracy</b>	<b>0.84</b>	<b>0.55</b>	<b>0.67</b>	<b>0.03</b>	<b>0.77</b>	<b>0.31</b>	<b>0.57</b>	<b>0.71</b>	<b>0.42</b>	<b>0.60</b>	<b>0.69</b>	<b>0.56</b>	<b>0.54</b>	<b>0.55</b>	<b>0.60</b>	<b>0.65</b>	<b>0.40</b>	<b>0.31</b>	<b>0.00</b>	<b>0.57</b>	<b>0.00</b>
<b>Kappa</b>	<b>0</b>	<b>0</b>	<b>0</b>	<b>0</b>	<b>0</b>	<b>0</b>	<b>0</b>	<b>0</b>	<b>0</b>	<b>0</b>	<b>0</b>	<b>0</b>	<b>0</b>	<b>0</b>	<b>0</b>	<b>0</b>	<b>0</b>	<b>0</b>	<b>0</b>	<b>0</b>	<b>0.52</b>

DSM

Class/Value	Water	Mixed Grass	Shadow	Dry Vegetation	Waterlogged Grass	Blackberry	Manuka	Other Tree (Dark)	Flax	Cabbage Tree	Kahikatea	Isolepis	Azolla	Reed	Dormant Tree	Sedge	Toetoe	Green Algae	Total	U_Accuracy	Kappa
Water	89	0	5	0	4	0	0	0	0	0	0	0	0	1	0	0	0	1	100	0.89	0
Mixed Grass	0	126	0	0	0	0	0	0	0	0	1	1	0	0	0	0	0	0	128	0.98	0
Shadow	1	0	16	0	0	0	0	0	0	0	0	0	0	0	0	0	0	0	17	0.94	0
Dry Vegetation	0	0	0	9	0	0	0	0	0	0	0	0	0	1	0	0	0	0	10	0.90	0
Waterlogged Grass	7	12	0	2	237	2	0	0	0	0	0	2	1	4	0	1	0	15	283	0.84	0
Blackberry	1	0	0	3	6	6	0	0	0	2	0	0	1	3	1	2	0	2	27	0.22	0
Manuka	0	3	0	0	0	1	6	0	2	0	1	0	0	0	0	0	1	0	14	0.43	0
Other Tree (Dark)	0	1	0	0	0	0	0	7	2	0	0	0	0	0	0	0	0	0	10	0.70	0
Flax	0	5	0	2	0	1	1	0	11	3	0	1	0	1	0	0	1	0	26	0.42	0
Cabbage Tree	0	0	0	1	1	0	0	0	2	9	0	1	0	0	0	0	1	0	15	0.60	0
Kahikatea	0	4	0	11	1	0	0	0	0	0	9	2	0	0	0	0	2	4	33	0.27	0
Isolepis	0	36	0	12	4	0	0	0	0	1	1	71	0	2	0	0	0	4	131	0.54	0
Azolla	0	0	0	1	0	0	0	0	0	0	0	0	9	0	0	0	0	0	10	0.90	0
Reed	0	2	0	14	0	0	0	0	2	0	0	0	0	36	0	1	0	0	55	0.65	0
Dormant Tree	0	0	0	5	0	0	0	0	0	0	0	0	0	2	4	0	0	5	16	0.25	0
Sedge	0	5	0	10	7	3	0	0	0	0	0	3	1	2	0	19	0	1	51	0.37	0
Toetoe	0	5	0	8	0	0	0	0	0	0	0	1	0	0	0	0	5	0	19	0.26	0
Green Algae	0	3	0	8	0	0	0	0	0	0	1	0	1	1	0	0	0	45	59	0.76	0
<b>Total</b>	<b>98</b>	<b>202</b>	<b>21</b>	<b>86</b>	<b>260</b>	<b>13</b>	<b>7</b>	<b>7</b>	<b>19</b>	<b>15</b>	<b>13</b>	<b>82</b>	<b>13</b>	<b>53</b>	<b>5</b>	<b>23</b>	<b>10</b>	<b>77</b>	<b>1004</b>	<b>0</b>	<b>0</b>
<b>P_Accuracy</b>	<b>0.91</b>	<b>0.62</b>	<b>0.76</b>	<b>0.10</b>	<b>0.91</b>	<b>0.46</b>	<b>0.86</b>	<b>1.00</b>	<b>0.58</b>	<b>0.60</b>	<b>0.69</b>	<b>0.87</b>	<b>0.69</b>	<b>0.68</b>	<b>0.80</b>	<b>0.83</b>	<b>0.50</b>	<b>0.58</b>	<b>0.00</b>	<b>0.71</b>	<b>0.00</b>
<b>Kappa</b>	<b>0</b>	<b>0</b>	<b>0</b>	<b>0</b>	<b>0</b>	<b>0</b>	<b>0</b>	<b>0</b>	<b>0</b>	<b>0</b>	<b>0</b>	<b>0</b>	<b>0</b>	<b>0</b>	<b>0</b>	<b>0</b>	<b>0</b>	<b>0</b>	<b>0</b>	<b>0</b>	<b>0.67</b>

### Stage Three – Summer

RGB ONLY

Class/Value	Water	Mixed Grass	Shadow	Isolepis	Dry Vegetation	Blackberry	Reeds	Sedge	Manuka	Other Tree (Dark)	Kahikatea	Azolla	Green Algae	Dormant Tree	Waterlogged Grass	Flax	Cabbage Tree	Rush	Total	U_Accuracy	Kappa
Water	63	0	0	0	0	0	0	0	0	0	0	0	0	0	2	0	0	0	65	0.97	0
Mixed Grass	0	121	0	23	7	0	0	3	0	0	0	0	5	0	0	0	1	1	161	0.75	0
Shadow	2	1	7	0	0	0	0	0	0	0	0	0	0	0	1	0	0	0	11	0.64	0
Isolepis	0	7	0	74	0	0	0	0	0	0	0	0	0	0	0	0	0	0	81	0.91	0
Dry Vegetation	0	1	0	0	71	0	0	0	0	0	0	2	16	1	1	0	0	0	92	0.77	0
Blackberry	0	3	0	0	0	12	1	0	1	3	0	0	0	0	0	1	0	0	21	0.57	0
Reeds	0	28	0	3	18	0	39	2	0	0	2	0	5	1	0	0	0	0	98	0.40	0
Sedge	0	18	0	24	0	1	4	18	0	0	0	0	0	0	0	0	0	0	65	0.28	0
Manuka	0	1	0	5	0	0	0	1	5	0	0	0	0	0	0	0	0	1	13	0.38	0
Other Tree (Dark)	0	11	0	6	0	0	0	2	0	6	0	0	0	0	0	0	0	0	25	0.24	0
Kahikatea	2	28	3	11	9	0	7	2	10	1	8	2	11	0	22	0	0	1	117	0.07	0
Azolla	0	0	0	0	0	0	0	0	0	0	0	24	2	0	0	0	0	0	26	0.92	0
Green Algae	0	0	0	0	0	0	0	0	0	0	0	1	19	0	0	0	0	0	20	0.95	0
Dormant Tree	0	0	0	0	2	0	0	0	0	0	0	4	1	3	1	0	0	0	11	0.27	0
Waterlogged Grass	0	1	0	1	1	0	0	0	0	0	0	1	0	0	26	0	0	0	30	0.87	0
Flax	1	6	0	0	4	2	10	0	0	1	2	0	1	0	1	16	1	0	45	0.36	0
Cabbage Tree	0	12	0	0	1	2	8	1	0	0	0	0	0	0	0	15	0	0	39	0.38	0
Rush	0	1	0	1	1	0	0	0	0	0	0	0	0	0	1	0	0	3	7	0.43	0
<b>Total</b>	<b>68</b>	<b>239</b>	<b>10</b>	<b>148</b>	<b>114</b>	<b>17</b>	<b>69</b>	<b>29</b>	<b>16</b>	<b>11</b>	<b>12</b>	<b>34</b>	<b>60</b>	<b>5</b>	<b>55</b>	<b>17</b>	<b>17</b>	<b>6</b>	<b>927</b>	<b>0.00</b>	<b>0</b>
<b>P_Accuracy</b>	<b>0.93</b>	<b>0.51</b>	<b>0.70</b>	<b>0.50</b>	<b>0.62</b>	<b>0.71</b>	<b>0.57</b>	<b>0.62</b>	<b>0.31</b>	<b>0.55</b>	<b>0.67</b>	<b>0.71</b>	<b>0.32</b>	<b>0.60</b>	<b>0.47</b>	<b>0.94</b>	<b>0.88</b>	<b>0.50</b>	<b>0.00</b>	<b>0.57</b>	<b>0</b>
<b>Kappa</b>	<b>0</b>	<b>0</b>	<b>0</b>	<b>0</b>	<b>0</b>	<b>0</b>	<b>0</b>	<b>0</b>	<b>0</b>	<b>0</b>	<b>0</b>	<b>0</b>	<b>0</b>	<b>0</b>	<b>0</b>	<b>0</b>	<b>0</b>	<b>0</b>	<b>0</b>	<b>0</b>	<b>0.53</b>

DSM

Class/Value	Water	Mixed Grass	Shadow	Isolepis	Dry Vegetation	Blackberry	Reeds	Sedge	Manuka	Other Tree (Dark)	Kahikatea	Azolla	Green Algae	Dormant Tree	Waterlogged Grass	Flax	Cabbage Tree	Rush	Total	U_Accuracy	Kappa
Water	64	0	0	0	0	0	0	0	0	0	0	0	0	0	1	0	0	0	65	0.98	0
Mixed Grass	0	124	0	24	1	0	0	2	0	0	0	0	4	0	0	0	1	1	157	0.79	0
Shadow	1	0	9	0	0	0	0	0	0	0	0	0	0	0	0	0	0	0	10	0.90	0
Isolepis	0	2	0	81	0	0	0	0	0	0	0	0	0	0	0	0	0	0	83	0.98	0
Dry Vegetation	0	0	0	0	83	0	0	0	0	0	0	1	4	0	1	0	0	0	89	0.93	0
Blackberry	0	2	0	0	0	12	0	0	1	2	0	0	0	0	0	0	0	0	17	0.71	0
Reeds	0	22	0	1	10	0	33	1	0	0	0	0	2	1	0	0	0	0	70	0.47	0
Sedge	0	29	0	23	0	0	6	23	0	0	0	0	0	0	0	0	0	0	81	0.28	0
Manuka	0	5	0	7	0	0	1	0	13	0	0	0	0	0	0	0	0	0	32	0.41	0
Other Tree (Dark)	0	8	0	2	0	1	1	3	0	8	0	0	0	0	0	0	0	0	23	0.35	0
Kahikatea	3	26	1	9	12	0	11	0	2	1	12	2	13	0	19	1	1	1	114	0.11	0
Azolla	0	0	0	0	0	0	0	0	0	0	0	26	1	0	0	0	0	0	27	0.96	0
Green Algae	0	0	0	1	1	0	0	0	0	0	0	2	34	0	0	0	0	0	38	0.89	0
Dormant Tree	0	0	0	0	3	0	0	0	0	0	0	3	1	4	1	0	0	0	12	0.33	0
Waterlogged Grass	0	0	0	0	0	0	0	0	0	0	0	0	0	0	26	0	0	0	26	1.00	0
Flax	0	8	0	0	4	3	9	0	0	0	0	0	1	0	0	16	0	0	41	0.39	0
Cabbage Tree	0	12	0	0	0	1	8	0	0	0	0	0	0	0	0	0	15	0	36	0.42	0
Rush	0	1	0	0	0	0	0	0	0	0	0	0	0	0	1	0	0	4	6	0.67	0
<b>Total</b>	<b>68</b>	<b>239</b>	<b>10</b>	<b>148</b>	<b>114</b>	<b>17</b>	<b>69</b>	<b>29</b>	<b>16</b>	<b>11</b>	<b>12</b>	<b>34</b>	<b>60</b>	<b>5</b>	<b>55</b>	<b>17</b>	<b>17</b>	<b>6</b>	<b>927</b>	<b>0.00</b>	<b>0</b>
<b>P_Accuracy</b>	<b>0.94</b>	<b>0.52</b>	<b>0.90</b>	<b>0.55</b>	<b>0.73</b>	<b>0.71</b>	<b>0.48</b>	<b>0.79</b>	<b>0.81</b>	<b>0.73</b>	<b>1.00</b>	<b>0.76</b>	<b>0.57</b>	<b>0.80</b>	<b>0.47</b>	<b>0.94</b>	<b>0.88</b>	<b>0.67</b>	<b>0.00</b>	<b>0.63</b>	<b>0</b>
<b>Kappa</b>	<b>0</b>	<b>0</b>	<b>0</b>	<b>0</b>	<b>0</b>	<b>0</b>	<b>0</b>	<b>0</b>	<b>0</b>	<b>0</b>	<b>0</b>	<b>0</b>	<b>0</b>	<b>0</b>	<b>0</b>	<b>0</b>	<b>0</b>	<b>0</b>	<b>0</b>	<b>0</b>	<b>0.60</b>

### Stage Three – Autumn

RGB ONLY

Class/Value	Water	Mud	Isolepis	Mixed Grass	Dry Vegetation	Shadow	Flax	Sedge	Cabbage Tree	Blackberry	Kahikatea	Bidens	Reed	Manuka	Other Tree (Light)	Dormant Tree	Green Algae	Rush	Total	U_Accuracy	Kappa
Water	42	0	0	0	0	0	0	0	0	0	0	0	1	0	0	0	0	0	43	0.98	0
Mud	1	14	0	0	0	0	0	0	0	0	0	0	0	0	0	0	0	0	15	0.93	0
Isolepis	0	0	247	20	0	0	0	1	0	0	0	2	0	0	0	0	0	0	270	0.91	0
Mixed Grass	0	0	21	58	2	0	0	2	0	1	0	0	1	0	0	0	2	0	87	0.67	0
Dry Vegetation	0	2	0	3	73	0	0	0	0	0	0	0	1	0	0	0	0	0	79	0.92	0
Shadow	0	0	0	0	0	10	0	0	0	0	0	0	0	0	0	0	0	0	10	1.00	0
Flax	0	0	0	1	3	1	22	1	0	3	1	0	22	2	0	0	0	1	57	0.39	0
Sedge	0	0	6	23	5	0	0	10	0	0	1	0	3	1	0	0	0	2	51	0.20	0
Cabbage Tree	0	0	2	20	2	0	6	5	11	6	1	2	8	0	3	0	1	0	67	0.16	0
Blackberry	0	0	9	11	0	1	2	0	0	6	1	7	3	1	10	0	0	1	52	0.12	0
Kahikatea	0	1	14	12	0	0	0	0	0	1	4	0	1	3	0	1	0	3	40	0.10	0
Bidens	0	0	3	3	0	0	0	0	0	0	0	19	0	0	0	0	0	0	25	0.76	0
Reed	0	0	1	10	26	0	2	2	0	1	3	0	34	1	0	0	0	1	81	0.42	0
Manuka	6	1	16	5	2	3	0	2	0	0	0	3	3	7	1	0	0	0	49	0.14	0
Other Tree (Light)	0	0	1	4	0	0	0	0	0	0	0	2	1	0	1	0	0	0	9	0.11	0
Dormant Tree	2	14	0	0	0	0	0	0	0	0	0	0	0	0	0	4	2	0	22	0.18	0
Green Algae	0	0	0	0	0	0	0	0	0	0	0	0	0	0	0	0	8	0	8	1.00	0
Rush	0	1	21	14	2	0	0	1	0	0	1	0	1	0	0	0	0	7	48	0.15	0
<b>Total</b>	<b>51</b>	<b>33</b>	<b>341</b>	<b>184</b>	<b>115</b>	<b>15</b>	<b>32</b>	<b>24</b>	<b>11</b>	<b>18</b>	<b>12</b>	<b>35</b>	<b>79</b>	<b>15</b>	<b>15</b>	<b>5</b>	<b>13</b>	<b>15</b>	<b>1013</b>	<b>0</b>	<b>0</b>
<b>P_Accuracy</b>	<b>0.82</b>	<b>0.42</b>	<b>0.72</b>	<b>0.32</b>	<b>0.63</b>	<b>0.67</b>	<b>0.69</b>	<b>0.42</b>	<b>1.00</b>	<b>0.33</b>	<b>0.33</b>	<b>0.54</b>	<b>0.43</b>	<b>0.47</b>	<b>0.07</b>	<b>0.80</b>	<b>0.62</b>	<b>0.47</b>	<b>0.00</b>	<b>0.57</b>	<b>0.00</b>
<b>Kappa</b>	<b>0</b>	<b>0</b>	<b>0</b>	<b>0</b>	<b>0</b>	<b>0</b>	<b>0</b>	<b>0</b>	<b>0</b>	<b>0</b>	<b>0</b>	<b>0</b>	<b>0</b>	<b>0</b>	<b>0</b>	<b>0</b>	<b>0</b>	<b>0</b>	<b>0</b>	<b>0</b>	<b>0.50</b>

DSM

Class/Value	Water	Mud	Isolepis	Mixed Grass	Dry Vegetation	Shadow	Flax	Sedge	Cabbage Tree	Blackberry	Kahikatea	Bidens	Reed	Manuka	Other Tree (Light)	Dormant Tree	Green Algae	C_18	Total	U_Accuracy	Kappa
Water	48	1	0	0	0	0	0	0	0	0	0	0	0	0	0	0	0	0	49	0.98	0
Mud	0	25	0	0	0	0	0	0	0	0	0	0	0	0	0	0	0	0	25	1.00	0
Isolepis	0	0	266	19	0	0	0	1	0	0	0	3	0	0	0	0	1	0	290	0.92	0
Mixed Grass	0	0	8	58	0	0	0	0	0	0	0	0	1	0	0	0	0	0	67	0.87	0
Dry Vegetation	0	2	0	0	68	0	0	0	0	0	0	0	1	0	0	0	0	0	71	0.96	0
Shadow	1	0	0	0	0	14	0	0	0	0	0	0	0	0	0	0	0	0	15	0.93	0
Flax	0	0	0	3	3	0	22	2	0	2	1	1	19	1	0	0	0	0	54	0.41	0
Sedge	0	0	4	18	0	0	0	13	0	1	1	0	3	1	0	0	0	0	41	0.32	0
Cabbage Tree	0	0	6	24	1	0	6	3	11	5	0	1	11	0	2	0	1	0	71	0.15	0
Blackberry	0	0	14	9	0	0	2	1	0	7	2	4	4	2	2	0	0	0	47	0.15	0
Kahikatea	0	0	8	11	1	0	1	0	0	1	5	0	1	0	0	0	0	2	30	0.17	0
Bidens	0	0	2	2	0	0	0	0	0	0	0	20	0	0	0	0	0	0	24	0.83	0
Reed	0	0	0	14	40	0	0	0	0	1	1	0	36	1	0	0	0	2	95	0.38	0
Manuka	2	0	16	7	0	1	0	2	0	0	0	4	3	8	0	0	0	0	43	0.19	0
Other Tree (Light)	0	0	2	5	0	0	0	0	0	1	0	2	0	0	11	0	0	0	21	0.52	0
Dormant Tree	0	4	1	0	0	0	0	0	0	0	0	0	0	0	0	5	0	0	10	0.50	0
Green Algae	0	0	0	0	0	0	0	0	0	0	0	0	0	0	0	0	11	0	11	1.00	0
Rush	0	1	14	14	2	0	1	2	0	0	2	0	0	2	0	0	0	11	49	0.22	0
<b>Total</b>	<b>51</b>	<b>33</b>	<b>341</b>	<b>184</b>	<b>115</b>	<b>15</b>	<b>32</b>	<b>24</b>	<b>11</b>	<b>18</b>	<b>12</b>	<b>35</b>	<b>79</b>	<b>15</b>	<b>15</b>	<b>5</b>	<b>13</b>	<b>15</b>	<b>1013</b>	<b>0</b>	<b>0</b>
<b>P_Accuracy</b>	<b>0.94</b>	<b>0.76</b>	<b>0.78</b>	<b>0.32</b>	<b>0.59</b>	<b>0.93</b>	<b>0.69</b>	<b>0.54</b>	<b>1.00</b>	<b>0.39</b>	<b>0.42</b>	<b>0.57</b>	<b>0.46</b>	<b>0.53</b>	<b>0.73</b>	<b>1.00</b>	<b>0.85</b>	<b>0.73</b>	<b>0.00</b>	<b>0.63</b>	<b>0.00</b>
<b>Kappa</b>	<b>0</b>	<b>0</b>	<b>0</b>	<b>0</b>	<b>0</b>	<b>0</b>	<b>0</b>	<b>0</b>	<b>0</b>	<b>0</b>	<b>0</b>	<b>0</b>	<b>0</b>	<b>0</b>	<b>0</b>	<b>0</b>	<b>0</b>	<b>0</b>	<b>0</b>	<b>0</b>	<b>0.57</b>

## Multispectral Tests: Stage One

RGB Only

Class\Value	Water	Mixed Grass	Isolepis	Dry Vegetation	Blackberry	Reed	Cabbage Tree	Flax	Other Tree (Dark)	Other Tree (Light)	Sedge	Bidens	Toetoe	Dormant Tree	Total	U_Accuracy	Kappa
Water	178	3	0	0	1	5	0	0	1	0	0	1	0	0	189	0.94	0
Mixed Grass	0	133	9	23	0	1	0	0	0	3	5	0	1	0	175	0.76	0
Isolepis	0	5	57	0	0	0	0	0	0	0	0	0	0	0	62	0.92	0
Dry Vegetation	0	3	0	37	0	1	0	0	0	0	1	0	0	0	42	0.88	0
Blackberry	0	14	5	1	4	1	1	8	0	0	1	0	2	0	37	0.11	0
Reed	1	6	2	5	0	31	0	8	1	0	4	6	2	0	66	0.47	0
Cabbage Tree	0	7	8	1	0	1	8	2	0	0	0	0	1	0	28	0.29	0
Flax	0	12	4	4	0	10	1	30	2	1	1	1	5	0	71	0.42	0
Other Tree (Dark)	1	4	26	1	1	1	1	3	22	4	0	0	3	0	67	0.33	0
Other Tree (Light)	0	0	8	0	0	0	2	0	0	2	0	0	0	0	12	0.17	0
Sedge	8	44	27	11	1	11	2	6	5	6	26	8	2	5	162	0.16	0
Bidens	0	1	0	3	0	3	0	0	0	0	0	3	0	0	10	0.30	0
Toetoe	1	21	2	19	1	2	1	0	0	2	5	0	12	1	67	0.18	0
Dormant Tree	3	1	0	6	0	1	0	0	0	0	1	0	1	1	14	0.07	0
<b>Total</b>	<b>192</b>	<b>254</b>	<b>148</b>	<b>111</b>	<b>8</b>	<b>68</b>	<b>16</b>	<b>57</b>	<b>31</b>	<b>18</b>	<b>44</b>	<b>19</b>	<b>29</b>	<b>7</b>	<b>1002</b>	<b>0</b>	<b>0</b>
<b>P_Accuracy</b>	<b>0.93</b>	<b>0.52</b>	<b>0.39</b>	<b>0.33</b>	<b>0.50</b>	<b>0.46</b>	<b>0.50</b>	<b>0.53</b>	<b>0.71</b>	<b>0.11</b>	<b>0.59</b>	<b>0.16</b>	<b>0.41</b>	<b>0.14</b>	<b>0.00</b>	<b>0.54</b>	<b>0.00</b>
<b>Kappa</b>	<b>0</b>	<b>0</b>	<b>0</b>	<b>0</b>	<b>0</b>	<b>0</b>	<b>0</b>	<b>0</b>	<b>0</b>	<b>0</b>	<b>0</b>	<b>0</b>	<b>0</b>	<b>0</b>	<b>0</b>	<b>0</b>	<b>0.48</b>

RGB + DSM

Class\Value	Water	Mixed Grass	Isolepis	Dry Vegetation	Blackberry	Reed	Cabbage Tree	Flax	Other Tree (Dark)	Other Tree (Light)	Sedge	Bidens	Toetoe	Dormant Tree	Total	U_Accuracy	Kappa
Water	174	3	1	0	0	5	0	0	1	0	0	0	0	1	185	0.94	0
Mixed Grass	0	128	6	27	0	2	0	0	0	1	7	1	1	0	173	0.74	0
Isolepis	0	5	53	0	0	0	0	0	0	0	0	0	0	0	58	0.91	0
Dry Vegetation	0	3	0	37	0	1	0	0	0	0	1	0	0	1	43	0.86	0
Blackberry	0	16	9	0	4	0	2	6	1	1	1	0	2	0	42	0.10	0
Reed	4	5	1	8	1	30	0	9	1	1	2	3	2	0	67	0.45	0
Cabbage Tree	0	7	10	0	0	1	7	1	0	0	1	0	0	0	27	0.26	0
Flax	0	15	3	4	0	9	1	28	0	2	4	1	9	0	76	0.37	0
Other Tree (Dark)	1	9	30	2	2	3	2	4	26	3	2	2	2	0	88	0.30	0
Other Tree (Light)	0	1	11	0	0	0	3	0	0	5	1	0	0	0	21	0.24	0
Sedge	3	33	20	9	1	8	0	8	2	3	20	4	2	3	116	0.17	0
Bidens	0	1	2	5	0	6	0	1	0	0	2	8	0	1	26	0.31	0
Toetoe	3	25	1	18	0	2	1	0	0	2	3	0	10	1	66	0.15	0
Dormant Tree	7	3	1	1	0	1	0	0	0	0	0	0	1	0	14	0.00	0
<b>Total</b>	<b>192</b>	<b>254</b>	<b>148</b>	<b>111</b>	<b>8</b>	<b>68</b>	<b>16</b>	<b>57</b>	<b>31</b>	<b>18</b>	<b>44</b>	<b>19</b>	<b>29</b>	<b>7</b>	<b>1002</b>	<b>0</b>	<b>0</b>
<b>P_Accuracy</b>	<b>0.91</b>	<b>0.50</b>	<b>0.36</b>	<b>0.33</b>	<b>0.50</b>	<b>0.44</b>	<b>0.44</b>	<b>0.49</b>	<b>0.84</b>	<b>0.28</b>	<b>0.45</b>	<b>0.42</b>	<b>0.34</b>	<b>0.00</b>	<b>0.00</b>	<b>0.53</b>	<b>0.00</b>
<b>Kappa</b>	<b>0</b>	<b>0</b>	<b>0</b>	<b>0</b>	<b>0</b>	<b>0</b>	<b>0</b>	<b>0</b>	<b>0</b>	<b>0</b>	<b>0</b>	<b>0</b>	<b>0</b>	<b>0</b>	<b>0</b>	<b>0</b>	<b>0.47</b>

RGB + MS

Class Value	Water	Mixed Grass	Isolepis	Dry Vegetation	Blackberry	Reed	Cabbage Tree	Flax	Other Tree (Dark)	Other Tree (Light)	Sedge	Bidens	Toetoe	Dormant Tree	Total	U_Accuracy	Kappa
Water	186	1	0	0	0	1	0	0	0	0	0	0	0	0	188	0.99	0
Mixed Grass	0	150	16	14	0	1	0	0	0	1	4	0	2	0	188	0.80	0
Isolepis	0	2	33	1	0	0	0	0	0	0	1	0	0	0	37	0.89	0
Dry Vegetation	0	1	0	43	0	3	0	0	0	0	1	0	2	0	50	0.86	0
Blackberry	0	6	5	1	6	0	0	1	1	0	1	1	0	0	22	0.27	0
Reed	2	16	26	9	0	45	2	9	1	1	1	2	6	1	121	0.37	0
Cabbage Tree	0	9	6	0	0	0	9	3	1	0	0	0	0	0	28	0.32	0
Flax	0	14	2	1	0	12	2	35	0	1	7	1	5	0	80	0.44	0
Other Tree (Dark)	0	3	25	1	1	1	1	4	27	2	0	0	0	0	65	0.42	0
Other Tree (Light)	0	0	2	0	0	0	1	1	0	6	1	0	1	0	12	0.50	0
Sedge	1	33	30	9	1	3	1	2	1	7	25	4	0	1	118	0.21	0
Bidens	0	0	0	1	0	0	0	0	0	0	1	11	0	0	13	0.85	0
Toetoe	0	18	2	31	0	1	0	2	0	0	2	0	12	0	68	0.18	0
Dormant Tree	3	1	1	0	0	1	0	0	0	0	0	0	1	5	12	0.42	0
<b>Total</b>	<b>192</b>	<b>254</b>	<b>148</b>	<b>111</b>	<b>8</b>	<b>68</b>	<b>16</b>	<b>57</b>	<b>31</b>	<b>18</b>	<b>44</b>	<b>19</b>	<b>29</b>	<b>7</b>	<b>1002</b>	<b>0</b>	<b>0</b>
<b>P_Accuracy</b>	<b>0.97</b>	<b>0.59</b>	<b>0.22</b>	<b>0.39</b>	<b>0.75</b>	<b>0.66</b>	<b>0.56</b>	<b>0.61</b>	<b>0.87</b>	<b>0.33</b>	<b>0.57</b>	<b>0.58</b>	<b>0.41</b>	<b>0.71</b>	<b>0.00</b>	<b>0.59</b>	<b>0.00</b>
<b>Kappa</b>	<b>0</b>	<b>0</b>	<b>0</b>	<b>0</b>	<b>0</b>	<b>0</b>	<b>0</b>	<b>0</b>	<b>0</b>	<b>0</b>	<b>0</b>	<b>0</b>	<b>0</b>	<b>0</b>	<b>0</b>	<b>0</b>	<b>0.54</b>

ALL ANCILLARIES

Class Value	Water	Mixed Grass	Isolepis	Dry Vegetation	Blackberry	Reed	Cabbage Tree	Flax	Other Tree (Dark)	Other Tree (Light)	Sedge	Bidens	Toetoe	Dormant Tree	Total	U_Accuracy	Kappa
Water	186	0	0	0	0	0	0	0	0	0	0	0	0	0	186	1.00	0
Mixed Grass	0	154	17	11	0	0	0	0	0	1	5	0	1	0	189	0.81	0
Isolepis	0	1	36	1	0	0	0	0	0	0	1	0	0	0	39	0.92	0
Dry Vegetation	0	1	0	45	0	1	0	0	0	0	1	0	2	0	50	0.90	0
Blackberry	0	7	6	1	6	0	0	1	1	0	1	1	0	0	24	0.25	0
Reed	3	18	27	9	0	47	2	9	1	2	1	1	5	0	125	0.38	0
Cabbage Tree	0	8	6	0	0	0	10	3	1	0	0	1	1	0	30	0.33	0
Flax	0	14	3	1	0	12	2	36	0	1	5	0	5	0	79	0.46	0
Other Tree (Dark)	0	3	22	1	1	1	1	4	27	1	0	0	0	0	61	0.44	0
Other Tree (Light)	0	0	2	0	0	0	0	1	0	7	1	0	0	0	11	0.64	0
Sedge	1	31	26	9	1	3	1	1	1	6	25	4	0	1	110	0.23	0
Bidens	0	0	0	1	0	0	0	0	0	0	1	12	0	0	14	0.86	0
Toetoe	0	17	2	29	0	3	0	2	0	0	3	0	14	0	70	0.20	0
Dormant Tree	2	0	1	3	0	1	0	0	0	0	0	0	1	6	14	0.43	0
<b>Total</b>	<b>192</b>	<b>254</b>	<b>148</b>	<b>111</b>	<b>8</b>	<b>68</b>	<b>16</b>	<b>57</b>	<b>31</b>	<b>18</b>	<b>44</b>	<b>19</b>	<b>29</b>	<b>7</b>	<b>1002</b>	<b>0</b>	<b>0</b>
<b>P_Accuracy</b>	<b>0.97</b>	<b>0.61</b>	<b>0.24</b>	<b>0.41</b>	<b>0.75</b>	<b>0.69</b>	<b>0.63</b>	<b>0.63</b>	<b>0.87</b>	<b>0.39</b>	<b>0.57</b>	<b>0.63</b>	<b>0.48</b>	<b>0.86</b>	<b>0.00</b>	<b>0.61</b>	<b>0.00</b>
<b>Kappa</b>	<b>0</b>	<b>0</b>	<b>0</b>	<b>0</b>	<b>0</b>	<b>0</b>	<b>0</b>	<b>0</b>	<b>0</b>	<b>0</b>	<b>0</b>	<b>0</b>	<b>0</b>	<b>0</b>	<b>0</b>	<b>0</b>	<b>0.56</b>

## Multispectral Tests: Stage Two

RGB Only

ClassValue	Water	Mixed Grass	Isolepis	Bidens	Flax	Cabbage Tree	Dry Vegetation	Dormant Tree	Green Algae	Sedge	Reed	Shadow	Other Tree (Dark)	Total	U_Accuracy	Kappa
Water	407	1	13	3	0	0	0	0	1	0	1	1	0	427	0.95	0
Mixed Grass	2	45	3	7	0	1	7	0	3	1	0	0	0	69	0.65	0
Isolepis	5	5	166	1	1	0	0	0	0	3	0	0	0	181	0.92	0
Bidens	0	0	1	52	2	0	2	0	0	1	0	0	0	58	0.90	0
Flax	4	9	11	3	18	6	8	0	1	1	5	3	2	71	0.25	0
Cabbage Tree	0	8	3	0	3	3	1	0	0	0	0	0	0	18	0.17	0
Dry Vegetation	0	5	0	0	0	0	16	0	0	0	0	0	0	21	0.76	0
Dormant Tree	2	0	4	0	0	0	5	0	0	0	0	0	0	11	0.00	0
Green Algae	0	0	0	0	0	0	0	0	1	0	0	0	0	1	1.00	0
Sedge	0	7	14	0	0	0	0	0	1	3	0	0	0	25	0.12	0
Reed	2	2	0	0	0	0	14	0	0	0	9	0	0	27	0.33	0
Shadow	0	0	0	0	0	0	0	0	0	0	0	2	0	2	1.00	0
Other Tree (Dark)	2	8	57	16	4	1	2	0	0	6	0	0	2	98	0.02	0
<b>Total</b>	<b>424</b>	<b>90</b>	<b>272</b>	<b>82</b>	<b>28</b>	<b>11</b>	<b>55</b>	<b>0</b>	<b>7</b>	<b>15</b>	<b>15</b>	<b>6</b>	<b>4</b>	<b>1009</b>	<b>0</b>	<b>0</b>
<b>P_Accuracy</b>	<b>0.96</b>	<b>0.50</b>	<b>0.61</b>	<b>0.63</b>	<b>0.64</b>	<b>0.27</b>	<b>0.29</b>	<b>0.00</b>	<b>0.14</b>	<b>0.20</b>	<b>0.60</b>	<b>0.33</b>	<b>0.50</b>	<b>0.00</b>	<b>0.72</b>	<b>0.00</b>
<b>Kappa</b>	<b>0</b>	<b>0</b>	<b>0</b>	<b>0</b>	<b>0</b>	<b>0</b>	<b>0</b>	<b>0</b>	<b>0</b>	<b>0</b>	<b>0</b>	<b>0</b>	<b>0</b>	<b>0</b>	<b>0</b>	<b>0.63</b>

RGB + DSM

ClassValue	Water	Mixed Grass	Isolepis	Bidens	Flax	Cabbage Tree	Dry Vegetation	Dormant Tree	Green Algae	Sedge	Reed	Shadow	Other Tree (Dark)	Total	U_Accuracy	Kappa
Water	403	0	9	0	0	0	2	0	1	0	0	1	0	416	0.97	0
Mixed Grass	3	40	8	11	0	1	8	0	2	1	0	0	0	74	0.54	0
Isolepis	5	3	163	0	1	0	0	0	0	2	0	0	0	174	0.94	0
Bidens	4	1	1	56	1	0	2	0	0	1	0	0	0	66	0.85	0
Flax	4	15	11	3	22	7	12	0	2	2	5	3	2	88	0.25	0
Cabbage Tree	0	11	4	0	1	3	0	0	0	0	0	0	0	19	0.16	0
Dry Vegetation	0	5	0	0	0	0	13	0	0	0	0	0	0	18	0.72	0
Dormant Tree	1	0	4	0	0	0	3	0	0	0	0	0	0	8	0.00	0
Green Algae	0	0	0	0	0	0	0	0	1	0	0	0	0	1	1.00	0
Sedge	0	6	9	0	0	0	0	0	1	3	0	0	0	19	0.16	0
Reed	1	1	0	1	0	0	13	0	0	0	10	0	0	26	0.38	0
Shadow	0	0	0	0	0	0	0	0	0	0	0	2	0	2	1.00	0
Other Tree (Dark)	3	8	63	11	3	0	2	0	0	6	0	0	2	98	0.02	0
<b>Total</b>	<b>424</b>	<b>90</b>	<b>272</b>	<b>82</b>	<b>28</b>	<b>11</b>	<b>55</b>	<b>0</b>	<b>7</b>	<b>15</b>	<b>15</b>	<b>6</b>	<b>4</b>	<b>1009</b>	<b>0</b>	<b>0</b>
<b>P_Accuracy</b>	<b>0.95</b>	<b>0.44</b>	<b>0.60</b>	<b>0.68</b>	<b>0.79</b>	<b>0.27</b>	<b>0.24</b>	<b>0.00</b>	<b>0.14</b>	<b>0.20</b>	<b>0.67</b>	<b>0.33</b>	<b>0.50</b>	<b>0.00</b>	<b>0.71</b>	<b>0.00</b>
<b>Kappa</b>	<b>0</b>	<b>0</b>	<b>0</b>	<b>0</b>	<b>0</b>	<b>0</b>	<b>0</b>	<b>0</b>	<b>0</b>	<b>0</b>	<b>0</b>	<b>0</b>	<b>0</b>	<b>0</b>	<b>0</b>	<b>0.62</b>

RGB + MS

ClassValue	Water	Mixed Grass	Isolepis	Bidens	Flax	Cabbage Tree	Dry Vegetation	Dormant Tree	Green Algae	Sedge	Reed	Shadow	Other Tree (Dark)	Total	U_Accuracy	Kappa
Water	404	0	4	0	0	0	0	0	1	0	0	0	0	409	0.99	0
Mixed Grass	0	46	3	4	0	0	4	0	0	0	0	0	0	57	0.81	0
Isolepis	7	3	193	3	0	0	0	0	0	2	0	0	1	209	0.92	0
Bidens	0	0	0	67	1	0	0	0	0	1	0	0	0	69	0.97	0
Flax	7	21	12	3	26	6	18	0	0	5	6	2	1	107	0.24	0
Cabbage Tree	0	5	1	0	1	5	0	0	0	0	0	0	0	12	0.42	0
Dry Vegetation	0	6	0	0	0	0	17	0	0	0	0	0	0	23	0.74	0
Dormant Tree	3	4	9	0	0	0	9	0	1	0	0	0	0	26	0.00	0
Green Algae	0	0	1	0	0	0	0	0	5	0	0	0	0	6	0.83	0
Sedge	0	1	6	0	0	0	1	0	0	3	0	0	0	11	0.27	0
Reed	3	0	5	0	0	0	6	0	0	0	9	0	0	23	0.39	0
Shadow	0	0	0	0	0	0	0	0	0	0	0	4	0	4	1.00	0
Other Tree (Dark)	0	4	38	5	0	0	0	0	0	4	0	0	2	53	0.04	0
<b>Total</b>	<b>424</b>	<b>90</b>	<b>272</b>	<b>82</b>	<b>28</b>	<b>11</b>	<b>55</b>	<b>0</b>	<b>7</b>	<b>15</b>	<b>15</b>	<b>6</b>	<b>4</b>	<b>1009</b>	<b>0</b>	<b>0</b>
<b>P_Accuracy</b>	<b>0.95</b>	<b>0.51</b>	<b>0.71</b>	<b>0.82</b>	<b>0.93</b>	<b>0.45</b>	<b>0.31</b>	<b>0.00</b>	<b>0.71</b>	<b>0.20</b>	<b>0.60</b>	<b>0.67</b>	<b>0.50</b>	<b>0.00</b>	<b>0.77</b>	<b>0.00</b>
<b>Kappa</b>	<b>0</b>	<b>0</b>	<b>0</b>	<b>0</b>	<b>0</b>	<b>0</b>	<b>0</b>	<b>0</b>	<b>0</b>	<b>0</b>	<b>0</b>	<b>0</b>	<b>0</b>	<b>0</b>	<b>0</b>	<b>0.70</b>

ALL ANCILLARIES

ClassValue	Water	Mixed Grass	Isolepis	Bidens	Flax	Cabbage Tree	Dry Vegetation	Dormant Tree	Green Algae	Sedge	Reed	Shadow	Other Tree (Dark)	Total	U_Accuracy	Kappa
Water	408	0	4	0	0	0	0	0	1	0	0	0	0	413	0.99	0
Mixed Grass	0	56	3	2	0	0	3	0	0	0	0	0	0	64	0.88	0
Isolepis	8	6	197	3	1	0	1	0	0	2	0	0	1	219	0.90	0
Bidens	0	0	0	68	1	0	0	0	0	1	0	0	0	70	0.97	0
Flax	4	9	12	4	24	5	11	0	0	5	5	0	1	80	0.30	0
Cabbage Tree	0	7	1	0	1	6	0	0	0	0	0	0	0	15	0.40	0
Dry Vegetation	0	3	0	0	0	0	20	0	0	0	0	0	0	23	0.87	0
Dormant Tree	4	2	10	0	0	0	9	0	1	0	0	0	0	26	0.00	0
Green Algae	0	0	1	0	0	0	0	0	5	0	0	0	0	6	0.83	0
Sedge	0	2	5	0	0	0	0	0	0	3	0	0	0	10	0.30	0
Reed	0	0	3	0	1	0	11	0	0	0	10	0	0	25	0.40	0
Shadow	0	0	0	0	0	0	0	0	0	0	0	6	0	6	1.00	0
Other Tree (Dark)	0	5	36	5	0	0	0	0	0	4	0	0	2	52	0.04	0
<b>Total</b>	<b>424</b>	<b>90</b>	<b>272</b>	<b>82</b>	<b>28</b>	<b>11</b>	<b>55</b>	<b>0</b>	<b>7</b>	<b>15</b>	<b>15</b>	<b>6</b>	<b>4</b>	<b>1009</b>	<b>0</b>	<b>0</b>
<b>P_Accuracy</b>	<b>0.96</b>	<b>0.62</b>	<b>0.72</b>	<b>0.83</b>	<b>0.86</b>	<b>0.55</b>	<b>0.36</b>	<b>0.00</b>	<b>0.71</b>	<b>0.20</b>	<b>0.67</b>	<b>1.00</b>	<b>0.50</b>	<b>0.00</b>	<b>0.80</b>	<b>0.00</b>
<b>Kappa</b>	<b>0</b>	<b>0</b>	<b>0</b>	<b>0</b>	<b>0</b>	<b>0</b>	<b>0</b>	<b>0</b>	<b>0</b>	<b>0</b>	<b>0</b>	<b>0</b>	<b>0</b>	<b>0</b>	<b>0</b>	<b>0.73</b>

## Multispectral Tests: Stage Three

RGB Only

Class/Value	Water	Mixed Grass	Dry Vegetation	Sedge	Bidens	Blackberry	Isolepis	Flax	Cabbage Tree	Other Tree (Dark)	Other Tree (Light)	Reed	Green Algae	Dormant Tree	Shadow	Kahikatea	Total	U_Accuracy	Kappa
Water	51	0	0	0	1	0	1	0	0	0	0	7	0	0	0	0	60	0.85	0
Mixed Grass	0	104	56	10	0	2	19	0	2	1	1	0	7	1	0	0	203	0.51	0
Dry Vegetation	0	5	59	1	0	0	0	0	0	0	0	2	0	2	0	0	69	0.86	0
Sedge	0	12	7	3	0	0	1	0	2	0	0	2	0	0	0	0	27	0.11	0
Bidens	0	0	0	0	4	0	0	0	0	0	0	17	0	0	0	0	21	0.19	0
Blackberry	8	20	8	11	7	19	14	6	5	3	9	6	1	0	0	0	117	0.16	0
Isolepis	0	9	2	0	12	0	208	0	0	1	1	5	0	0	0	0	238	0.87	0
Flax	0	0	0	0	0	0	0	13	0	0	0	1	0	0	0	0	14	0.93	0
Cabbage Tree	0	2	0	0	1	0	1	0	0	0	0	1	0	0	0	0	5	0.00	0
Other Tree (Dark)	0	2	4	0	5	0	0	0	0	5	0	2	0	0	2	0	20	0.25	0
Other Tree (Light)	0	0	0	0	1	0	0	0	0	0	2	1	1	0	0	0	5	0.40	0
Reed	0	3	17	0	4	1	0	2	1	0	0	36	0	0	0	0	64	0.56	0
Green Algae	0	0	0	0	0	0	0	0	1	0	0	0	5	0	0	0	6	0.83	0
Dormant Tree	0	0	8	0	0	0	0	0	0	0	0	0	0	5	0	0	13	0.38	0
Shadow	0	0	0	0	0	0	0	0	0	0	0	0	0	0	5	0	5	1.00	0
Kahikatea	2	19	11	5	23	1	77	5	1	4	4	10	0	0	5	6	173	0.03	0
<b>Total</b>	<b>61</b>	<b>176</b>	<b>172</b>	<b>30</b>	<b>58</b>	<b>23</b>	<b>321</b>	<b>26</b>	<b>12</b>	<b>14</b>	<b>17</b>	<b>90</b>	<b>14</b>	<b>8</b>	<b>12</b>	<b>6</b>	<b>1040</b>	<b>0</b>	<b>0</b>
<b>P_Accuracy</b>	<b>0.84</b>	<b>0.59</b>	<b>0.34</b>	<b>0.10</b>	<b>0.07</b>	<b>0.83</b>	<b>0.65</b>	<b>0.50</b>	<b>0.00</b>	<b>0.36</b>	<b>0.12</b>	<b>0.40</b>	<b>0.36</b>	<b>0.63</b>	<b>0.42</b>	<b>1.00</b>	<b>0.00</b>	<b>0.50</b>	<b>0.00</b>
<b>Kappa</b>	<b>0.00</b>	<b>0.00</b>	<b>0.00</b>	<b>0.00</b>	<b>0.00</b>	<b>0.00</b>	<b>0.00</b>	<b>0.00</b>	<b>0.00</b>	<b>0.00</b>	<b>0.00</b>	<b>0.00</b>	<b>0.00</b>	<b>0.00</b>	<b>0.00</b>	<b>0.00</b>	<b>0.00</b>	<b>0.00</b>	<b>0.43</b>

RGB + DSM

Class/Value	Water	Mixed Grass	Dry Vegetation	Sedge	Bidens	Blackberry	Isolepis	Flax	Cabbage Tree	Other Tree (Dark)	Other Tree (Light)	Reed	Green Algae	Dormant Tree	Shadow	Kahikatea	Total	U_Accuracy	Kappa
Water	53	1	0	0	1	2	0	0	0	0	0	5	0	0	0	0	62	0.85	0
Mixed Grass	0	101	54	13	0	1	20	0	3	0	0	0	6	1	0	0	199	0.51	0
Dry Vegetation	0	3	60	1	0	0	0	0	0	0	0	2	0	2	0	0	68	0.88	0
Sedge	0	18	7	1	0	1	3	0	0	1	2	2	0	0	0	0	35	0.03	0
Bidens	0	0	0	0	5	0	0	0	0	0	1	17	0	0	0	0	23	0.22	0
Blackberry	6	22	10	8	12	18	41	4	4	4	8	11	1	0	0	0	149	0.12	0
Isolepis	1	7	3	1	8	0	207	0	0	0	1	2	0	0	0	1	231	0.90	0
Flax	0	0	0	0	0	0	1	13	0	1	0	2	0	0	1	0	18	0.72	0
Cabbage Tree	0	3	1	0	0	0	4	0	1	0	0	0	0	0	0	0	9	0.11	0
Other Tree (Dark)	0	1	1	2	1	0	0	0	0	2	1	1	0	0	1	1	11	0.18	0
Other Tree (Light)	0	1	0	0	2	0	0	0	0	1	2	1	0	0	0	0	7	0.29	0
Reed	0	3	24	1	5	1	0	2	1	0	0	40	0	0	0	0	77	0.52	0
Green Algae	0	1	0	0	0	0	0	0	1	0	0	0	7	0	0	0	9	0.78	0
Dormant Tree	1	0	5	0	0	0	0	0	0	0	0	0	0	5	0	0	11	0.45	0
Shadow	0	0	0	0	0	0	0	0	0	1	0	0	0	0	10	0	11	0.91	0
Kahikatea	0	15	7	3	24	0	45	7	2	4	2	7	0	0	0	4	120	0.03	0
<b>Total</b>	<b>61</b>	<b>176</b>	<b>172</b>	<b>30</b>	<b>58</b>	<b>23</b>	<b>321</b>	<b>26</b>	<b>12</b>	<b>14</b>	<b>17</b>	<b>90</b>	<b>14</b>	<b>8</b>	<b>12</b>	<b>6</b>	<b>1040</b>	<b>0</b>	<b>0</b>
<b>P_Accuracy</b>	<b>0.87</b>	<b>0.57</b>	<b>0.35</b>	<b>0.03</b>	<b>0.09</b>	<b>0.78</b>	<b>0.64</b>	<b>0.50</b>	<b>0.08</b>	<b>0.14</b>	<b>0.12</b>	<b>0.44</b>	<b>0.50</b>	<b>0.63</b>	<b>0.83</b>	<b>0.67</b>	<b>0.00</b>	<b>0.51</b>	<b>0.00</b>
<b>Kappa</b>	<b>0.00</b>	<b>0.00</b>	<b>0.00</b>	<b>0.00</b>	<b>0.00</b>	<b>0.00</b>	<b>0.00</b>	<b>0.00</b>	<b>0.00</b>	<b>0.00</b>	<b>0.00</b>	<b>0.00</b>	<b>0.00</b>	<b>0.00</b>	<b>0.00</b>	<b>0.00</b>	<b>0.00</b>	<b>0.00</b>	<b>0.44</b>

RGB + MS

Class\Value	Water	Mixed Grass	Dry Vegetation	Sedge	Bidens	Blackberry	Isolepis	Flax	Cabbage Tree	Other Tree (Dark)	Other Tree (Light)	Reed	Green Algae	Dormant Tree	Shadow	Kahikatea	Total	U_Accuracy	Kappa
Water	58	0	0	0	0	0	0	0	0	0	0	3	0	0	1	0	62	0.94	0
Mixed Grass	0	135	51	4	1	0	12	1	6	0	4	3	1	1	0	0	219	0.62	0
Dry Vegetation	0	0	69	0	0	0	0	0	0	0	0	1	0	3	0	0	73	0.95	0
Sedge	0	9	11	12	2	2	8	0	0	2	1	3	0	0	0	0	50	0.24	0
Bidens	0	0	8	1	21	0	1	1	1	0	0	1	0	0	0	0	34	0.62	0
Blackberry	0	4	2	2	3	13	20	0	0	3	2	0	0	0	0	2	51	0.25	0
Isolepis	0	10	2	1	11	1	222	0	0	1	3	1	0	0	0	0	252	0.88	0
Flax	0	0	0	0	0	0	0	16	1	0	0	1	0	0	0	0	18	0.89	0
Cabbage Tree	0	0	0	0	0	0	7	0	4	0	0	1	0	0	0	0	12	0.33	0
Other Tree (Dark)	0	7	0	2	9	2	8	1	0	7	0	2	0	0	1	3	42	0.17	0
Other Tree (Light)	0	5	0	5	2	0	3	4	0	0	6	2	1	0	0	0	28	0.21	0
Reed	2	2	23	3	6	3	5	3	0	0	1	71	2	0	1	0	122	0.58	0
Green Algae	0	0	0	0	0	0	0	0	0	0	0	0	10	0	0	0	10	1.00	0
Dormant Tree	1	0	5	0	0	0	0	0	0	0	0	1	0	4	0	0	11	0.36	0
Shadow	0	0	0	0	0	0	0	0	0	0	0	0	0	0	9	0	9	1.00	0
Kahikatea	0	4	1	0	3	2	35	0	0	1	0	0	0	0	0	1	47	0.02	0
<b>Total</b>	<b>61</b>	<b>176</b>	<b>172</b>	<b>30</b>	<b>58</b>	<b>23</b>	<b>321</b>	<b>26</b>	<b>12</b>	<b>14</b>	<b>17</b>	<b>90</b>	<b>14</b>	<b>8</b>	<b>12</b>	<b>6</b>	<b>1040</b>	<b>0</b>	<b>0</b>
<b>P_Accuracy</b>	<b>0.95</b>	<b>0.77</b>	<b>0.40</b>	<b>0.40</b>	<b>0.36</b>	<b>0.57</b>	<b>0.69</b>	<b>0.62</b>	<b>0.33</b>	<b>0.50</b>	<b>0.35</b>	<b>0.79</b>	<b>0.71</b>	<b>0.50</b>	<b>0.75</b>	<b>0.17</b>	<b>0.00</b>	<b>0.63</b>	<b>0.00</b>
<b>Kappa</b>	<b>0.00</b>	<b>0.00</b>	<b>0.00</b>	<b>0.00</b>	<b>0.00</b>	<b>0.00</b>	<b>0.00</b>	<b>0.00</b>	<b>0.00</b>	<b>0.00</b>	<b>0.00</b>	<b>0.00</b>	<b>0.00</b>	<b>0.00</b>	<b>0.00</b>	<b>0.00</b>	<b>0.00</b>	<b>0.00</b>	<b>0.57</b>

ALL ANCILLARIES

Class\Value	Water	Mixed Grass	Dry Vegetation	Sedge	Bidens	Blackberry	Isolepis	Flax	Cabbage Tree	Other Tree (Dark)	Other Tree (Light)	Reed	Green Algae	Dormant Tree	Shadow	Kahikatea	Total	U_Accuracy	Kappa
Water	57	0	0	0	0	0	0	0	0	0	0	2	0	0	0	0	59	0.97	0
Mixed Grass	0	133	47	3	0	0	12	0	5	0	2	2	1	1	0	0	206	0.65	0
Dry Vegetation	0	0	69	0	0	0	0	0	0	0	0	2	0	3	0	0	74	0.93	0
Sedge	0	8	11	13	1	1	9	0	0	1	1	3	0	0	0	0	48	0.27	0
Bidens	0	0	9	1	18	1	1	0	0	0	0	2	0	0	0	0	32	0.56	0
Blackberry	0	5	3	3	3	16	22	2	0	4	4	1	0	0	0	1	64	0.25	0
Isolepis	0	10	1	1	13	0	227	0	0	0	2	1	0	0	0	1	256	0.89	0
Flax	0	0	0	0	0	0	0	16	1	0	0	2	0	0	0	0	19	0.84	0
Cabbage Tree	0	1	0	0	0	0	6	0	5	0	0	1	0	0	0	0	13	0.38	0
Other Tree (Dark)	0	7	0	2	11	1	8	0	0	6	0	1	0	0	1	3	40	0.15	0
Other Tree (Light)	0	6	0	5	2	1	3	3	1	1	6	1	1	0	0	0	30	0.20	0
Reed	1	2	26	2	6	2	5	5	0	0	2	70	2	0	1	0	124	0.56	0
Green Algae	0	0	0	0	0	0	0	0	0	0	0	0	10	0	0	0	10	1.00	0
Dormant Tree	3	0	5	0	0	0	0	0	0	0	0	2	0	4	0	0	14	0.29	0
Shadow	0	0	0	0	0	0	0	0	0	0	0	0	0	0	10	0	10	1.00	0
Kahikatea	0	4	1	0	4	1	28	0	0	2	0	0	0	0	0	1	41	0.02	0
<b>Total</b>	<b>61</b>	<b>176</b>	<b>172</b>	<b>30</b>	<b>58</b>	<b>23</b>	<b>321</b>	<b>26</b>	<b>12</b>	<b>14</b>	<b>17</b>	<b>90</b>	<b>14</b>	<b>8</b>	<b>12</b>	<b>6</b>	<b>1040</b>	<b>0</b>	<b>0</b>
<b>P_Accuracy</b>	<b>0.93</b>	<b>0.76</b>	<b>0.40</b>	<b>0.43</b>	<b>0.31</b>	<b>0.70</b>	<b>0.71</b>	<b>0.62</b>	<b>0.42</b>	<b>0.43</b>	<b>0.35</b>	<b>0.78</b>	<b>0.71</b>	<b>0.50</b>	<b>0.83</b>	<b>0.17</b>	<b>0.00</b>	<b>0.64</b>	<b>0.00</b>
<b>Kappa</b>	<b>0.00</b>	<b>0.00</b>	<b>0.00</b>	<b>0.00</b>	<b>0.00</b>	<b>0.00</b>	<b>0.00</b>	<b>0.00</b>	<b>0.00</b>	<b>0.00</b>	<b>0.00</b>	<b>0.00</b>	<b>0.00</b>	<b>0.00</b>	<b>0.00</b>	<b>0.00</b>	<b>0.00</b>	<b>0.00</b>	<b>0.58</b>

## Appendix C: Full-Page Maps

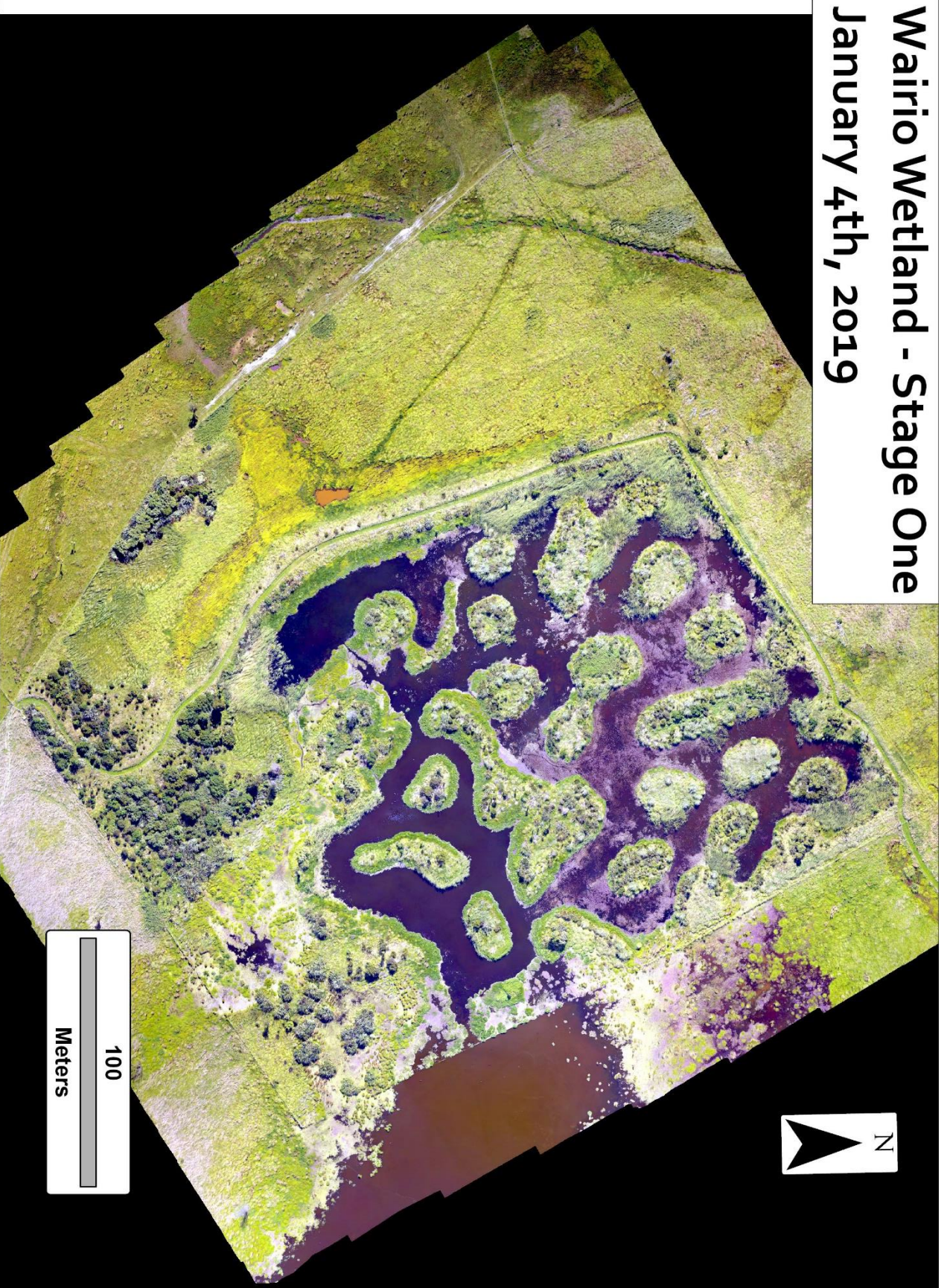
### C.1 True-Colour Camera Orthomaps



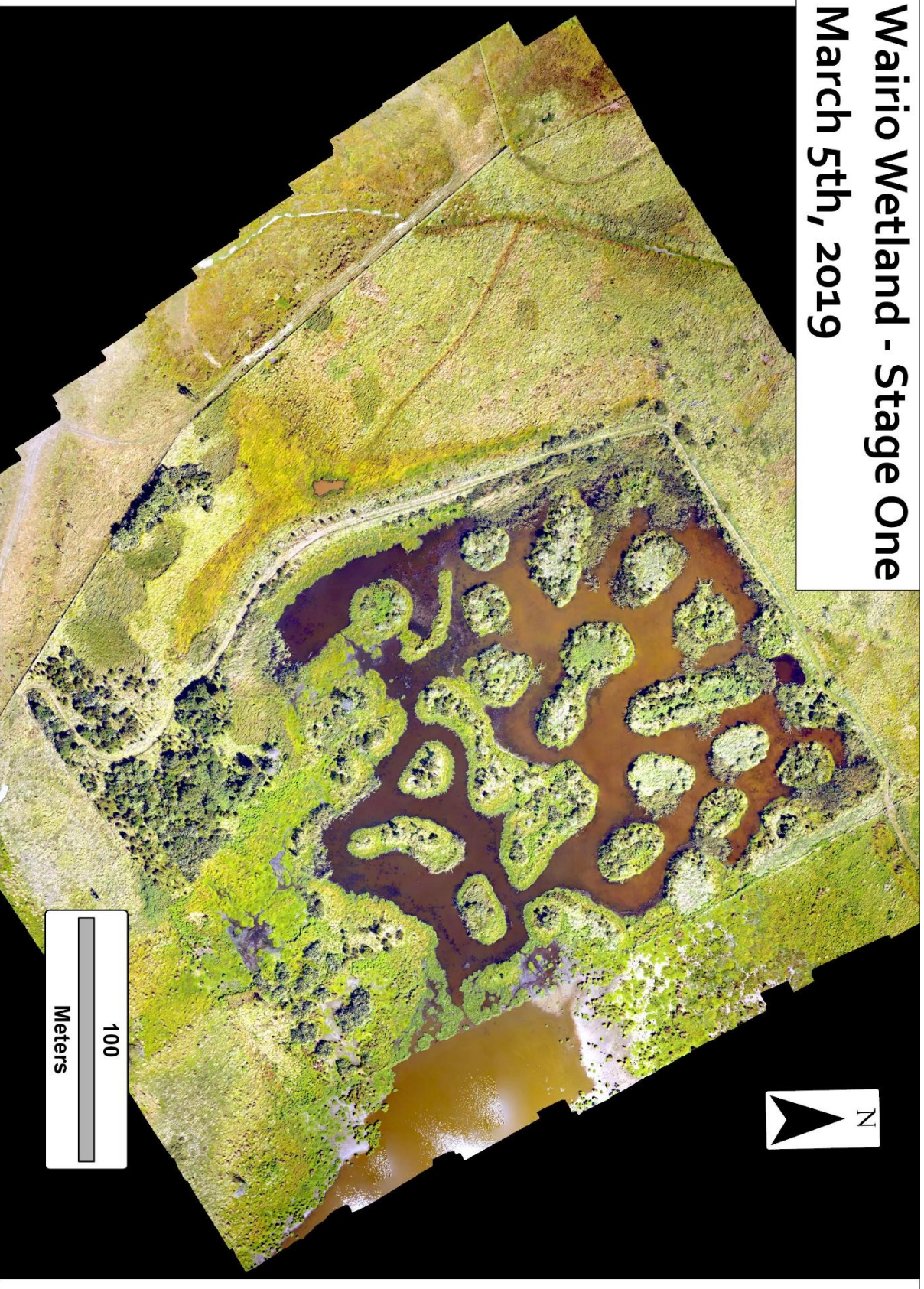
Wairio Wetland - Stage One  
October 6th, 2018



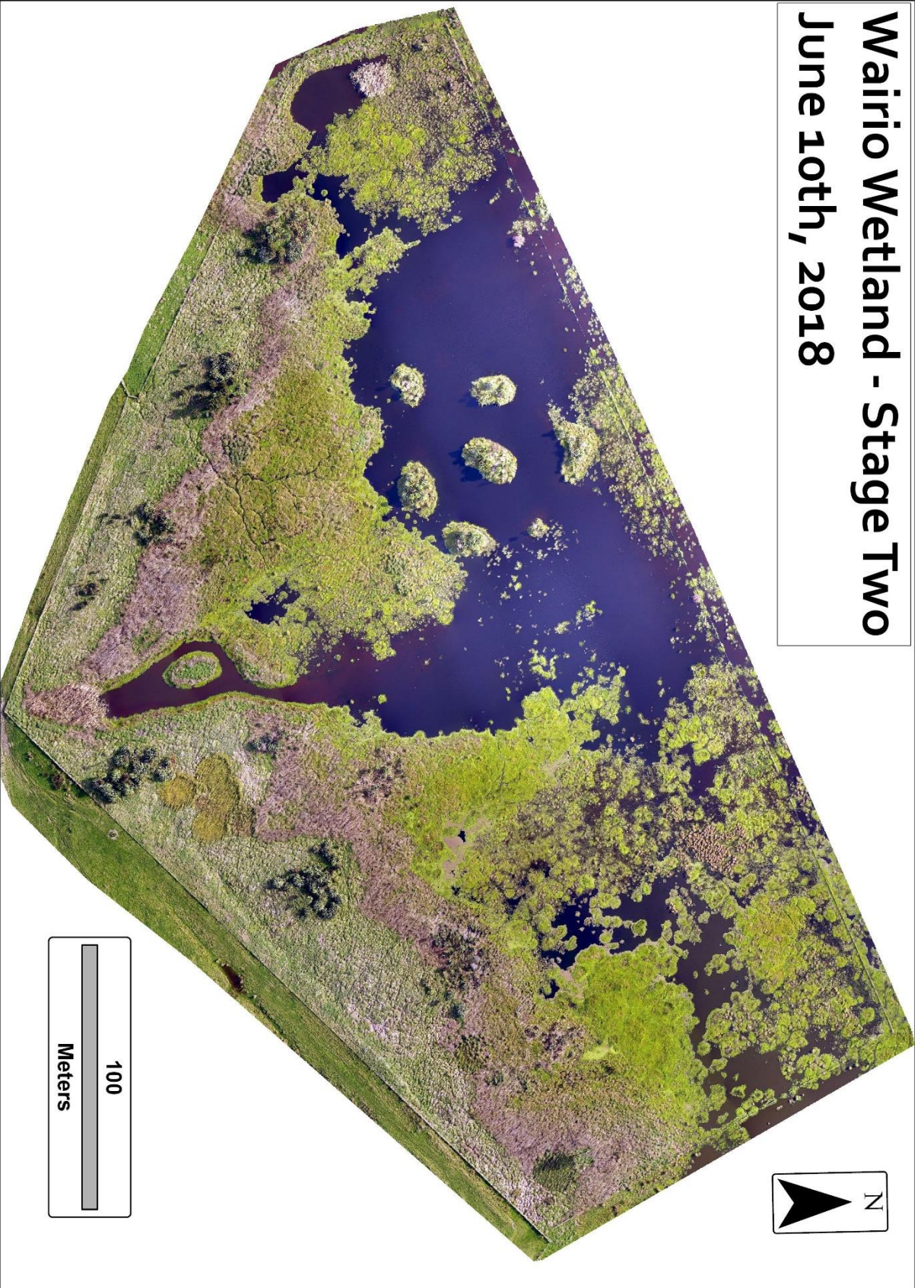
**Wairio Wetland - Stage One  
January 4th, 2019**



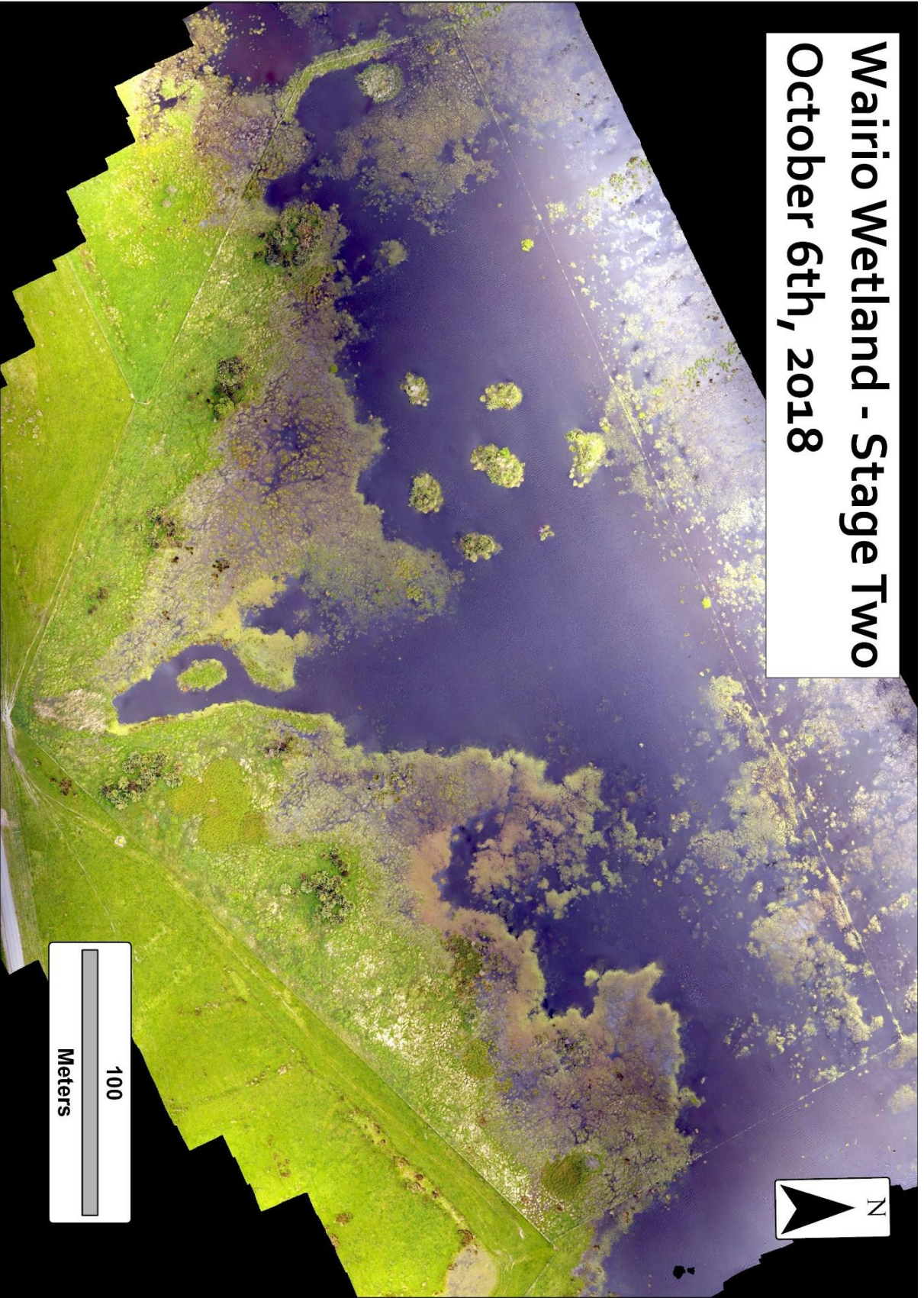
# Wairio Wetland - Stage One March 5th, 2019



**Wairio Wetland - Stage Two**  
**June 10th, 2018**



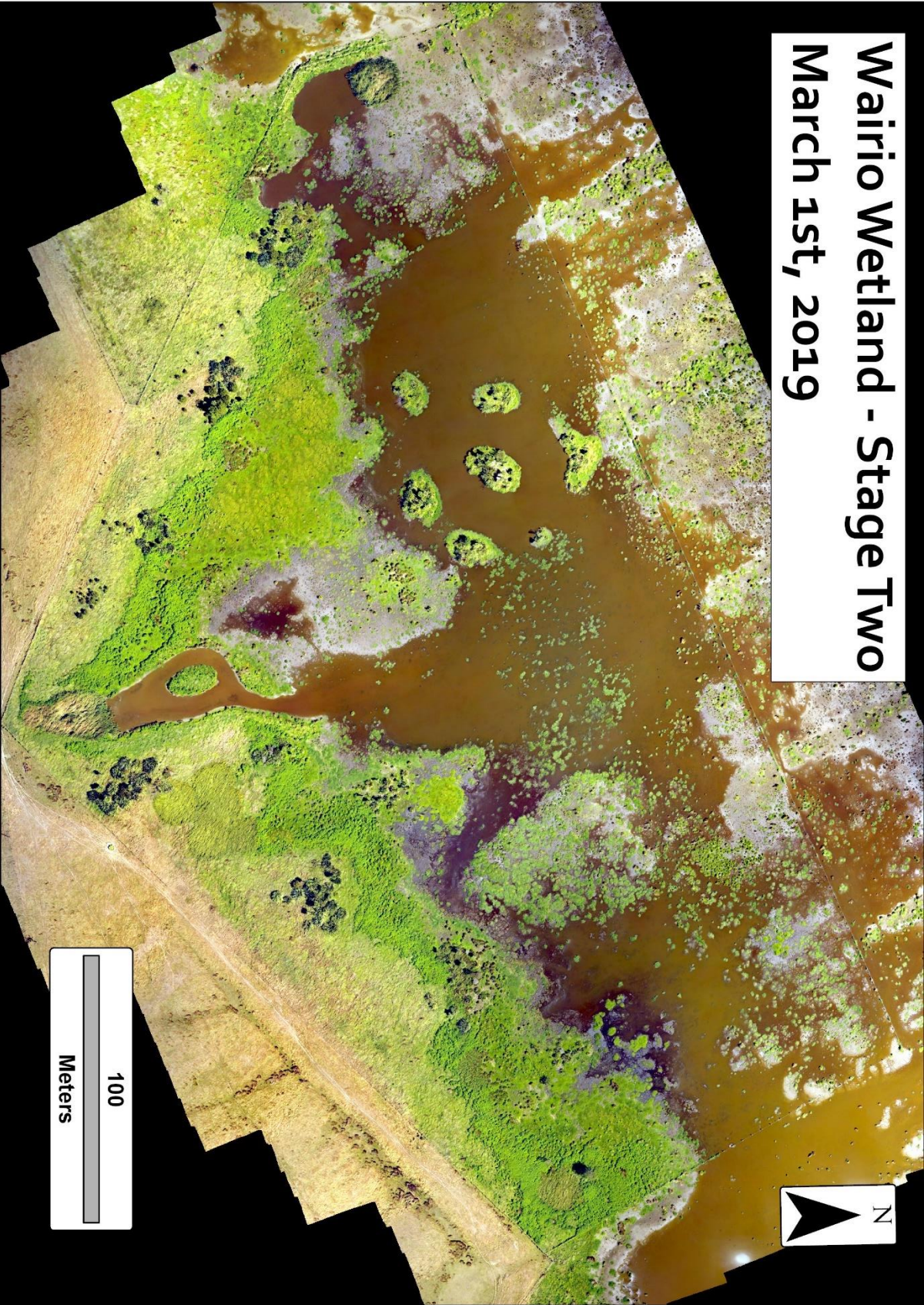
# Wairio Wetland - Stage Two October 6th, 2018



**Wairio Wetland - Stage Two  
January 4th, 2019**

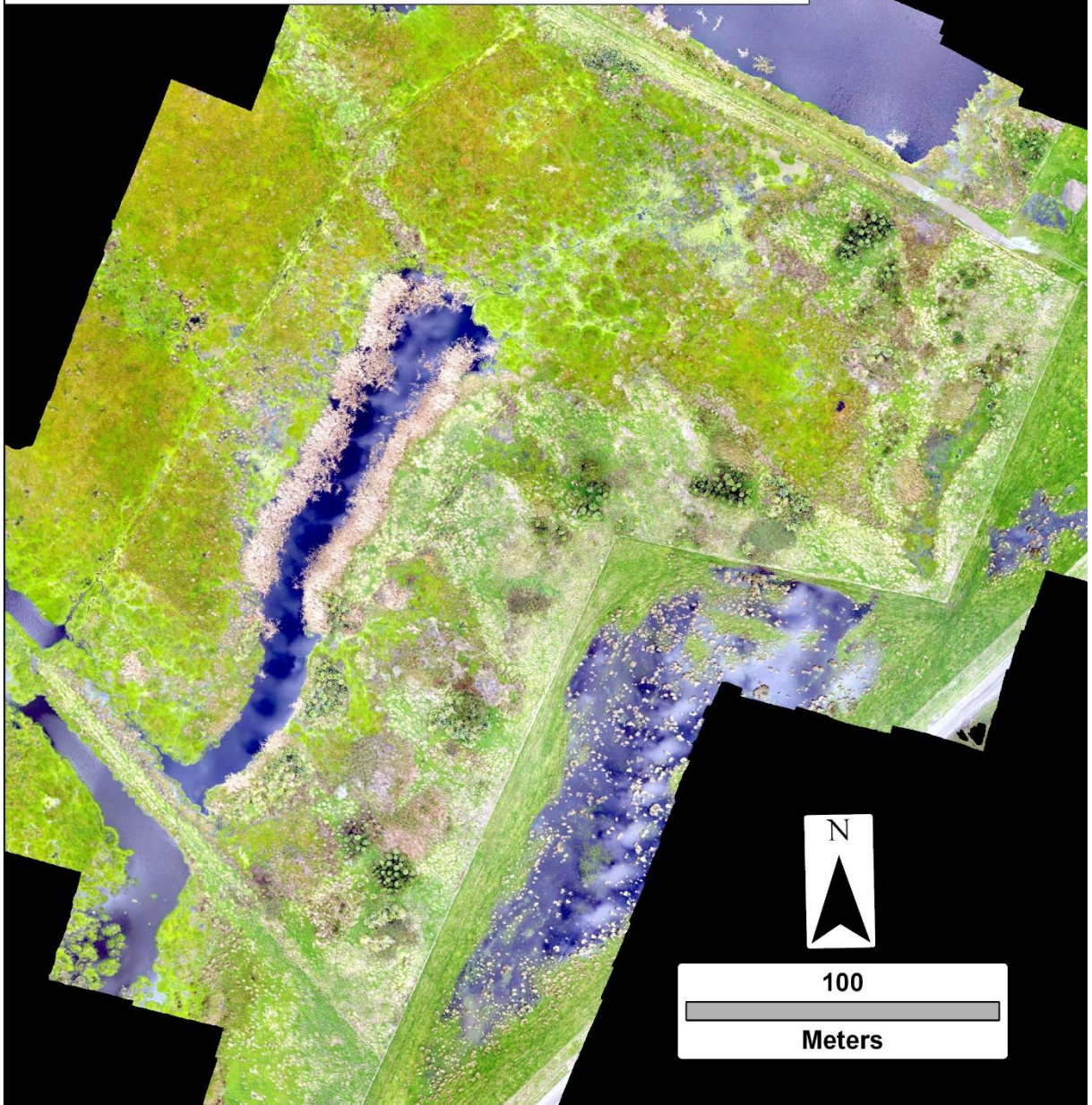


**Wairio Wetland - Stage Two  
March 1st, 2019**

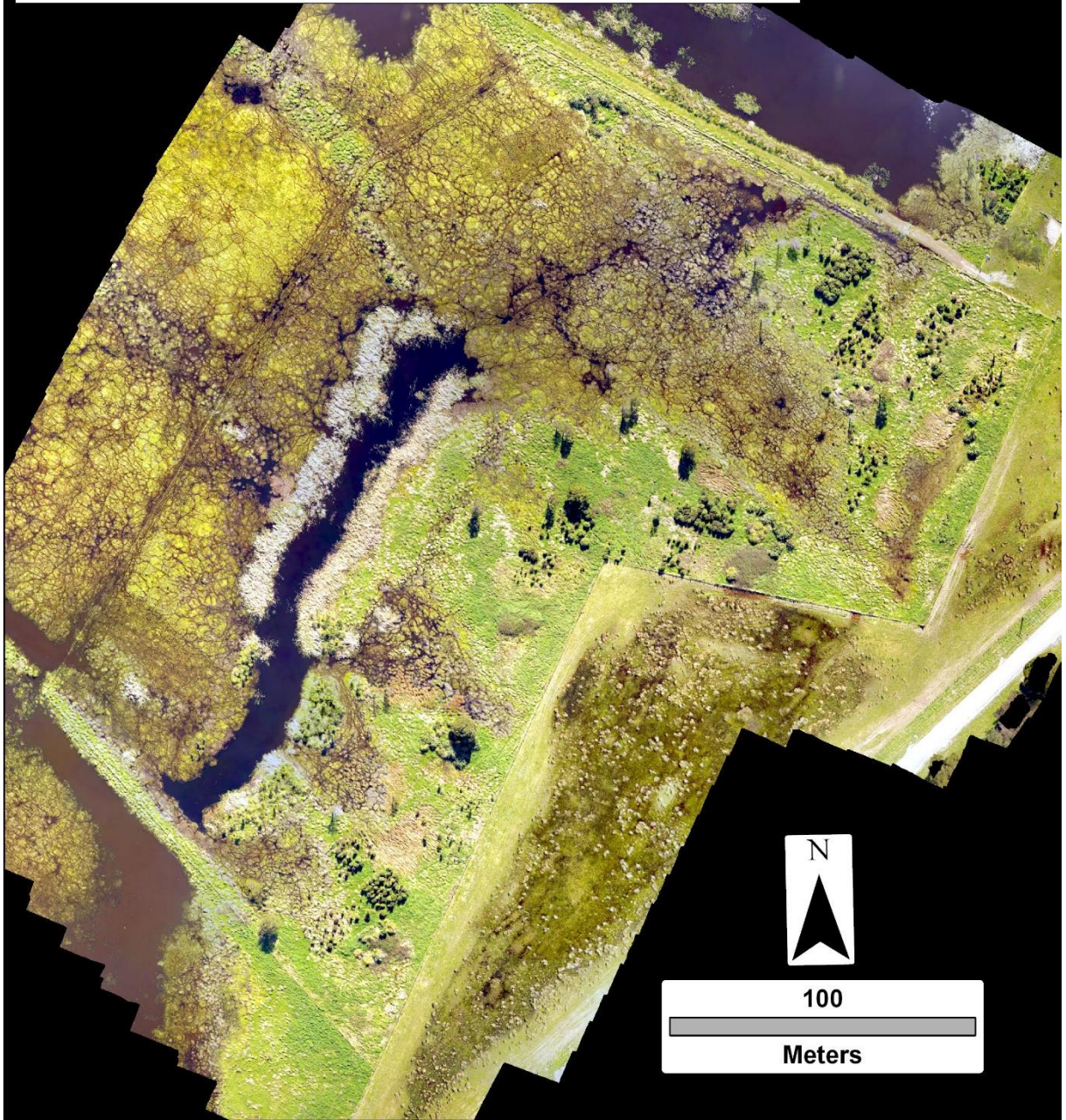


# Wairio Wetland - Stage Three

June 15th, 2019



# Wairio Wetland - Stage Three September 15th, 2019



# Wairio Wetland - Stage Three

## January 4th, 2019



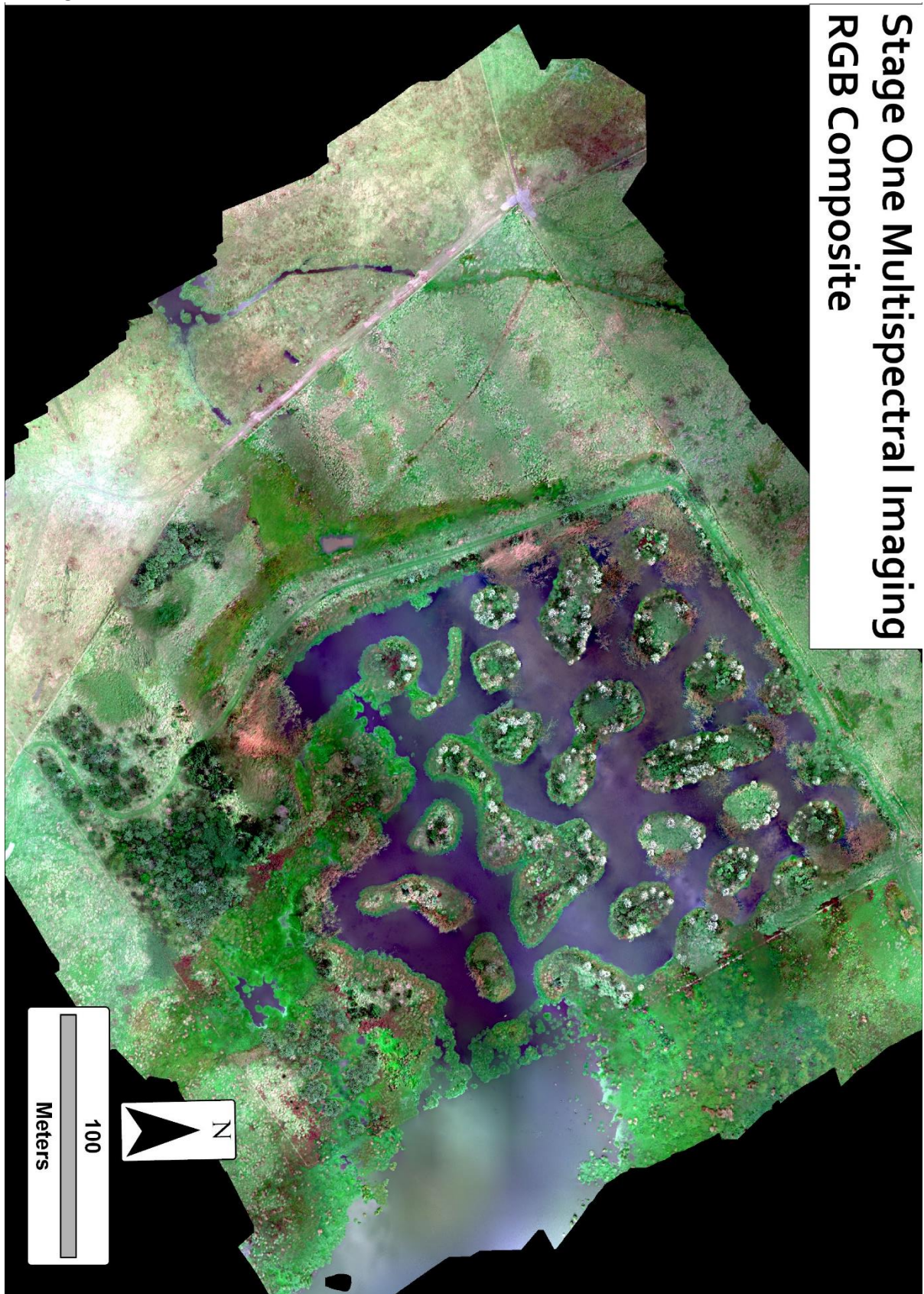
# Wairio Wetland - Stage Three

March 1st, 2019

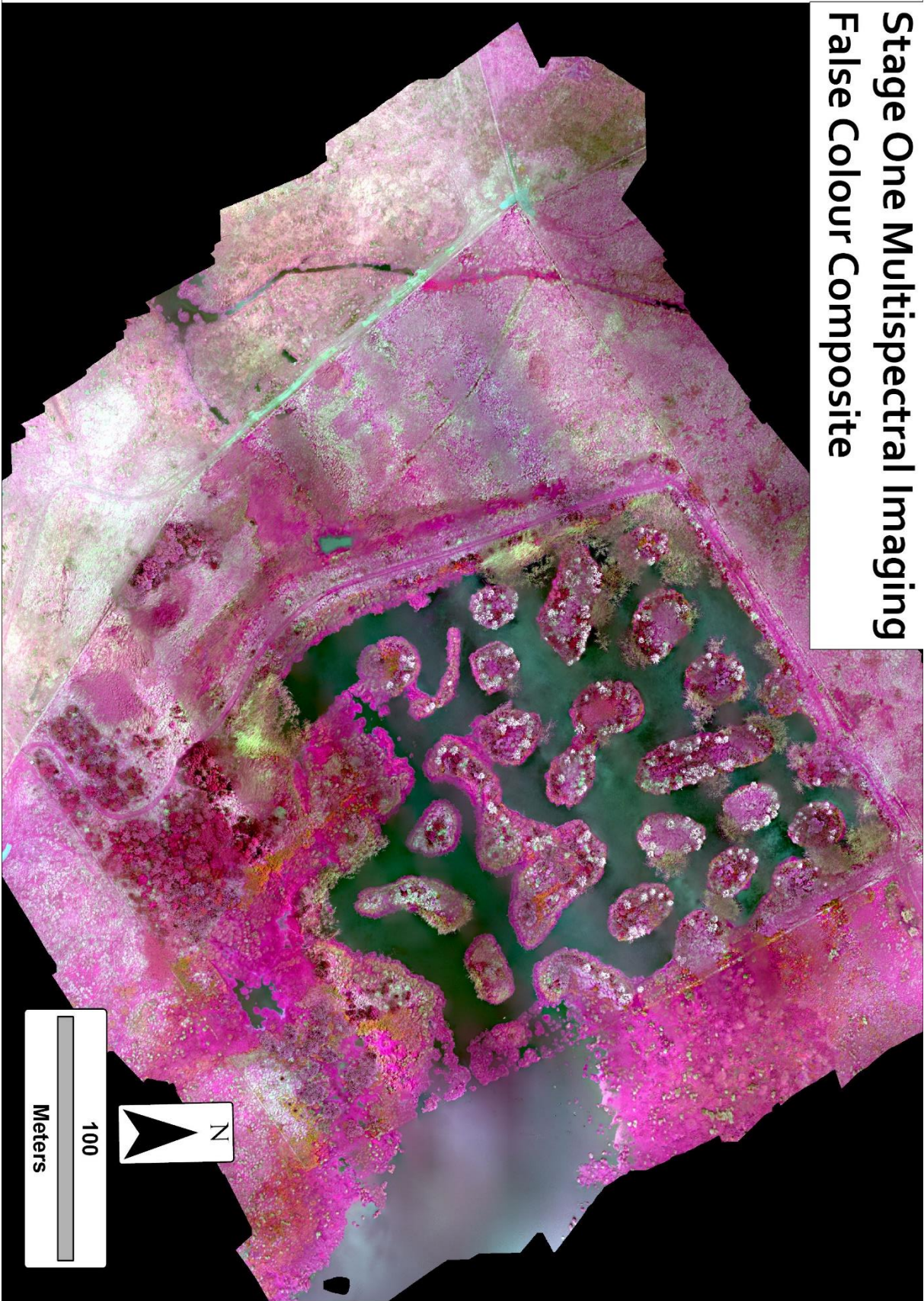


## C.2 Multispectral Camera Imagery

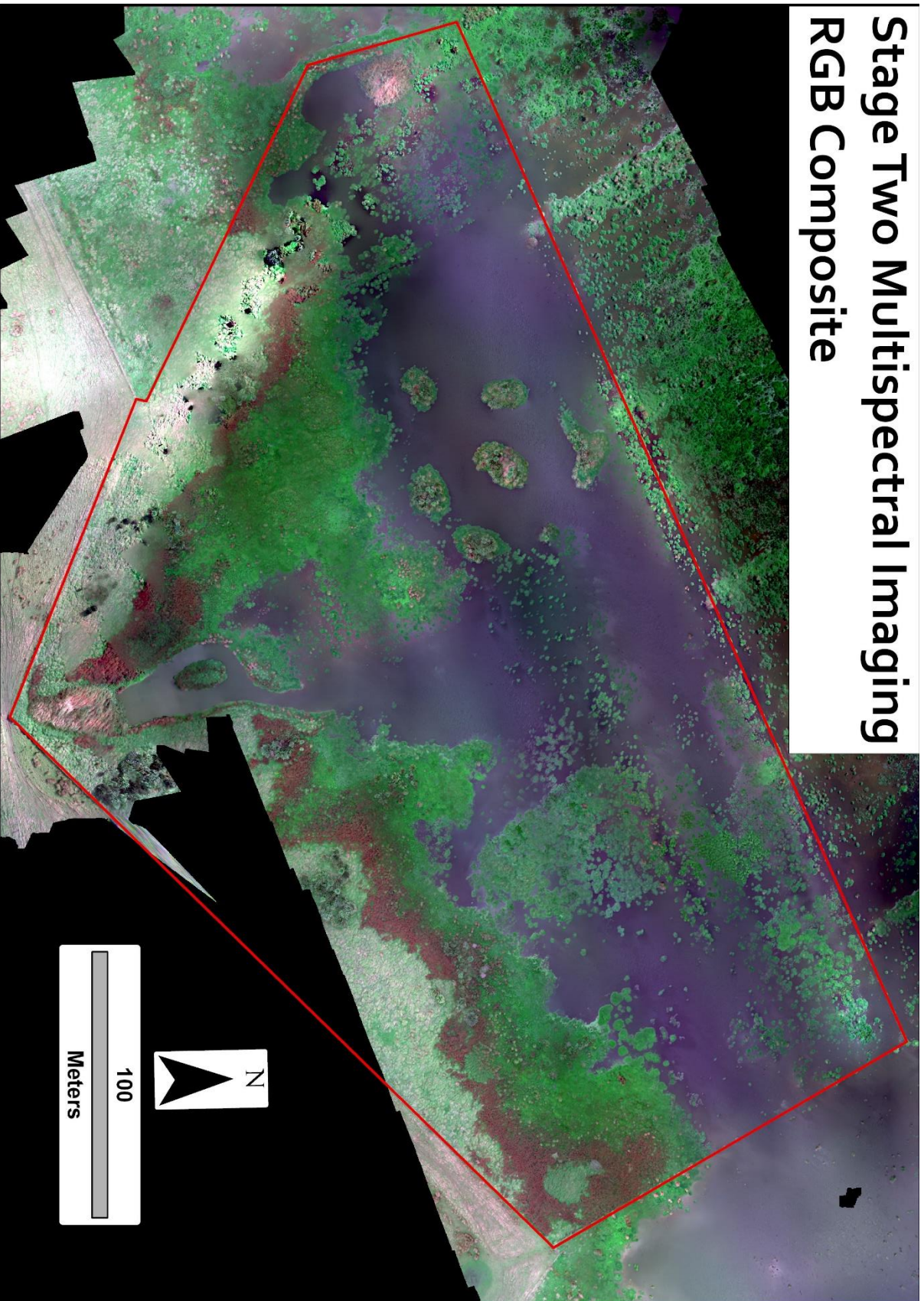
Two orthomosaics are presented here: the true-colour composite produced from the red, green and blue bands, used as the base RGB map for the multispectral tests, and a false-colour composite produced from the NIR, Red and Green bands to demonstrate the spectral separability in the NIR and RE ranges.



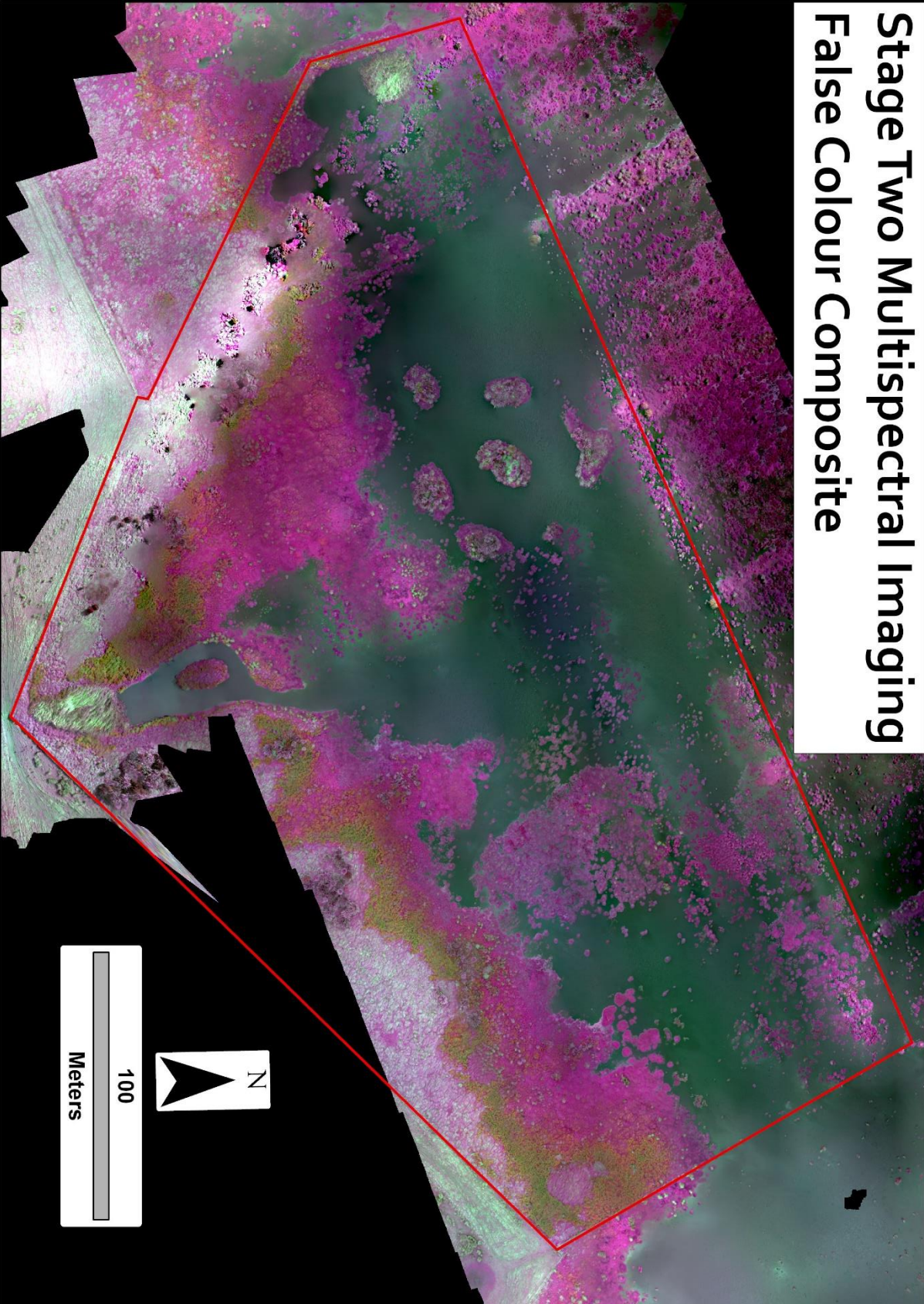
# Stage One Multispectral Imaging False Colour Composite



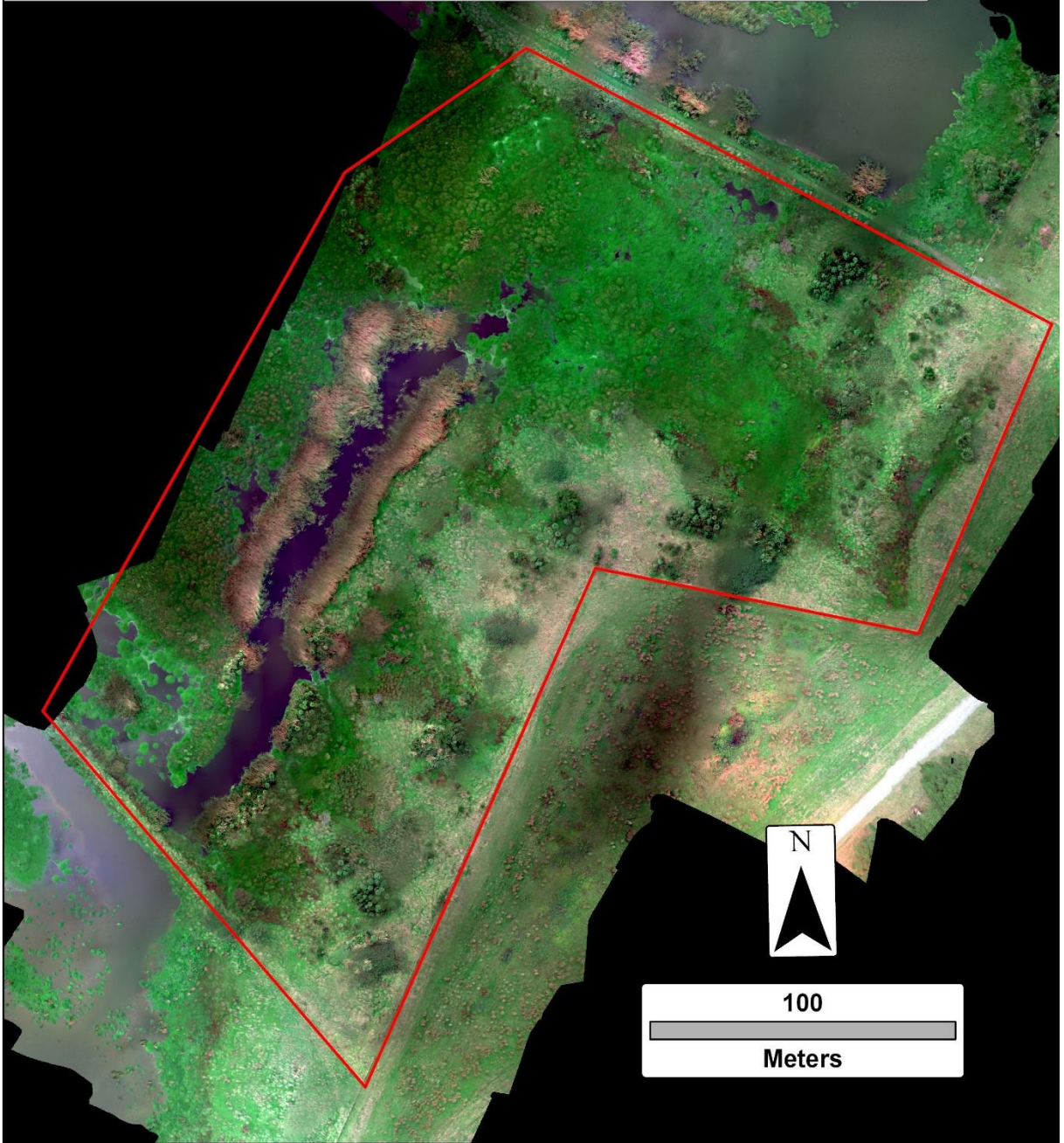
# Stage Two Multispectral Imaging RGB Composite



# Stage Two Multispectral Imaging False Colour Composite



# Stage Three Multispectral Imaging RGB Composite



# Stage Three Multispectral Imaging False Colour Composite

